OPEN ACCESS

January 2022
ISSN 1996-0786
DOI: 10.5897/AJEST
www.academicjournals.org

ACADEMIC JOURNALS
expand your knowledge

About AJEST

African Journal of Environmental Science and Technology (AJEST) provides rapid publication (monthly) of articles in all areas of the subject such as Biocidal activity of selected plant powders, evaluation of biomass gasifier, green energy, Food technology etc. The Journal welcomes the submission of manuscripts that meet the general criteria of significance and scientific excellence. Papers will be published shortly after acceptance. All articles are peer-reviewed

Indexing

The African Journal of Environmental Science and Technology is indexed in:

CAB Abstracts, CABI's Global Health Database, Chemical Abstracts (CAS Source Index), China National Knowledge Infrastructure (CNKI), Dimensions Database, Google Scholar, Matrix of Information for The Analysis of Journals (MIAR), Microsoft Academic

AJEST has an h5-index of 14 on Google Scholar Metrics

Open Access Policy

Open Access is a publication model that enables the dissemination of research articles to the global community without restriction through the internet. All articles published under open access can be accessed by anyone with internet connection.

The African Journal of Environmental Science and Technology is an Open Access journal. Abstracts and full texts of all articles published in this journal are freely accessible to everyone immediately after publication without any form of restriction.

Article License

Article Copyright

Self-Archiving Policy

The African Journal of Environmental Science and Technology is a RoMEO green journal. This permits authors to archive any version of their article they find most suitable, including the published version on their institutional repository and any other suitable website.

Please see http://www.sherpa.ac.uk/romeo/search.php?issn=1684-5315

Digital Archiving Policy

The African Journal of Environmental Science and Technology is committed to the long-term preservation of its content. All articles published by the journal are preserved by Portico. In addition, the journal encourages authors to archive the published version of their articles on their institutional repositories and as well as other appropriate websites.

https://www.portico.org/publishers/ajournals/

Metadata Harvesting

The African Journal of Environmental Science and Technology encourages metadata harvesting of all its content. The journal fully supports and implement the OAI version 2.0, which comes in a standard XML format. See Harvesting Parameter

Memberships and Standards

Academic Journals strongly supports the Open Access initiative. Abstracts and full texts of all articles published by Academic Journals are freely accessible to everyone immediately after publication.

All articles published by Academic Journals are licensed under the Creative Commons Attribution 4.0 International License (CC BY 4.0). This permits anyone to copy, redistribute, remix, transmit and adapt the work provided the original work and source is appropriately cited.

Crossref is an association of scholarly publishers that developed Digital Object Identification (DOI) system for the unique identification published materials. Academic Journals is a member of Crossref and uses the DOI system. All articles published by Academic Journals are issued DOI.

Similarity Check powered by iThenticate is an initiative started by CrossRef to help its members actively engage in efforts to prevent scholarly and professional plagiarism. Academic Journals is a member of Similarity Check.

CrossRef Cited-by Linking (formerly Forward Linking) is a service that allows you to discover how your publications are being cited and to incorporate that information into your online publication platform. Academic Journals is a member of CrossRef Cited-by.

Academic Journals is a member of the International Digital Publishing Forum (IDPF). The IDPF is the global trade and standards organization dedicated to the development and promotion of electronic publishing and content consumption.

Contact

Editorial Office: ajest@academicjournals.org

Help Desk: helpdesk@academicjournals.org

Website: http://www.academicjournals.org/journal/AJEST

Submit manuscript online http://ms.academicjournals.org

Academic Journals
73023 Victoria Island, Lagos, Nigeria
ICEA Building, 17th Floor,
Kenyatta Avenue, Nairobi, Kenya.

Table of Content

Variability of the magnetospheric electric field due to high-speed solar wind convection from 1964 to 2009 1
Gnanou Inza, Zoundi Christian, Kaboré Salfo and Ouattara Frédéric

Optimizing community participation in the management of Yala Wetland Ecosystem, Lake Victoria Basin, Kenya: The Yala Hub Framework 10
Douglas O. Odero and Victor A. O. Odenyo

Isotherms, kinetic and thermodynamic studies of methylene blue adsorption on chitosan flakes derived from African giant snail shell 37
Olaosebikan Abidoye Olafadehan, Victor Ehigimetor Bello, Kehinde Olawale Amoo and Adebukola Morufat Bello

Vol. 16(1), pp. 1-9, January 2022
DOI: 10.5897/AJEST2021.3075
Article Number: 07F381E68408
ISSN: 1996-0786

http://www.academicjournals.org/AJEST

ACADEMIC JOURNALS
expand your knowledge

African Journal of Environmental Science and Technology

Full Length Research Paper

Variability of the magnetospheric electric field due to high-speed solar wind convection from 1964 to 2009

Gnanou Inza, Zoundi Christian*, Kaboré Salfo and Ouattara Frédéric

Laboratoire de Recherche en Energétique et Météorologie de l'Espace (LAREME), Université Norbert Zongo, Koudougou, Burkina Faso.

Received 19 October, 2021; Accepted 10 December, 2021

Focusing on the classification of solar winds into three types of flux: (1) slow winds, (2) fluctuating winds, and (3) high speed-solar winds HSSW (V ≥ 450 km/s on average day), the influence of the convection electric field (E_M) via the flow of HSSWs during storms in the internal magnetosphere and on the stability of magnetospheric plasma at high latitudes was investigated. The study involved 1964-2009 period, which encompasses solar cycles 20, 21, 22 and 23. The results show a weak correlation of the frozen electric field profiles with the HSSWs overall solar cycles and a very large number of HSSWs recorded in cycle 23. Particular attention has been paid to solar cycle 22 which rather presents a fairly disturbed profile with sudden variations in solar flux and E_M field; however, solar cycle 21 records the lowest level of HSSW. Overall, over all the studied solar cycles, it can be seen that the E_M field from HSSWs of very low intensity increases progressively from solar cycle 20 to cycle 23, respectively with a minimum occurrence of 8.48% and a maximum of 9.36%. The results reached show, on one hand, that the magnetosphere is very stable from 15:00UT to 21:00UT, and on the other hand, that there is a significant transfer of mass in the night sector (21:00UT-24:00UT) than on the day side (00:00UT-15:00UT) for all solar cycles over the long period of 45 years.

Key words: Solar cycle, solar wind, magnetosphere, geomagnetic convection, electric field.

INTRODUCTION

Magnetospheric convection electric field (E_M) is a key parameter in all existing theories when it comes to the mechanism of magnetic disturbances in the upper atmosphere. These disturbances, more intense via the solar flux at high speed, can have a possible impact on human health (Schwenn, 2006; Belisheva, 2019; Abdullrahman and Marwa, 2020; Hapgood et al., 2021) as well as technological systems (satellites, planes, telecommunications, etc).

Magnetospheric convection is seen as a fundamental driver of magnetospheric processes (Dungey, 1961; Axford and Hines, 1964). Component of the ionosphere/ magnetosphere coupling, E_M specifies the motion of the plasma in the internal magnetosphere (Matsui et al., 2008). It contributes with the corotating electric field related to the rotation of the earth to the magnetospheric electric field (Khazanov et al., 2004; Maus, 2017).

Considerable progress has been made on the study of

*Corresponding author. E-mail: zounchr@yahoo.fr.

the E_M field (Kivelson, 1976; He et al., 2010; Kunduri et al., 2018). These include the study of magnetospheric electric fields and their variation with geomagnetic activity, numerical simulations on the internal magnetosphere-ionosphere convection, the study of the small-scale magnetospheric electric field observed by the Double Star TC-1 satellite (Matsui et al., 2008; Kivelson, 1976).

However, its large-scale study is poorly understood due to its low value in time and space (Fälthammar, 1989; Matsui et al., 2003). Also, this field measurement is technically very difficult, except in the relatively dense plasma of the ionosphere (Fälthammar, 1989). Indeed, first measurements were made from rockets and satellites at low latitude, while measurements at high latitude and in the magnetopause were made much later. Even today, only a few missions have included direct measurements of the magnetospheric electric field in high latitude regions such as the "Parker Solar Probe" mission launched on August 12, 2018 in Florida and "ESA S SMILE" class mission whose launch is scheduled for 2023. Therefore, many studies used data from the electric field on one hand and the magnetic field on the other hand, acquired at high latitudes (Kim et al., 2013; Kunduri et al., 2018) and at latitudes equatorial (Kelley et al., 1979; Fejer and Scherliess, 1995; Fejer et al., 2007). Since there is no way to determine directly the E_M field overall distribution, various empirical and mathematical models have been provisionally constructed, with varying degrees of complexity (Wu et al., 1981; Pierrard et al., 2008; Matsui et al., 2013).

This paper is interested in the study of the geo-efficiency of the inner magnetosphere for 1964-2009 period. The aim was to compare the dynamics of the earth's magnetosphere under two hall cycles when it is impacted by the very energetic particles of the high-speed solar wind. In this study, to determine the E_M field, linear model of Wu et al. (1981) validated by Revah and Bauer (1982) is used, a rather empirical model with a confidence level of 99% and a correlation of 97%. The objective of the study is to show the influence of HSSW on the E_M field per solar cycle.

DATA AND METHODOLOGY

The dawn-dusk electric field strength is specified empirically by the magnetic index Kp distributed in 3 h steps (Maynard and Chen, 1975; Thomsen, 2004). In doing so, data used in this present article are taken over 3-h steps so as to cover a period of 45 years. All data were extracted from CDPP site via the link «https://cdpp-archive.cnes.fr/». A comparison was made with the data available on OMNIWeb (http://omniweb.gsfc.nasa.gov/form/dx1.html) and a filtering was performed. The two surprising peaks of the frozen electric field (in mV/m) and solar wind velocities V (in km/s) were considered as erroneous and removed. In this paper, the data are called good or reliable, when simultaneously the parameters Ey, V, Aa (geomagnetic index) and Bz (component of the interplanetary magnetic field IMF) are available. The data inventory for the period1964-2009 is shown in Table 1.

The hourly values of the Ey (in mV/m) are converted into E_M (in mV/m) using the law of field transformation (Wu et al., 1981) according to the equation:

$$E_M = 0,13 E_y + 0,09 \quad (1)$$

Since we cannot isolate the behavior of part of the solar winds from that of the whole in the case of turbulent flow, it would be necessary to take a holistic view. Using this approach, we calculated the daily (Equations 2 and 3) and annual (Equation 4 and 5) averages of the frozen field and the solar wind speeds:

$$V = \frac{1}{24}\sum_{i=1}^{n} V_i \quad (2)$$

$$E = \frac{1}{24}\sum_{i=1}^{n} E_i \quad (3)$$

where V_i and E_i are respectively the hourly values of solar wind speed V and the frozen electric field E.

$$V = \frac{1}{n}\sum_{j=1}^{n} V_j \quad (4)$$

$$E = \frac{1}{n}\sum_{j=1}^{n} E_j \quad (5)$$

where V_j and E_j are respectively the daily values of V and E with n = 365 or 366.

RESULTS AND DISCUSSION

High-speed solar winds from 1964 to 2009

Figure 1 shows high speed solar winds annual averages evolution from 1964 to 2009. Part of our study period was not influenced by high-speed solar winds. It was found that the solar wind speeds maximum are generally observed at the end of the cycle, that is to say in the years of the descending phases. This finding is in agreement with other previous studies (Richardson and Hilary, 2012; Zerbo et al., 2012; Mursula et al., 2015; Borovsky, 2020).

The observed peaks in 1974, 1986, 1994 and 2003 belong, respectively to solar cycles 20 (1964-1976), 21 (1976-1986), 22 (1986-1996) and 23 (1996-2009). The more important peak was observed in 2003 with an annual average speed of 608.50 km/s (Zerbo et al., 2013; Kaboré and Ouattara, 2018). The year 2003 presents the frequent occurrence of high-speed solar winds with a peak of 1189 km/s recorded on October 31, 2003 (Tanskanen et al., 2005 ; Reeves et al., 2011). The year 2003 is a solar cycle 23 year, for the longest time, which recorded over 76% of HSSWs.

In addition, we examined a number of correlations (Table 2). It noticed that the profiles of the solar flux speed V and the frozen field have no dependency ratios. This is confirmed by the curves in Figure 2.

Table 1. Data inventory per solar cycle.

Cycle	Start/End	Total days	Total days when HSSW are recorded	Occurrences of HSSW (%)	Occurrences of reliable data (%)
Cycle 20	August 1964 / March 1976	2796	1220	43.6	68
Cycle 21	March 1976 / September 1986	2892	1241	42.9	75.2
Cycle 22	September 1986 / May 1996	2421	1019	42.1	69.9
Cycle 23	May 1996 / January 2009	4593	2356	51.3	99.6

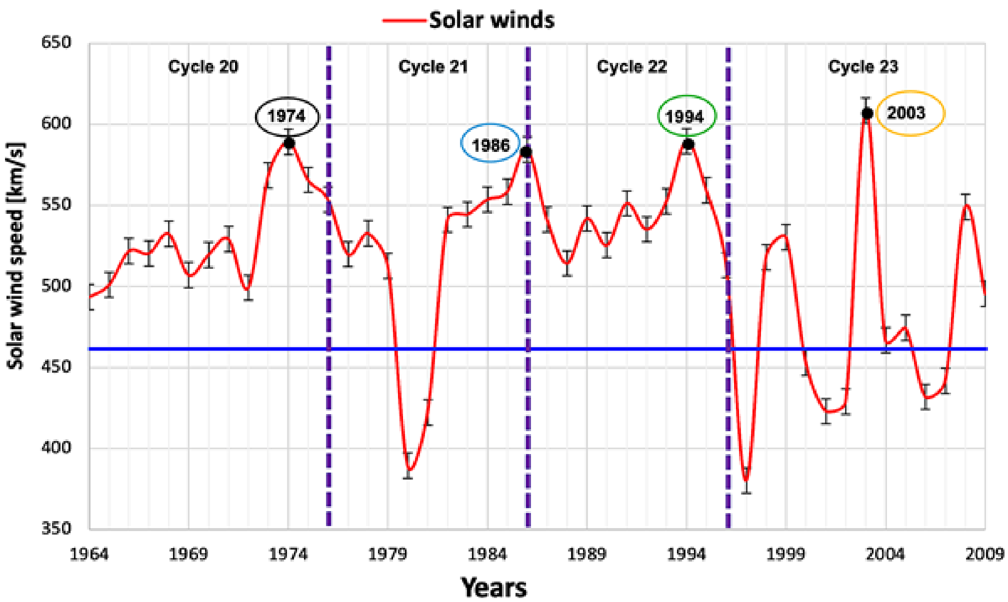

Figure 1. Evolution of annual averages of high-speed solar wind velocities from 1964 to 2009.

Table 2. Correlation between Aa and Kp indices and solar wind parameters from 1964-2009.

Parameter	V & Ey	V & Aa	V & Bz	Ey & Bz	Aa & Kp
Correlation	-0.04	0.75	0.04	-0.95	0.97

The absence of correlation between V and Ey and then between V and Bz observed, confirms the mechanism of protection of the magnetosphere from solar and planetary phenomena. Our results are in good agreement with those of Maggiolo et al. (2017), Poudel et al. (2019), and El-Borie et al. (2020).

In addition, the graphs in Figure 3 show that the Ey field and the Bz component of the interplanetary magnetic field (IMF) are in phase opposition. The average values of Ey and Bz fields obtained, are 0.031 mV/m and -0.013 nT, respectively. According to Tsurutani et al. (1988) and Herdiwijaya (2019), negative values of IMF-Bz in geocentric solar magnetospheric GSM coordinates, refer to the south direction. The negative correlation of IMF-Bz with the Ey value of the frozen electric field in the solar wind, indicates that the southern orientation of IMF-Bz could be responsible for the initiation of magnetic substorms. Probably, daily fluctuations of the magnetic and electric effects of the magnetospheric origin currents would play a very important role in the magnetic reconnection rate.

Solar wind velocities vary with distance traveled and time, but changes from solar minimum to solar maximum produce larger effects (Richardson et al., 2001). To better understand the temporal variability of high-speed solar winds over the long 45 years period, the data were averaged over 24 h in order to more visually capture the trend of the variations (Figure 4).

On the graph of Figure 4, a peak is reached at 12:00UT and the minima are observed at night until sunrise. In

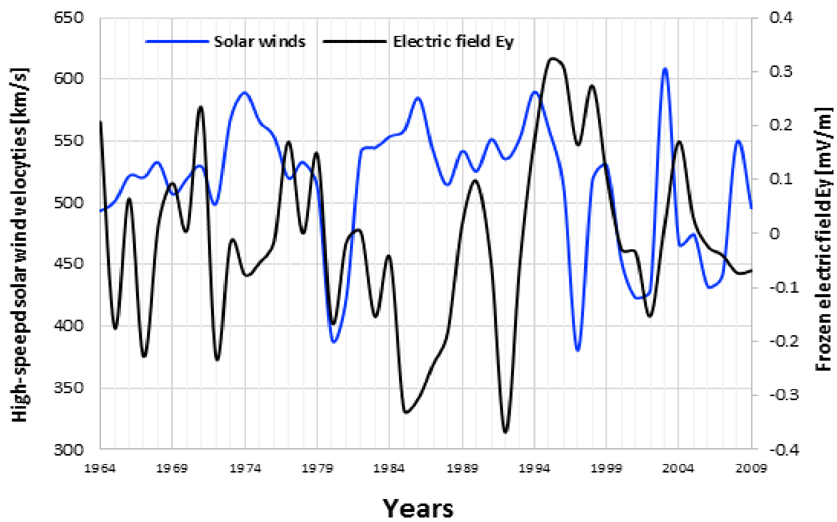

Figure 2. Comparative profiles of fast solar wind speeds and frozen electric field from 1964-2009.

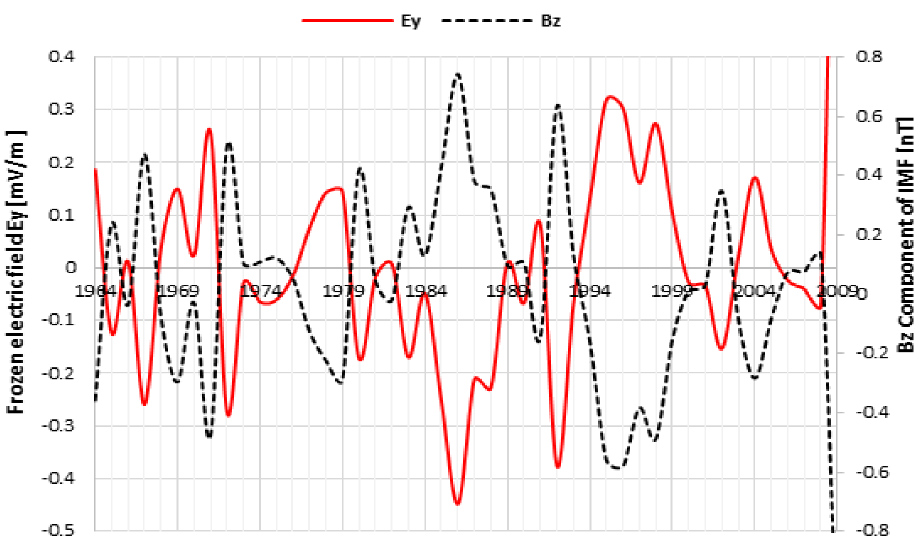

Figure 3. Comparative profiles of the frozen field and the Bz component of the IMF from 1964-2009.

doing so, we can hypothesize that the high-speed solar winds experience an acceleration from sunrise up to 12:00UT and after 12:00UT, undergo a deceleration. This result corroborates that of Navia (2018). However, the low correlation (r = 0.43) between HSSW and time may be due to the temporal cadence or variety of the solar wind considered in this study.

Magnetospheric electric field from 1964 to 2009

Figure 5 represents the daily variability of the magnetospheric electric field from 1964-2009. In this figure, linear regression curves plotted in dotted lines, are obtained from the least squares method. Plot shows three trends, two increasing and one decreasing with relatively different correlations at different times of the day. This leads respectively to the low daily averages 0.090 mV/m for the first trend, 0.088 mV/m for the second trend, and 0.089 mV/m for the last trend. Over 1964-2009 period, we find that with universal time (UT), correlation of the E_M field is much weak (r = 0.16) from 00:00 to 15:00 UT, better (r = −0.98) from 15:00 to 21:00 UT, and excellent (r = 1) from 21:00 to 24:00 UT. The first

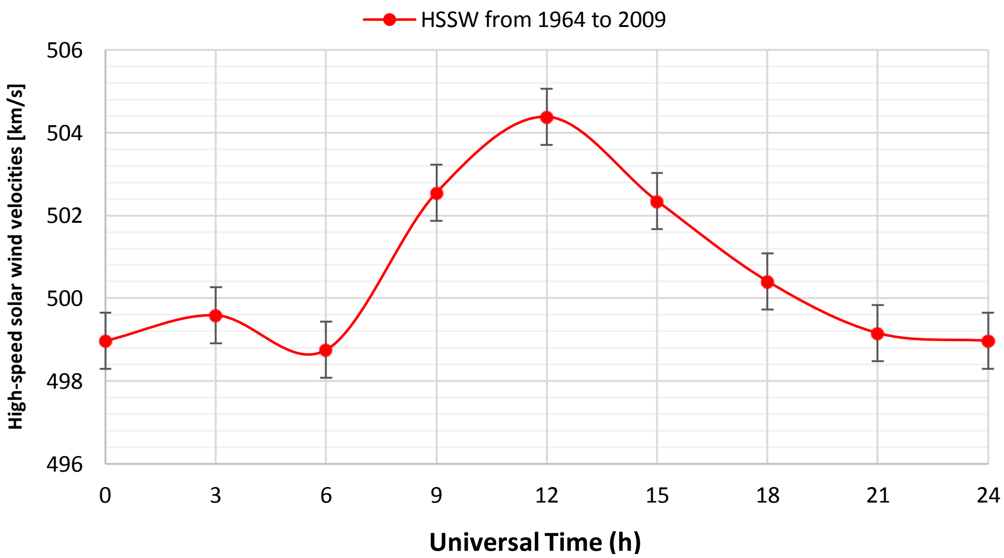

Figure 4. Average velocities evolution of the HSSW as a function of time.

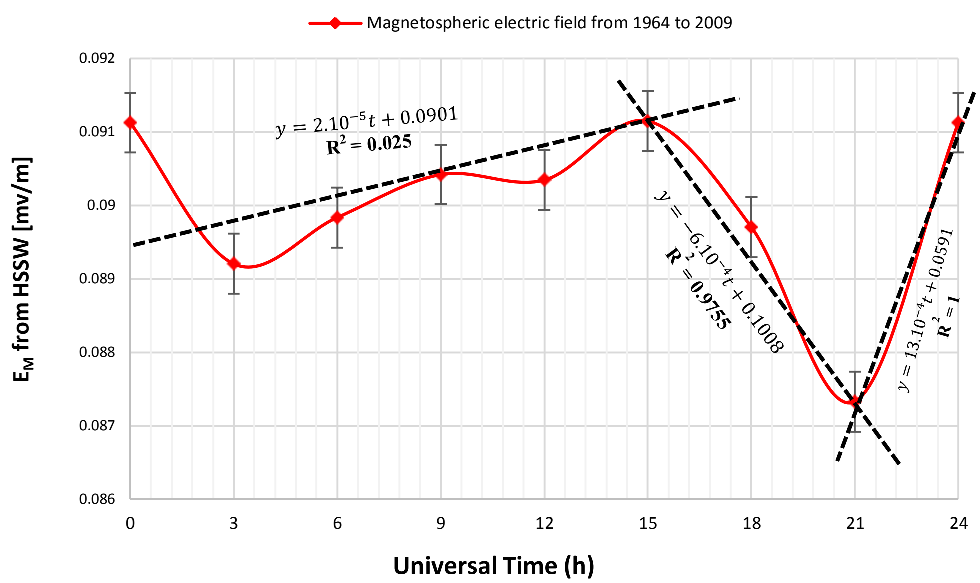

Figure 5. Evolution of E_M from HSSW as a function of time.

increasing trend from 00:00 to 15:00 TU with a slope of $+2.10^{-5}$ mV/m.s, shows the main phase of the magnetic storm (Partamies et al., 2011). The onset of this phase corresponds to the beginning of the IMF change from north to south. During this main phase, we find that the sustained E_M field, is directed southward until 21:00UT. According to several works (Nishimura et al., 2009; Partamies et al., 2011), the IMF southward change implies the intensification of the ring current; and according to Gonzalez et al. (1994), since the geomagnetic storm is identified by the intensification of this type of current, we can conclude in this study that the increasing phase of E_M field expresses the phase of increasing geomagnetic activity. These authors have confirmed that a south-facing IMF triggers the increase of the convective electric field in the inner magnetosphere, however they do not specify the time at which this increase is perceptible. Our study suggests that the intensification of the ring current took place from 00:00 to 15:00 UT for all the solar cycles 20 to 23 studied.

The next trend is decreasing from 15:00 to 21:00 UT with a slope of -6.10^{-4} mV/m.s. According to several

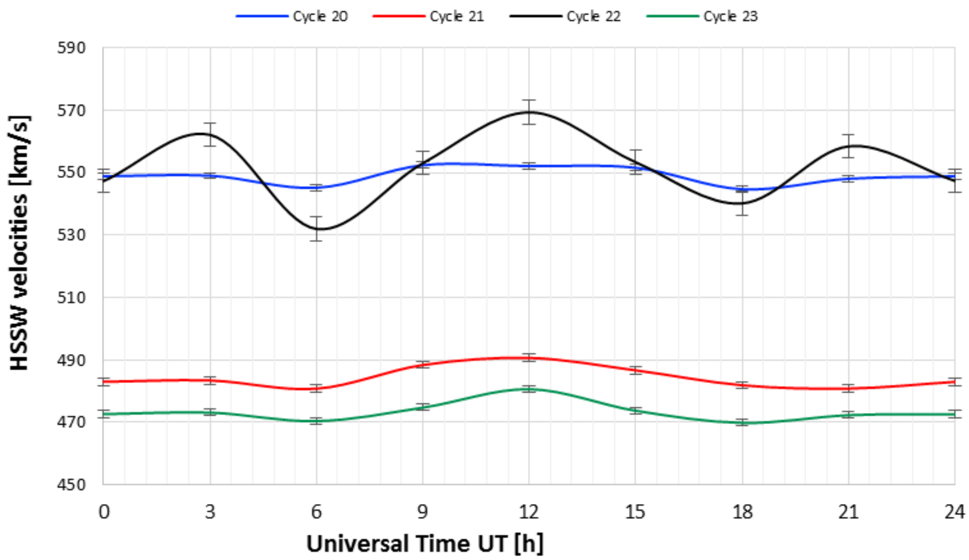

Figure 6. Average velocities evolution of the HSSW as a function of time.

authors (Gonzalez et al., 1994; Nishimura et al., 2009; Partamies et al., 2011; Kaboré and Ouattara, 2018), the decaying phase of E_M field is due to the change of IMF from South to North. In view of this argument and for the whole solar cycles 20 to 23, we can confirm that IMF maintains northward from 15:00 UT until 21:00 UT, and turns southward again after 21:00 UT. During this decreasing phase, there is a dissipation of energy by the inner magnetosphere. In this paper, this dissipation observed over a period of 03 h, is corroborated by the work of Partamies et al. (2011) and Kaboré and Ouattara (2018). This result leads us to suggest that the dissipation of solar-derived energy by the earth's magnetosphere via HSSWs, varies according to the phases of magnetic substorms, in particular, when the IMF is oriented North. Moreover, based on the assumptions that, magnetospheric convection is weakened when IMF shifts from South to North (Kelley et al., 1979; Kaboré and Ouattara, 2018), it could be suggested in this study that the inner magnetosphere is much stable between 15:00 and 21:00 UT. Moreover, the phase changes of the IMF occur around 15:00 UT on the day side and then 21:00 UT on the night side.

Finally, the night side increase phase (21:00-24:00 UT) with a slope of $+13.10^{-4}$ mV/m.s of the E_M field may be due to the magnetic reconnection. This reconnection affecting the plasma dynamics, observed in the night sector (21:00-24:00 UT), would be consistent with the reconnection model proposed in the open magnetosphere concept which illustrates the principle of field line and plasma transport (Dungey, 1961; Lilensten and Blelly, 2000). The consequence of a reconnection with a south-facing IMF is the massive entry of charged particles into the inner magnetosphere. However, facing the sun, direct entries of solar wind particles are possible depending on the magnetic state of the Sun. The particles which find themselves in the magnetosphere, undergo a strong acceleration towards the earth under the combined effect of the electric field and the IMF variations. In sum, fluctuations of the magnetospheric electric field resulting from the high-speed solar winds, observed in this article, are responsible for the initiation of substorms. The intensity of these substorms increases in the mornings and evenings, while they decrease in the afternoons.

Distribution of E_M field and HSSW per solar cycle

In order to study the occurrence of the E_M field on each solar cycle, temporal evolutions of HSSWs have been represented in Figure 6. The graphs show large amplitudes of HSSWs for even solar cycles (cycles 20 and 22), and low amplitudes for odd ones (cycles 21 and 23). This result corroborates the work of Takalo (2021).

The graphs in Figure 6 reveal the existence of abrupt variations and large amplitudes of HSSWs for solar cycle 22. This may be due, on the one hand, to the fact that the polar coronal holes were more developed for this cycle (Issautier, 2003); and on the other hand, to the high occurrence of storms recorded in this solar cycle 22 (Echer et al., 2008; Nagatsuma et al., 2015; Pokharia et al., 2018). As a result, cycle 22 remains the most "magnetically disturbed" solar cycle, with HSSWs peaking at 569.35 km/s. These observed geomagnetic disturbances are attributed to magnetospheric electric fields due to HSSWs. This observation is in good agreement with that made by other authors (Nishida, 1966;

Table 3. E_M field and HSSW balance for solar cycles 20, 21, 22 and 23.

Cycle	Period	Averages [km/s]	E_M [mV/m]%
Cycle 20	1964-1976	550.34	8.48
Cycle 21	1976-1986	485.10	8.59
Cycle 22	1986-1996	551.18	9.02
Cycle 23	1996-2009	473.64	9.36

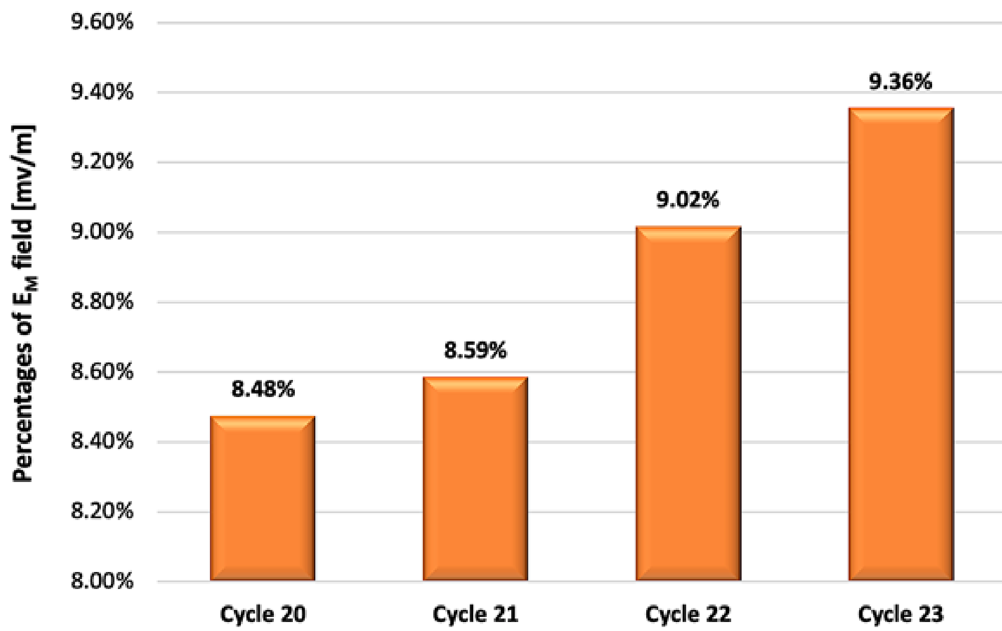

Figure 7. Distribution of E_M field from HSSW for the 20-23 solar cycles.

Kikuchi et al., 1996). The graphs in Figure 6 show that cycles 21 and 23 experienced low amplitudes of the high-speed solar winds HSSWs with peaks of 490.66 and 480.63 km/s, respectively around 12:00 UT. Column 5 of Table 1 and Column 3 of Table 3 corroborate this fact. Table 3 gives the averages of the HSSWs velocities and the results of various occurrences of the E_M field for the four solar cycles.

The fourth column of Table 3 shows low occurrences of E_M field for all solar cycles studied. The lowest 8.48% occurrence is recorded in cycle 20 and the highest 9.36% in cycle 23. It is important to emphasize that, for our study period, almost all Ey field values of solar cycle 20 are negative (with an average of −0.038 mV/m), hence the weak contribution of E_M field. Solar cycle 23 is the most exceptional. With an average duration of around 13 years, cycle 23 records 2356 days of HSSW (Table 1), slightly more than the double of the days recorded by each of the other solar cycles. As a result, cycle 23 is distinguished by remarkable years both for its majestic phenomena (09 major geomagnetic storms from 1997 to 2001, strong solar flares in 2003, violent magnetic storms in 2004, etc.) and for the intensity of its solar activity (Belov et al., 2005; Trichtchenko et al., 2007; Zerbo et al., 2012). The low proportion of E_M fields corroborates the work of Bharati et al. (2019). The same authors also predicted a significant decrease in E_M field occurrences for the last three solar cycles (22-24). Figure 7 shows E_M field distributions from the HSSWs from 1964 to 2009 period. Globally, we noticed an increasing and almost linear evolution of the occurrences. As the depression of the geomagnetic activity level is underlined by several works (Schatten, 2003; Maris and Maris, 2009; Bharati, 2019) with solar cycle 23 being the weakest of the last three, we can confirm that E_M field and geomagnetic activity are progressing in phase opposition.

Conclusion

Various parameters of solar origin have been used in this study to understand the dynamics of the earth's magnetosphere under the impact of high-speed solar winds (HSSW). For 1964-2009 period, about 85% of the years were under the influence of HSSW. Among these years, four were remarkable with peaks generally observed at the end of the solar cycle around 12:00 UT, which confirms the intensification of HSSW around noon UT. Daily statistical analysis of HSSW populations showed three phases of magnetic substorms manifestations: from 00:00-15:00 UT, from 15:00-21:00 UT then from 21:00-24:00 UT. These three periods are respectively characterized by the main phase of the magnetic storm, the dissipation of the solar energy initially stored by the inner magnetosphere during the first phase, and the magnetic reconnection at night. The results obtained showed that the changes of IMF orientation during these three phases, were observed at 15:00 UT on the day side and 21:00 UT on the night side. Our results confirm that the inner magnetosphere was very stable from 15:00-21:00 UT, and disturbed from 00:00-15:00 UT then 21:00-24:00 UT. For all the solar cycles studied, E_M field oscillated between minima (0.087 mV/m around 06:00 UT and 0.089 mV/m around 21:00 UT) and maximum 0.091 mV/m at 15:00 UT. Overall, E_M field was very weak (~0.090 mV/m overall studied cycles) and increased progressively from 8.48% (cycle 20) to 9.36% (cycle 23). Of the solar cycles studied, the even-numbered cycles were highly perturbed, with solar cycle 22 the most active.

CONFLICT OF INTERESTS

The authors have not declared any conflict of interests.

ACKNOWLEDGEMENTS

The authors thank the OMNIWeb team and CDPP for the databases.

REFERENCES

Abdullrahman HM, Marwa AM (2020). The Effects of Solar Activity and Geomagnetic Disturbance on Human Health. Open Access Journal of Biomedical Science 2(5).

Axford WI, Hines CO (1964). Comments on “a hydromagnetic theory of geomagnetic storms” by J.H. Piddington. Planetary Space Science 12(6):660-661.

Belisheva NK (2019). The Effect of Space Weather on Human Body at the Spitsbergen Archipelago. In Arctic Studies-A Proxy for Climate Change. IntechOpen.

Belov A, Baisultanova L, Eroshenko E, Mavromichalaki H, Yanke V, Pchelkin V, Plainaki C, Mariatos G (2005). Magnetospheric effects in cosmic rays during the unique magnetic storm on November 2003. Journal of Geophysical Research 110(A9).

Bharati K, Amar K, Durbha SR, Gurbax SL (2019). Diminishing activity of recent solar cycles (22–24) and their impact on geospace. Journal of Space Weather and Space Climate 9(A1).

Borovsky JE (2020). What magnetospheric and ionospheric researchers should know about the solar wind. Journal of Atmospheric and Solar-Terrestrial Physics 204:105271.

Dungey JW (1961). Interplanetary magnetic field and the auroral zones. Physical Review Letters 6(2):47-48.

Echer E, Gonzalez WD, Tsurutani BT, Gonzalez ALC (2008). Interplanetary conditions causing intense geomagnetic storms (Dst ≤ −100 nT) during solar cycle 23 (1996-2006). Journal of Geophysical Research: Space Physics 113(A5).

El-Borie MA, El-Taher AM, Thabet AA, Bishara AA, (2020). The Interconnection between the Periodicities of Solar Wind Parameters Based on the Interplanetary Magnetic Field Polarity (1967–2018): A Cross Wavelet Analysis. Solar Physics 295(9).

Fälthammar CG (1989). Electric fields in the magnetosphere —a review, Planetary and Space Science 37(8):899-914.

Fejer BG, Jensen JW, Kikuchi T, Abdu MA, Chau JL (2007). Equatorial ionospheric electric fields during the November 2004 magnetic storm. Journal of Geophysical Research 112(A10).

Fejer BG, Scherliess L (1995). Time dependent response of equatorial ionospheric electric fields to magnetospheric disturbances. Geophysical Research Letters 22(7):851-854.

Gonzalez WD, Joselyn JA, Kamide Y, Kroehl HW, Rostoker G, Tsurutani BT, Vasyliunas VM (1994). What is a geomagnetic storm? Journal of Geophysical Research 99(4):5771-5792.

Hapgood M, Angling MJ, Attrill G, Bisi M, Cannon PS, Dyer C, Eastwood P, Elvidge S, Gibbs M, Harrison RA, Hord C, Horne RB, Jackson DR, Jones B, Machin S, Mitchell CN, Preston J, Rees J, Rogers NC, Routledge G, Ryden K, Tanner R, Thomson AWP, Wild JA, Willis M (2021). Development of Space Weather Reasonable Worst-Case Scenarios for the UK National Risk Assessment. Space Weather 19(4).

He ZH, Liu ZX, Chen T, Shen C, Li X, Carr C, Rème H (2010). The large-scale magnetospheric electric field observed by Double Star TC-1, Annales Geophysicae 28(9):1625-1631.

Herdiwijaya D (2019). Distribution of solar energetic particles and magnetic field orientations related to strong geomagnetic storms in solar cycle 24. Journal of Physics: Conference Series 1204:012121.

Issautier K (2003). Large-scale structure of the polar solar wind at solar maximum: ULYSSES/URAP observations. AIP Conference Proceedings.

Kaboré S, Ouattara F (2018). Magnetosphere convection electric field (MCEF) time variation from 1964 to 2009: Investigation on the signatures of the geoeffectiveness Coronal Mass Ejections 13(20):273-281.

Kelley MC, Fejer BG, Gonzales CA (1979). An explanation for anomalous equatorial ionospheric electric fields associated with a northward turning of the interplanetary magnetic field. Geophysical Research Letters 6(4):301-304.

Khazanov GV, Liemohn MW, Newman TS, Fok MC, Ridley AJ (2004). Magnetospheric convection electric field dynamics andstormtime particle energization: case study of the magneticstorm of 4 May 1998. Annales Geophysicae 22(2):497-510.

Kikuchi T, Lühr H, Kitamura T, Saka O, Schlegel K (1996). Direct penetration of the polar electric field to the equator during a DP2 event as detected by the auroral and equatorial magnetometer chains and the EISCAT radar. Journal of Geophysical Research: Space Physics 101(A8):17161-17173.

Kim H, Cai X, Clauer CR, Kunduri BSR, Matzka J, Stolle C, and Weimer DR (2013). Geomagnetic response to solar wind dynamic pressure impulse events at high-latitude conjugate points. Journal of Geophysical Research: Space Physics 118(10):6055-6071.

Kivelson MG (1976). Magnetospheric electric fields and their variation with geomagnetic activity. Reviews of Geophysics 14(2):189.

Kunduri BSR, Baker JBH, Ruohoniemi JM, Sazykin S, Oksavik K, Maimaiti M, Chi PJ, Engebretson MJ (2018). Recent Developments in Our Knowledge of Inner Magnetosphere-Ionosphere Convection. Journal of Geophysical Research: Space Physics 123:7276-7282.

Lilensten J, Blelly PL (2000). Du soleil à la Terre : Aéronomie et Météorologie de l’Espace. Collection Grenoble Sciences. Presses Universitaires de Grenoble, 416.

Maggiolo R, Hamrin M, De Keyser J, Pitkänen T, Cessateur G, Gunell H, Maes L (2017). The Delayed Time Response of Geomagnetic Activity to the Solar Wind. Journal of Geophysical Research: Space Physics 122(11):109-127.

Maris G, Maris O (2009). Rapid solar wind and geomagnetic variability during the ascendant phases of the 11-yr solar cycles. Proceedings of the International Astronomical Union 5(S264):359-362.

Matsui H, Puhl-Quinn PA, Jordanova VK, Khotyaintsev Y, Lindqvist PA, Torbert RB (2008). Derivation of inner magnetospheric electric field (UNH-IMEF) model using Cluster data set, Annales Geophysicae 26:2887-2898.

Matsui H, Quinn JM, Torbert RB, Jordanova VK, Baumjohann W, Puhl-Quinn PA, Paschmann G (2003). Electric field measurements in the inner magnetosphere by Cluster EDI. Journal of Geophysical Research 108(A9).

Matsui H, Torbert RB, Spence HE, Khotyaintsev YV, Lindqvist PA (2013). Revision of empirical electric field modeling in the inner magnetosphere using Cluster data. Journal of Geophysical Research: Space Physics 118(7):4119-4134.

Maus S (2017). A corotation electric field model of the Earth derived from Swarm satellite magnetic field measurements. Journal of Geophysical Research: Space Physics 122(8):8733-8754.

Maynard NC, Chen AJ (1975). Isolated Cold Plasma Regions: Observations and Their Possible Production Mechanisms. Journal of Geophysical Research 80(7).

Mursula K, Lukianova R, Holappa L (2015). Occurrence of high-speed solar wind streams over the grand modern maximum. The Astrophysical Journal 801(1):30.

Nagatsuma T, Kataoka R, Kunitake M (2015). Estimating the solar wind conditions during an extreme geomagnetic storm: a case study of the event that occurred on March 13–14, 1989. Earth, Planets and Space 67(1).

Navia CE, Marcel MN de O, Augusto CRA, (2018). The Highest Geomagnetic Storms of the Solar Cycle Observed at Ground Level. Extreme Weather.

Nishida A (1966). Formation of plasmapause, or magnetospheric plasma knee, by the combined action of magnetospheric convection and plasma escape from the tail. Journal of Geophysical Research 71(23):5669-5679.

Nishimura Y, Kikuchi T, Wygant J, Shinbori A, Ono T, Matsuoka A, Nagatsuma T, Brautigam D (2009). Response of convection electric fields in the magnetosphere to IMF orientation change. Journal of Geophysical Research 114(A9).

Partamies N, Juusola I, Tanskanen E, Kauristie K, Weygand JM, Ogawa Y (2011). Substorms during different phases. Annales Geophysicae 29(11):2031-2043.

Pierrard V, Khazanov GV, Cabrera J, Lemaire J (2008). Influence of the convection electric field models on predicted plasmapause positions during magnetic storms. Journal of Geophysical Research 113(A8).

Pokharia M, Prasad L, Bhoj C, Mathpal C (2018). A comparative study of geomagnetic storms for solar cycles 23 and 24. Journal of Astrophysics and Astronomy 39(5).

Poudel P, Simkhada S, Adhikari B, Sharma D, Nakarmi JJ (2019). Variation of Solar Wind Parameters along with the understanding of Energy Dynamics within the Magnetospheric System during Geomagnetic Disturbances. Earth and Space Science 6(2):276-293.

Revah I, Bauer P (1982). Rapport d'activité du Centre de Recherches en Physique de l'environnement Terrestre et Planétaire, Note technique CRPE/115, 38-40 Rue du Général Leclerc 92131 Issy-Les Moulineaux.

Richardson IG, Cliver EW, Cane HV (2001). Sources of geomagnetic storms for solar minimum and maximum conditions during 1972–2000. Geophysical Research Letters 28(13):2569-2572.

Richardson IG, Hilary VC (2012). Solar wind drivers of geomagnetic storms during more than four solar cycles. Journal of Space Weather and Space Climate 2(1).

Schatten KH (2003). Solar activity and the solar cycle. Advances in Space Research 32(4):451-460.

Schwenn R (2006). Space Weather: The Solar Perspective. Living Reviews in Solar Physics 3(2).

Takalo J (2021). Comparison of Geomagnetic Indices During Even and Odd Solar Cycles SC17 – SC24: Signatures of Gnevyshev Gap in Geomagnetic Activity. Solar Physics 296(1):1-16.

Thomsen MF (2004). Why Kp is such a good measure of magnetospheric convection. Space Weather 2(11).

Trichtchenko L, Zhukov A, Van DLR, Stankov SM, Jakowski N, Stanisławska I, Juchnikowski G, Wilkinson P, Patterson G, Thomson AWP (2007). Space weather events: Real-time observations and forecasts. Space Weather 5(6).

Tsurutani BT, Gonzalez WD, Tang F, Akasofu SI, Smith EJ (1988). Origin of interplanetary southward magnetic fields responsible for major magnetic storms near solar maximum (1978–1979). Journal of Geophysical Research 93(A8):8519.

Wu L, Gendrin R, Higel B, Berchem J (1981). Relationships between the solar wind electric field and the magnetospheric convection electric field. Geophysical Research Letters 8(10):1099-1102.

Zerbo JL, Amory-Mazaudier C, Ouattara F (2013). Geomagnetism during solar cycle 23: Characteristics. Journal of Advanced Research 4(3):265-274.

Zerbo JL, Amory-Mazaudier C, Ouattara F, Richardson JD (2012). Solar wind and geomagnetism: toward a standard classification of geomagnetic activity from 1868 to 2009. Annales Geophysicae 30(2):421-426.

Vol. 16(1), pp. 10-36, January 2022
DOI: 10.5897/AJEST2020.2940
Article Number: 949B69668423
ISSN: 1996-0786

http://www.academicjournals.org/AJEST

ACADEMIC JOURNALS
expand your knowledge

African Journal of Environmental Science and Technology

Full Length Research Paper

Optimizing community participation in the management of Yala Wetland Ecosystem, Lake Victoria Basin, Kenya: The Yala Hub Framework

Douglas O. Odero* and Victor A. O. Odenyo

School of Environmental Studies, University of Eldoret Box 1125-30100, Eldoret /Retouch Africa International Limited, P. O. Box 69259-00622 Nairobi, Kenya.

Received 4 November, 2020; Accepted 28 January, 2021

Wetlands are particularly important environmental assets whose sustainability requires meaningful participation of the riparian communities in their management. Yala Wetland is an important resource whose key challenges involve land and water resource use for competing interests which prompted Siaya and Busia County regional Governments to initiate preparation, a Land Use Plan (LUP)/Strategic Environmental Assessment (SEA) to resolve these. A LUP/SEA Framework with Yala Project Advisory Committee (YPAC) for local communities guided the planning process and implementation. Concurrently, an action research was conducted to assess the level and effectiveness of Yala Wetland community participation in the SEA/LUP processes and improve the outcomes. Research data was derived from 410 respondents from 60 local community groups, 34 key informant interviews, 187 students and satellite images. The Spectrum of Public Participation Model revealed that wetland communities' participation was at lower levels (Inform (17%) and Consult (83%) while the measure of effectiveness on 10 indicators were poor (20%) and unsatisfactory (80%) thus not meaningful nor effective. Consequently, Yala Hub Framework was developed, occasioning significant improvements in the final LUP. The study concluded that effective community participation determines and influences effective implementation of decisions made and that increased participation through deliberate intervention will eventually increase the effectiveness of community development and encourage long-term sustainability.

Key words: Yala Hub Framework, community participation, strategic environmental assessment, land use planning, wetland.

INTRODUCTION

Wetlands are one of the world's most important environmental assets which provide homes for large, diverse biota as well as significant economic, social and cultural benefits related to timber, fisheries, hunting, recreational and tourist activities. Yala Wetland is an important resource shared by Siaya and Busia counties of Kenya. It supports the livelihoods of surrounding communities, including water, papyrus and fisheries,

*Corresponding author. E-mail: douglas.ouma7@gmail.com.

among others, and provides vital ecosystem services such as purification and storage of water. It also acts as a carbon sink, thus regulating global and local climatic conditions and is internationally recognized as a Key Biodiversity Area that hosts globally and nationally threatened bird, fish and mammal species. The wetland is also an important agricultural asset that has attracted both local farmers and external agricultural interests (EANHS, 2018).

Wetlands constitute an important resource for riparian communities and therefore it is important that they participate in their management. Community participation in natural resource management has evolved from the realization that people living with natural resources should be responsible for their management and benefit from using the resources (Ostrom, 1990; WWF, 2006; Bond, 2006; Lockie and Sonnenfeld, 2008; GoK, 2010a; Hardin, 1968; IUCN, 2009). The Aarhus Convention of 1998 states that citizens must not only have access to information but must also be entitled to participate in decision making and have access to justice in environmental matters (DETR, 2000; Stec et al., 2000). However, participation of local communities in seeking solutions to wetlands resources use remains a grave challenge as managers of participation processes engage in low level consultations that do not empower them to co-manage these resources alongside government agencies mandated to do so (GoK, 2010a; Springate-Baginski et al., 2009; Okello et al., 2009; Olson, 1965). Besides, the dynamics of communities' participation and their activities on the wetland are not clearly understood despite wetland's continued degradation in size and value (Dobiesz and Lester, 2009; Dugan, 1993).

The Papyrus Wetlands challenges and public participation

A synthesis of research and policy priorities for papyrus wetlands presented in Wetlands Conference in 2012 concluded that more research on the governance, institutional and socio-economic aspects of papyrus wetlands is needed to assist African governments in dealing with the challenges of conserving wetlands in the face of growing food security needs and climate change (van Dam et al., 2014). The other three priorities identified were the need for: better estimates of the area covered by papyrus wetlands as limited evidence suggest that the loss of papyrus wetlands is rapid in some areas; a better understanding and modelling of the regulating services of papyrus wetlands to support trade-off analysis and improve economic valuation; and, research on papyrus wetlands should include assessment of all ecosystem services so that trade-offs can be determined as the basis for sustainable management strategies ('wise use').

In Africa, wetlands degradation is on the increase as wetland ecosystems are relied upon to lessen industrial, urban and agricultural pollution and supply numerous services and resources (Nasongo et al., 2015; Kansiime et al., 2007). Similarly, lack of recognition of the traditional values of these wetlands, desire for modernisation and failure to appreciate their ecological role aggravate their degradation (Maclean et al*.,* 2003; Panayotou, 1994).

Public participation

Public participation has been the focus of many Environmental Impact Assessments (EIAs) and Strategic Impact Assessment (SEA) studies globally (Doelle and Sinclair, 2005; Hartley and Wood, 2005). This article defines public participation as the process of ensuring that those who have an interest or stake in a decision are involved in making that decision. The many ways that organizations interpret and use the term public participation can be resolved into a range of different types of participation. This range from passive participation, where people are told what is to happen and act out predetermined roles, to self-mobilisation, where people take initiatives largely independent of external institutions. Participation has become a key element in the discussion concerning development particularly in natural resources management (Cooke and Kothari, 2001). Today, the concept is seen as a magic bullet by development agencies who are making participation one, if not the core element of development (Michener, 1998).

According to the International Association of Public Participation (IAP2, 2008) public participation consists of five levels: Information (lowest level, where participation does not go beyond information provision), consultation, involvement, collaboration and empowerment (highest level, where the public are given a final say on the project decision.

Models and Types of Participation

Participation has been studied and different models offered to show the levels and challenges therein. The models include the ladder of citizen participation (Arnstein, 1969) which show the hierarchies of participation from non-participation, to tokenism and to citizen power with meaningful happening at the apex (citizen control); *the wheel* model with four levels namely inform, consult, participate and empower (Davidson, 1998); and the spectrum model with five levels from inform, consult, involve, collaborate and empower (Stuart, 2017; Gaventa, 2004) and citizen as partners with five levels from Information and transaction, consultation, deliberative involvement, government – led active participation and citizen-led active participation (OECD, 2001).

Table 1. Spectrum of public participation.

	Inform	**Consult**	**Involve**	**Collaborate**	**Empower**
	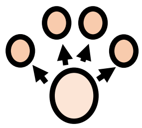	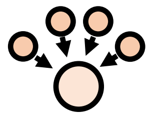	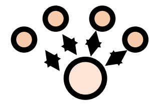	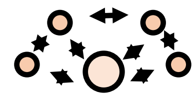	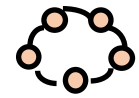
Goal	To provide balanced and objective information in a timely manner.	To obtain feedback on analysis, issues, alternatives and decisions.	To work with the public to make sure that concerns and aspirations are considered and understood.	To partner with the public in each aspect of the decision-making.	To place final decision making in the hands of the public.
Promise	“we will keep you informed”	“We will listen to and acknowledge your concerns”	“We will work with you to ensure your concerns and aspirations are directly reflected in the decisions made	“we will look to you for advice and innovations and incorporate this in decisions as much as possible”	“We will implement what you decide”

(Adapted from IAP2 Spectrum of public participation, Stuart, 2017)

Spectrum of public participation

The Spectrum of Public Participation was developed by the International Association of Public Participation (IAP2) to help clarify the role of the public (or community) in planning and decision-making, and how much influence the community has over planning or decision-making processes (Stuart, 2017; IAP2, 2008; Gaventa, 2004). It identifies five levels of public participation (or community engagement) from inform, consult, involve, collaborate and empower shown in Table 1.

The further to the right on the Spectrum, the more influence the community has over decisions, and each level can be appropriate depending on the context. It is important to recognize they are levels, not steps. For each level it articulates the public participation goal and the promise to the public. The first level the Inform level of public participation does not actually provide the opportunity for public participation at all, but rather provides the public with the information they need to understand the agency decision-making process. Some practitioners suggest that the Inform level should be placed across the Spectrum (e.g. above or below it) to demonstrate that “effective engagement with stakeholders at all levels on the Spectrum requires a strategic flow of information” (Chappell, 2016). Since Arnstein (1969) proposed a ladder of citizen participation, almost 50 years ago (ranging from manipulation and therapy, to delegated power and citizen control) there have been several attempts to classify levels of community engagement. The Spectrum of Public Participation is one of the best attempts so far (Stuart, 2017).This study therefore uses Spectrum of public participation to assess the level of community participation in Yala SEA/LUP processes.

White ’s (1996) work on the forms and functions of participation distinguish four forms of participation: nominal, instrumental, representative and transformative. She reasons that each form has different functions, and argues actors ‘at the top’ (more powerful) and ‘at the grass roots’ (less powerful) have different perceptions of and interests in each form. Nominal participation is often used by more powerful actors to give legitimacy to development plans. Instrumental participation sees community participation being used as a means towards a stated end – often the efficient use of the skills and knowledge of community members in project implementation. Representative participation involves giving community members a voice in the decision-making and implementation process of projects or policies that affect them. Transformative participation results in the empowerment of those involved, and as a result alter the structures and institutions that lead to marginalization and exclusion.

White’s work helps us to think about the politics of participation (hidden agendas and the dynamic relationships between more and less powerful actors). It is only in ‘transformative participation’ that the power holders are in solidarity with the less powerful to take actions and shape decisions. White emphasizes that this framework needs to be seen as something dynamic, and that a single intervention can include more than one form of participation. One type of participation may not in itself be ‘better’ than another. Different types of public participation are appropriate in different situations, with different objectives and with different stakeholders. Some stakeholders have a greater right to more control of the process than others, some have greater capacity to participate than others and some are quite happy to participate less in some decisions- allowing others such as representative organizations or politicians to take decisions for them.

Emerging lessons and good practices of public participation

From these six project areas carried out in Participation in Planning Water management options, European Union (EU) life environment wise use of flood plain project notes the following six early lessons as emerging on when to do participation (Harrison et al., 2001):

1. Scale: Participation exercises have taken place at a variety of scales with some areas involving communities to consider issues at river catchment level whilst others have broken down into sub catchments or even more local areas along the catchment. Catchment level discussions have generally taken place more with organizations than with individual members of the community.
2. Context: Always the degree to which participation has been successful in involving people, getting views, or even aiming at consensus, has depended greatly on issues of context. These include political contexts, employment contexts, issues contexts, such as flooding, water quality and on cultural contexts relating to a history or not of co-operation and participation.
3. Transferability: Many of the methods including mapping, surveys, timelines etc have been used in the WUF project areas and the experience has been valuable to test different techniques for different issues and with different stakeholders. Flexibility of using techniques is essential and so it is important to have a wide range of techniques. Techniques are transferable but need to be applied and adapted to local circumstances.
4. Training/ capacity/resources: Participation can be resource hungry though some areas have saved costs through using local networks and facilities. The main resource investment is usually time. Techniques for participation vary and the more complex ones need careful training and professional implementation.
5. Processes of participation – early involvement of communities in the decision making process has led to gradual decision making and planning and helped achieve consensus amongst stakeholders.
6. Partnership working – using local host organizations can not only save time and money but also help build up trust and ongoing relationships – especially in cross border situations if the host has a history of cross border working.

Effectiveness of public participation using emerging lessons and World Bank indicators

From the application of participatory approaches in various projects and subsequent emerging lessons and the World Bank public participation lessons (World Bank, 1998:2002, Harrison et al. 2001) some 10 indicators have been identified as key in evaluating public participation effectiveness namely:

1. Objectives – why do participation? what are the objectives – this is a vital reference point for evaluation.
2. Contexts for the participation – helps evaluation. Was participation, for example, part of a larger strategy. political contexts, economic.
3. Levels of Involvement – all to do with how early you involve people, how much power is handed over and when.
4. Who was involved, how chosen – mistakes made (by who?)
5. What methods were used, maps, interviews etc. – did they work?
6. Innovation –of method or just participation itself for the area
7. Commitment – to use or not?
8. Inputs – time, money etc. and results in relation to those inputs
9. Outputs, hard outputs, reports, posters, press, completed survey forms
10. Outcome – most important culmination of the evaluation.

The indicators point at different elements of public participation and this study will use the 10 indicators as well as spectrum of public participation to evaluate community participation framework of Yala Land Use Planning. The synergy of the two methods would help bring the best of each other as well as complement each where they have weaknesses. The World Bank's Internal Learning Group on Participatory Development conducted a study in 1994 to measure the benefits and costs of their participatory projects. A total of 42 participatory projects were analyzed and compared with equivalents. The principal benefits were found to be increased uptake of services; decreased operational costs; increased rate of return; and increased incomes of stakeholders. But it was also found that the absolute costs of participation were greater, though these were offset by benefits: the total staff time in the design phase (42 projects) was 10-15% more than non-participatory projects; and the total staff time for supervision was 60% more than non-participatory projects (loaded at front end). It is increasingly clear that if the process is sufficiently interactive, then benefits can arise both within local communities and for external agencies and their professional staff.

Okello et al. (2009) study on public participation in SEA in Kenya concludes that it was unsatisfactory. The study noted that Environmental Management and Coordination Act (EMCA) of 1999 and its 2015 amendment and Environmental Impact Assessment Audit Regulations 2003 (EIAAR) did not have provisions detailing consultation with the public during SEA and that knowledge and awareness of the public at all levels of society were found to be poor (EMCA, 2015). The undoings of public participation included information inaccessibility in terms of readability and physical access, inadequate awareness of the public on their roles and rights during EIA, incomprehensible language and incomplete regulation for public participation during SEA. Those undoings have to be overcome if public participation in Kenya is to be improved and moved to higher levels (that is, collaboration-empowerment) of participation on the spectrum of public participation level.

Therefore, this study uses cumulatively the 10 indicators to measure the effectiveness of community participation in Yala Wetland Land Use Planning. The synergy of the two methods (spectrum model and 10 Indicators) brought the best of each other as well as complemented each other where they had weaknesses. Thus, Yala Project Advisory Committee (YPAC) framework weaknesses were identified and consequently an addendum to the framework designed to optimize participation of Yala wetland communities in the then ongoing SEA/LUP processes called the Yala RAPPEF-CF-IR Hub framework simply called the Yala Hub Framework. The Yala RAPPEF-CF-IR-Hub is a 5- steps facilitative model used to optimize YPAC framework participation but was also deployed in Siaya County Integrated Development Planning (CIDP) with substantial success Odero, 2021.

Rationale for Effective Community Participation in Yala Wetland SEA and LUP

Yala Wetland is facing many challenges that revolve around land and water resource use for competing interests and also from catchment degradation (GOK, 2018; Odhengo et al., 2018a; Ondere, 2016; Odero, 2015a, 2015b; Muoria et al., 2015; van Heukelom, 2013; Raburu, 2012; Thenya and Ngecu, 2017; Onywere et al., 2011; GOK, 2010b; Kenya Wetland Forum, 2006; Lihanda et al., 2003; Otieno et al., 2001; GOK, 1987). Additionally, the weak frameworks for stakeholder participation especially the local communities in resources management created suspicion and tension among various interest groups in the wetland. These challenges pointed to the need for a well-considered LUP that would provide a rational and scientific basis for future development and use of the resource. This situation prompted and encouraged County Governments of Siaya and Busia, and Nature Kenya to initiate processes that culminated in the present effort to prepare a LUP that will help resolve these challenges so that Yala Wetland will be able to sustainably support local residents' livelihoods while its ecological integrity and that of its associated ecosystems is protected.

Preliminary processes implemented by Inter-ministerial Technical Committee (IMTC) and a Deltas Management Secretariat prepared a LUP Framework to guide the planning process and was agreed upon by stakeholders. The IMTC's responsibility is coordination, policy and planning processes of major deltas in Kenya. The Framework was as result of a participatory and collaborative process that involved various stakeholders at the local, county and national levels. As required by Kenya Constitution article 69(1) and part VIII section 87-92 and 115 of County Government Act, 2012 on devolution provisions, and part 2 section 6 (1-2) Public Participation Bill, 2020 provided for participation of local communities in the Yala SEA and LUP process through a Yala Project Advisory Committee (YPAC) (GOK, 2010; GOK, 2012a, b, c and d, GOK,2020).

This paper seeks to first, determine the level of community participation in the ongoing SEA and LUP processes; second; to determine the effectiveness of community participation in the ongoing Yala Wetland SEA and LUP processes; and, consequently, to develop a framework for optimizing community participation in the ongoing Yala Wetland SEA and LUP processes and Yala Wetland ecosystem management.

MATERIALS AND METHODS

The Yala Wetland Area

Yala Wetland is located on the North eastern shoreline of Lake Victoria between 33° 50' E to 34° 25'E longitudes to 0° 7'S to 0° 10'N latitude (Figure 1), and is situated on the deltaic sediments of the confluence of both Nzoia and Yala Rivers where they enter the north-eastern corner of Lake Victoria. It is highly valued by local communities (NEMA, 2016). Yala Wetland is Kenya's third largest wetland after Lorian Swamp and Tana Delta and has a very delicate ecosystem. It is shared between Siaya and Busia counties of Kenya and covers an area of about 20,756 ha (about 207 Km^2) (JICA, 1987; LBDA, 1989; Odhengo et al., 2018b).

Yala Wetland and its environment have a high population density (KNBS, 2009). The Siaya County side had human population density estimated at 393 per Km^2 in 2009 while Busia County had a higher concentration of up to 527 persons per Km^2 (KNBS, 2009). Based on the 2019 National Census Results, the population of Siaya and Busia Counties were 743,946 with a growth rate of 1.7% and 833,760 with a growth rate of 3.1% respectively. The population of the planning area (wetland and its buffer of 5km radius) was estimated at 130,838 in 2014 and was projected to be 171,736 in 2030 and 241,280 in 2050 (KNBS, 2009). The mean household size was 5.05, although population density in the wetland and adjacent areas were not uniform. High population concentrations were found in the Busia County side around the banks of Nzoia River and to the South in Siaya County side around Usenge town and north of Lake Kanyaboli (KNBS, 2009). The study focused on the communities inside and within 5km from the wetland boundaries because their propensity to use the wetland is inversely related to travel distance (Abila, 2002). The study also extended to communities living in the upper Yala cluster (lower catchment of river Yala) whose activities affect the Yala Wetland water flow and quality (IWMI, 2014).

Environmental livelihoods of the wetland communities

Yala Wetland has diverse scenic sites that attract visitors from Kenya and beyond. Such attractions include Ramogi Hills, sandy beaches of Usenge, sand dunes around Osieko beach, Oxbow

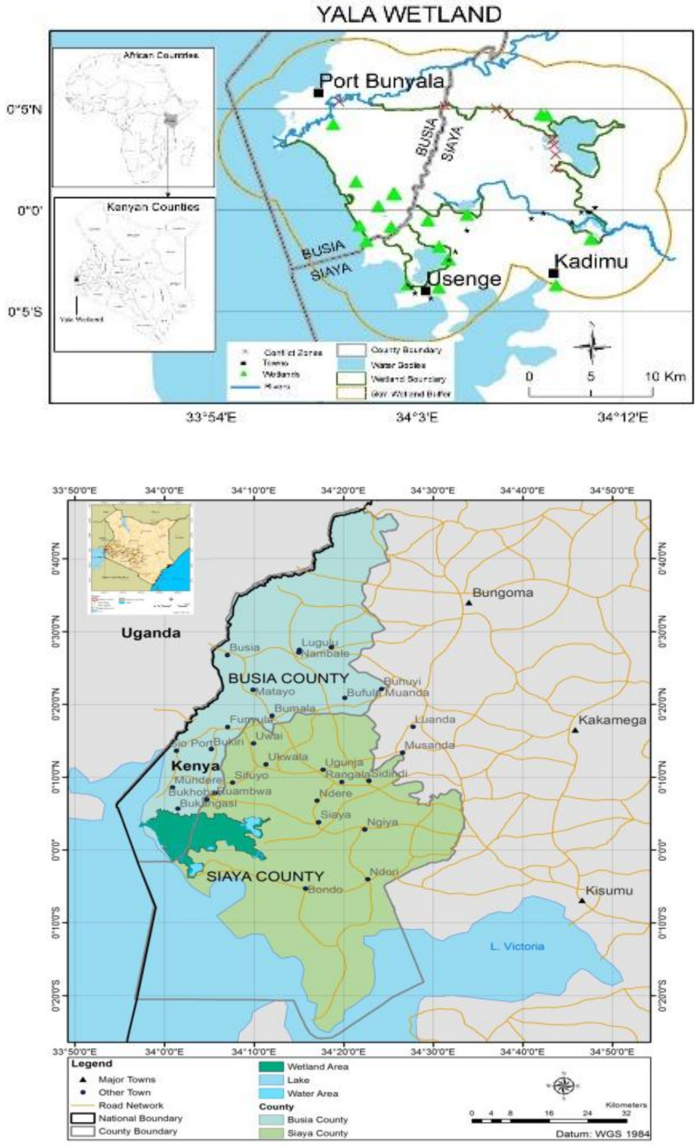

Figure 1. Location of Yala Wetland in Lake Victoria Basin.
Source a: Author; Source b: Simonit and Perrings (2011).

lakes, migratory birds, and endangered wildlife species among others. Potential tourist attractions in the Yala Wetland include the scenic appeal, bird watching, wildlife viewing, sport fishing, boat riding, outdoor sports and several cultural and traditional ceremonies. However, tourism potential for the area is largely unexploited and poorly developed in the area at present. Muoria et al (2015) estimated that visitors to Yala Swamp contribute Kshs 1,170,200 (USD$1,170.2) annually to the local economy. This is a very low value compared to the estimated potential of Kshs 499,912,500 (USD$ 499,912.5) estimated by Kabubo-Mariara et al (Unpublished data**)** who used the willingness to pay method (Yala Wetland ICCA, 2020).

Cultural diversity

The communities of Yala Wetland have diverse cultural practices and beliefs, some of which can be exploited for tourism and for conservation. Local communities have strong attachments to the wetland because of their social, cultural and spiritual importance. Some religious or spiritual purposes include baptism, traditional passage rites and ceremonies appeasing evil spirits, cleansing, as shrines etc. The communities also promote indigenous knowledge and practices on environmental functions and values that are essential for their survival such as the use of medicinal herbs. Some villages in the wetland are taken as custodian of clan spirits hence the residents consider it their duty to protect the graves and shrines of their departed clan members (Odero, 2021). However, there is lack of sound documentation and uptake of indigenous knowledge in biodiversity conservation.

Scientific and educational values

The Yala Wetland has immense potential for scientific research, formal and informal education, and training values. The wetland ecosystem is ideal for excursions and fieldwork for learning institutions. The wetland can also serve as important reference areas for monitoring environmental vulnerability such as floods, drought and climate change.

Carbon sequestration

Yala Wetland is among the most effective ecosystems for carbon storage. The Yala wetland vegetation takes up carbon from the atmosphere and converts it into plant biomass during the process of photosynthesis. The Yala wetland therefore is a giant 'sink' which is recovering the greenhouse gas, carbon dioxide, from the atmosphere. In many wetlands, waterlogged soil conditions prevent decomposition of the plant material thereby retaining carbon in the form of un-decomposed organic matter (Peat). The long retention of carbon in wetlands prevents excessive amounts of atmospheric carbon, thereby reducing global warming. The retained carbon is easily released into the atmosphere wherever peat lands are drained and exposed to fires. A detailed study of carbon storage in the Yala Wetlands was performed in 2015/2016 (Muoria et al., 2015) and confirmed that the present wetland is storing close to 15 million tonnes of carbon within the papyrus swamp, with less than 1 million tonnes stored in the remaining areas (reclaimed farmland and immature papyrus). This study further revealed that natural and semi-natural papyrus dominated habitats is better carbon sinks than drained farmed areas.

Biodiversity

The Yala Wetland, which is the largest papyrus swamp in the Kenyan portion of Lake Victoria, is an exceptionally rich and diverse ecosystem, containing many rare, vulnerable and endangered species of plants and animals (EANHS, 2018). The wetland is almost entirely covered in stands of papyrus.

Over 30 mammal species have been recorded in the Wetland. They include the Sitatunga (*Tragecephalus spekeii*), a shy and rare semi-aquatic antelope that is nationally listed as Endangered (Thomas et al., 2016; Wildlife Act, 2013; KWS, 2010). The Wetland provides an important refuge for Lake Victoria cichlid fish, many of which have been exterminated in the main lake by the introduction of the non-native predatory fish, Nile Perch *(Lates niloticus)*. Recent surveys in Lake Kanyaboli recorded 19 fish species within nine families, which included all the two critically endangered cichlids species: *Oreochromis esculentus* and *Oreochromis variabilis* (IUCN, 2018; KWS, 2010; Ogutu, 1987a; Ogutu, 1987b). The fishes use the wetland as a breeding ground, nursery, and feeding grounds (Aloo, 2003).

The Yala Wetland climate has a variable rainfall pattern that generally increases from the lake shore to the hinterland (Ekirapa and Kinyanjui, 1987; Awange et al., 2008). The mean annual rainfall ranges from 1050-1160 mm and is bimodal. The mean annual daily maximum and minimum temperatures are 28.9 and 15.9°C respectively – giving a mean annual temperature of 24.4°C (Luedeling, 2011; Semenov, 2008).

The hydrological conditions within the Yala Wetland are characterized by five main water sources namely: inflows from the Yala River, seepage from River Nzoia, flooding from both rivers, backflow from Lake Victoria, local rainfall and lakes within Yala Wetland (Okungu and Sangale, 2003). River Yala is the main source of water for the wetland and other satellite lakes. The naturalized mean monthly discharge is 41.1 m^3/s. The lowest flows barely fall under 5m^3 /s in the months of January to March while the highest discharge of 300 m^3/s occur in the months of April/May and August/ September. The minimum suspended silt load of River Yala Water is 543 ppm (BirdLife, 2018; Sangale et al., 2012; Okungu and Sangale, 2003).

Originally, the Yala River flowed through the eastern wetland (now 'reclaimed') into Lake Kanyaboli, then into the main wetland, and finally into Lake Victoria via a small gulf. The Yala flow is now diverted directly into the main wetland, and a silt-clay dike cuts off Lake Kanyaboli, which receives its water from the surrounding catchment and through back-seepage from the wetland. A culvert across the confluence of the Yala, some metres above the level of Lake Victoria, has cut off the gulf on the lake and, through back-flooding, created Lake Sare (BirdLife, 2018; Gichuki et al., 2005). This river flows on a very shallow gradient through small wetlands and saturated ground over its last 30 km before entering Lake Victoria through its own delta. The soils in this region have a very high clay content which impedes ground water flow but there is known to be a gradual movement of seepage water into the northern fringes of the Wetland. Flooding occurs annually and the very high discharge rates mean that the river channels are overtopped with floodwater passing into Yala Wetland. Parts of the western wetland lie below the level of Lake Victoria and are constantly filled with backflow in addition to being subjected to flooding from the lake and upper catchment. Annual rainfall in Lake Victoria Basin (LVB) encompasses a bimodal pattern. The Yala/ Nzoia catchment has high precipitation in the Northern highland (1,800-2,000 mm per annum) and low in the South-Western lowlands (800-1,600 mm per annum). Local rainfall contributes to Yala Wetland water. The water balance for Yala Wetland also includes the water retained within the three freshwater lakes found within the wetland: Kanyaboli (10.5 km^2), Sare (5 km^2) and Namboyo (1 km^2). Lake Kanyaboli has a catchment area of 175 km^2 and a mean depth of 3 metres. Lake Sare is an average of 5 m deep and Lake Namboyo has a depth of between 10 to 15 m (NEMA, 2016; Owiyo et al., 2014; Dominion Farms, 2003; Envertek Africa Consult Limited, 2015).

Action research design

Given the nature of the Yala wetland "wicked problems", action research was the best methodology to unravel participation issues therein. Action research methodologies would assist the "actor" in improving and/or refining his or her actions (Stringer, 1999; Mills, 2000). Also, it seeks transformative change through the simultaneous process of taking action and doing research, which are linked together by critical reflection (Lewin, 1946; Johnson, 1976). Thus, action research is problem centered, client centered, and action oriented. It involves the client system in a diagnostic, active-learning, problem-finding and problem-solving process. The research was done under the regulations and guidance of School of Environmental Studies who subjected the study through its internal review processes and enriched the final outcome-The Yala Hub Framework. The study permit was obtained from the Kenya National Commission for Science, Technology and Innovation.

Sampling and data collection

The study used non- random purposive and stratified sampling to collect data. A total of 410 respondents from 60 local community groups participated in focus group discussions (FGDs) from the swamp and adjacent buffer zones (Table 2). The target organizations that were actively involved in wetland conservation within the last five years; have been affected in one way of the other with projects within Yala Wetland, have been a member of an interest group during a LUP/SEA studies in Yala Wetland, have been involved in research and training in in Environmental conservation, EIA or SEA. The community organizations included beach management units (BMUs), Environmental Conservation groups (Yala Swamp conservancy organization, Environmental volunteers), women groups (Nyiego,), youth groups (Hawinga Boda

Table 2. Breakdown of community members who took part in the study.

Gender	Number	Over 35 years	Youths (under 35years)	Person with disability
Male	223 (54.3 %)	116 (52.0 %)	106 (47.5%)	1 (0.5 %))
Female	187 (45.6 %)	96 (51.3 %)	91 (48.7 %)	
Total	410	212(51.7%)	197(48.1%)	1(0.2%)

Source: Author

Boda, smallholder farmer's cooperatives, Weavers Umbrella group, Lake Kanyaboli Nurseries, religious leaders' associations, sand harvesters, Yala Swamp Site Support (YSSG), YPAC members.

The 60 community organizations were drawn from all the sublocations/ wards of Yala wetland and buffer zones. Each community organization had only one group of 10 persons participating in FGD irrespective of the total membership. The community organizations membership ranged between 8-60 persons with mixed economic abilities but drawn by the mission and ideals of the specific group. The age of members ranged between 15-85 years while the youngest organizations were five years while the oldest was 30 years old. The 10 respondents invited to participate in the FDGs were chosen to represent diversity within the group and the FGDs were held in convenient locations for local communities. The respondents were mainly group members, active and retired civil servants, teachers, retired teachers, respectable elders who were deemed as custodian of communities' information and religious leaders.

The FGDs are very advantageous, as Natasha et al. (2005) maintain since they allow collecting substantial data from many people within a very short period. The structure of these FGDs was kept to a minimum, allowing feelings and characterizations to emerge from the participants themselves (Dawson et al., 1993; Krueger and Casey, 2009) on background information about the wetland, their opinions, ideas, perceptions, and beliefs and experiences that influenced their interactions in the wetland and their involvement in its management over the years (Likert,1932). Data were recorded both by written notes and video recordings.

Key informant interviews with 34 highly respected elders and change makers from Usenge, Usigu, Kombo, Hawinga, Uhembo, Bunyala were conducted between April and June 2016. The elders were considered by communities as custodians of the Yala Wetland historical, cultural and indigenous knowledge information. Information received was corroborated with other literature on Yala Wetland to provide historical and contextual information. These informants included deputy chairperson of the Luo Council of Elders from Yimbo, an elder who had also established a Yala community museum in Kombo beach at the shores of Lake Kanyaboli; an elder from Misori Kaugagi; an elder and a youth from Bunyala islands. They narrated the history of the wetland, significant events and trends and their implications. These interviews were video recorded and later used for analysis of the research data and the identity of respondents is concealed in the findings. At the end of each interview session and end of the day the researcher set aside time to record research activities for the day, his observations and experiences for the day and critical reflection in the researcher's journal (Deveskog, 2013; Greene, 1995; Leggio, 1995). Leggio (1995) in her PhD dissertation titled *Magic* wand notes: In the last decade, I made some major transitions in my life and the process of writing has helped me think through some of the decisions involved. Writing is a powerful way to create one's life as well as to record and reflect on it (p.82.).

Data were also collected from 187 students who participated through essays writing, debates, poems and artistic works on the Yala Wetland issues and were rewarded for outstanding performance as shown in Plate 1. These were drawn from primary (12), secondary (5) and post- secondary polytechnics and colleges (2) in Yala wetland and its buffer zone. The data were part of what the modified community participation Yala community participation framework brought to the SEA/LUP processes. The qualitative data require triangulation and the data from the learning institutions helped with triangulation as well as bringing students' perspectives to the study.

Sample size determination for this research was based on judgment with respect to the quality of information desired and the respondents' availability that fit the selection criteria of active involvement in Yala swamp conservation activities (Sandelowski, 1995). According to Neuman (1997) it is acceptable to use judgment in non-random purposive sampling and reiterates that there is no 'magic number'. Thus, the 410 community respondents, 34 key informants and 187 students were representative of the wetland communities who were actively involved its management (Figure 2).

Data analysis

Qualitative data were analyzed in using content analysis methods. Content analysis technique allowed the researcher to categorize and code the collected information based on participants' responses to each question or major themes that emerged from FGDs, in-depth interviews, essays, debates and artworks. Content analysis as Babbie (2015) argues is useful since it captures well the content of communications generated through interviews, essays and FGDs in an inductive manner, where themes were generated based on emerging similarities of expression in the data material. Many of these elements provided quotations in the write-up of research findings and other similar elements were quantified using descriptive statistics to give a sense of the emerging themes and their relative importance according to the respondents. Priority ranking of issues was done to arrive at overall prioritization of issues by wetland communities that informed the final LUP content. The study dealt more with people's perception than with statistically quantifiable outputs. Thus, data analysis to gauge these perceptions was done by calculating percentage response (Neuman, 1997). The response rates were calculated using the following formula.

$$Response(\%) = {}^{x}/_{y} * 100$$

Where x: respondent groups who gave feedback and y total number of respondent groups. To grade the percentage response, a modification of Lee's (2000) EIA study review package was used (Table 3).

Schools essays, debates and artwork analysis

A select team of panelists that adjudicated the learning institutions entries comprised the Researcher, one Research Supervisor from

Plate 1. Yala SSG Chairperson (right) presents a certificate of merit to a pupil of Nyakado Primary School for emerging as the best in an essay writing competition on children's dream/vision for Yala swamp in the school. The Head teacher and researcher overseeing the award ceremony.

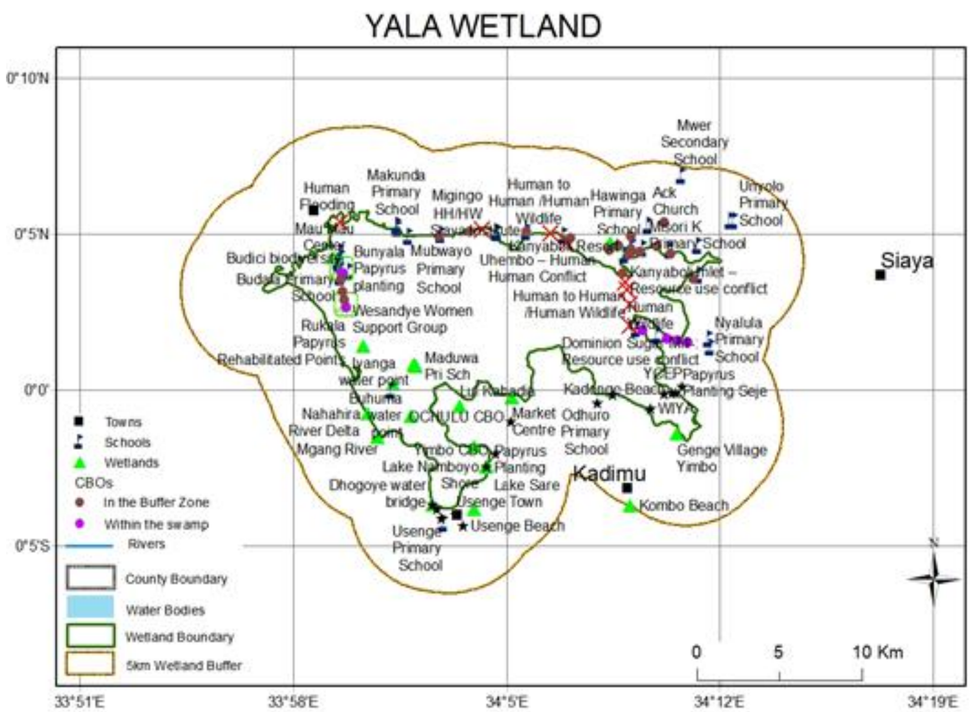

Figure 2. The geolocations of Community Organizations and Schools in the Yala Wetland Ecosystem mapped during the study.
Source: Author

SES, Program Manager from Nature Kenya), Research Assistant from SES and Siaya County Director of Education. Each panelist marked the 187 essays and art works, guided by the following parameters: background information, context, creativity, vision and

Table 3. Grading of responses.

	Grade (%)	Rank
1	1-16	Very poor
2	17-33	Poor
3	34-50	Unsatisfactory
4	51-67	Satisfactory
5	68-83	Good
6	84-100	Excellent

dream all seen as identification of appropriate key challenges of the Yala Wetland and prescription of potential solutions that address the identified challenges with the potential highest score being forty marks. These parameters were based on the issues that SEA and LUP were investigating to inform the development of Yala Wetland LUP and ecosystem management starting with the vision of Yala LUP, understanding the contextual and historical information about the wetland and finally key environmental issues and what actions are required to ensure sustainable management of the Yala ecosystem. Table 4 shows the adjudication criteria for students' submissions.

The individual panelist scores were recorded and the average score tabulated to arrive at the overall score for the entries. The top 3 students from every school were awarded prizes as well as participating institutions. The essays school entries were further analyzed using content analysis to itemize environmental issues, desired future and strategies for attaining that future for inclusion in the final SEA and LUP outcomes. Satellite images from Google Earth provided detailed photographic evidence of the condition of Yala Wetland and its various land use changes over years. These satellite images also helped to determine the current size of the wetland in line with revised definition of the wetland in EMCA 2015. Satellite images and GIS analysis were used variously to determine land cover/land use changes (EMCA, 2015; Turner, 1998; Liverman et al., 1998; Chambers, 2006; Ampofo et al., 2015; Lillesand and Kiefer, 1987).

Literature review was conducted on public participation, policies, laws and relevant studies that provided secondary data and a valuable source of additional information for triangulation of data generated by other means during the research and this has also been used by many researchers (Friis-Hansen and Duveskog, 2012; IYSLP, 2017).

Overall, a multidisciplinary research using case study design employed exploratory action research with both qualitative and quantitative methods of data collection and analysis. Appreciative Inquiry (AI) methodology and participatory approaches and secondary data were used in data collection and analysis (Dweck, 2008; Cooperrider and Leslie, 2006). The secondary data include policy and legal frameworks, wetland ecosystem management guidelines and procedures, relevant studies to Yala wetland and other sensitive ecosystems elsewhere. This qualitative research was supported by quantitative methods on how contextual factors and processes affected the planning and management of Yala wetland ecosystem. Corbin and Strauss (1990) noted that quantitative and qualitative methods are tools that complement each other, while Greene (1995) in her doctoral research demonstrated the value of journaling as research methodology for in-depth reflection by the researcher and vital in action research designs. Greene (1995) says "learning to write is a matter of learning to shatter the silences, of making meaning, of learning to learn" (p.108).

The Yala project advisory committee

YPAC was the main mechanism for representing the communities of the Yala Wetland in the Yala LUP whose role was to discuss the findings of the SEA and LUP processes and content and obtain views from the wetland communities. The YPAC members were tasked to guide and instruct their own communities on the role and purpose of the LUP and SEA; to provide effective communication vertically and horizontally; to minimize misinformation and were collectively responsible for common good.

YPAC consisted of 46 members drawn from local communities and reported to the Inter-County Technical Committee (ICTC). The YPAC organ represented various interests namely ecotourism, cultural groupings/heritage; conservation; religion; islanders; fisherman; hunters; persons with disability, transporters; handicraft; farmers; investors; wildlife (honorary warden); county technical officers (lands, livestock, water, fisheries, crops, forests); sand harvesters; the youth; administration (ward, sub-county); and voluntary scout.The National Government and the County Government officers participated in YPAC meetings as observers and adjudicated on any internal disagreements.

RESULTS

Assessment of Yala Project Advisory Committee (YPAC) Framework

During the period of LUP development, YPAC held over six meetings. The main challenge of YPAC's members was how to report back the deliberations and seek inputs from a large number of their constituencies (e.g. some over 200 persons). As a result of logistical constraints, they presented their own views and received inputs from only those around them. This offered limited local community participation. Similarly, they were unable to seek broader view of their representation to enrich YPAC meetings and feedback to draft SEA and LUP reports thereby limiting the quality of community participation in SEA and LUP development. Thus, YPAC framework membership was narrow with respect to representation and quality given the entire spatial area of wetland and its buffer zone. Additionally, the YPAC members had inadequate logistics and skills required to undertake their roles and responsibilities.

Assessing the level of community participation in SEA/LUP process using spectrum of public participation model

The level of community participation in SEA/LUP using Spectrum of Public Participation Model was at low levels (draft 1 SEA/LUP "Inform (17%) and Consult (83%) levels. But, the application of the Yala Community Participation framework (The Yala Hub Framework) significantly improved community participation (draft 2 SEA/LUP Consult (50%) and Involve (50%)" and draft 3 SEA/LUP at (Involve level (80%) and Collaboration level (20%). Figure 3 show the levels of communities'

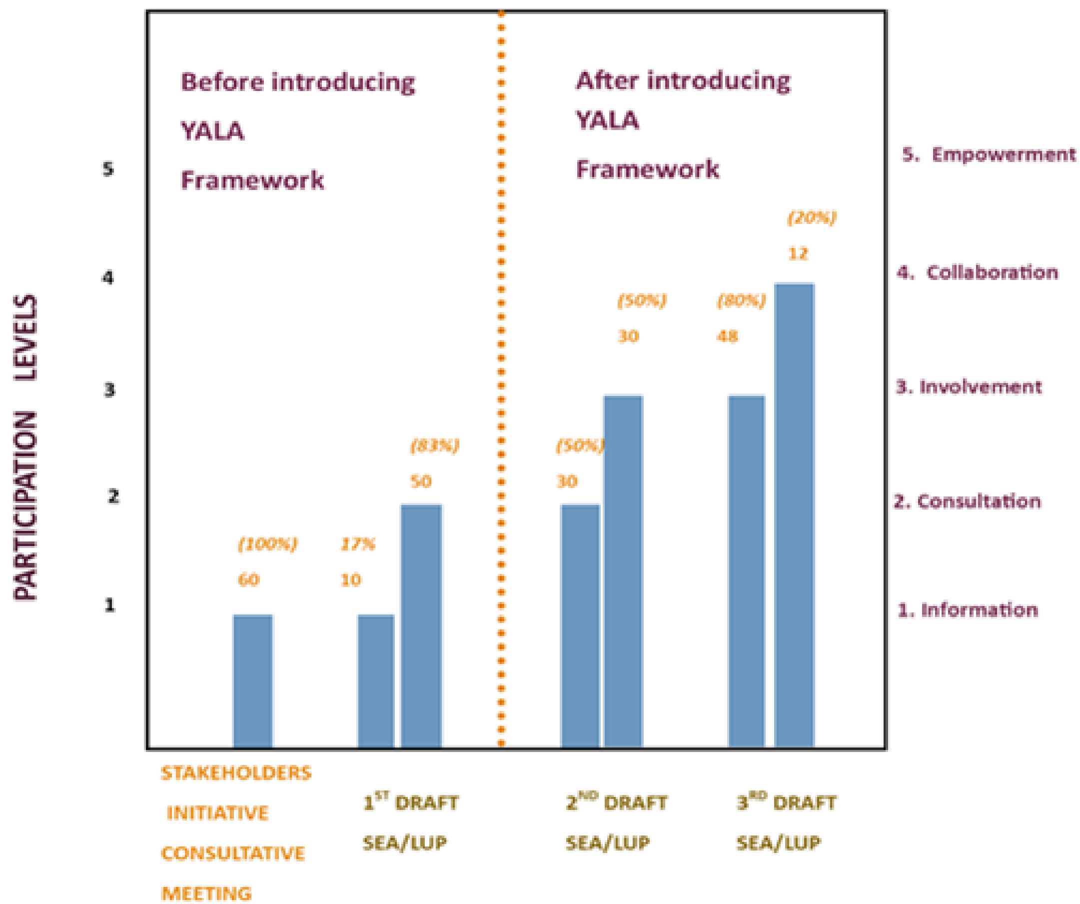

Figure 3. Level of communities' participation in SEA/LUP activities using spectrum of public participation model.

involvement in various SEA/LUP processes and various drafts of the plan.

DISCUSSION

With application of Yala Community participation framework in the existing YPAC framework with its identified weaknesses, the wetland communities felt that the process ensured their concerns and aspirations were therefore directly reflected in SEA and LUP and that together with the Government they would implement the resultant LUP recommendations.

Thus, the Yala Hub Framework was an optimizer for community participation in the LUP development that understood the Yala wetland context to enhance their participation. This finding is supported by best practices in public participation that noted the need to overcome personal and institutional barriers to public participation, understanding context (political contexts, employment contexts, issues contexts, such as flooding and on cultural contexts relating to a history of co-operation and participation (Harrison et al, 2001,GOK, 2020).

Assessing effectiveness of communities' participation in SEA/LUP processes using 10 indicators for public participation

The Community participation in SEA/LUP processes were evaluated for effectiveness using the 10 Indicators for public participation effectiveness. The results of effectiveness with the original YPAC participation framework and the results after the application of the Yala Hub framework. The results reveal communities' participation effectiveness in SEA/LUP was poor (2 indicators) and unsatisfactory (8 indicators) with YPAC. However, with the application of Yala Hub framework, the effectiveness moved to satisfactory (3 indicators) and good (7 indicators) as shown in Figure 4. The results also show that YPAC framework was poor in levels of involvement of people (30%) and commitment to community participation (30%).The overall score on YPAC effectiveness was 41% (unsatisfactory) but this moved 68% (good) with the application of Yala Hub framework. There was a shift in all 10 indicators with introduction of the Yala Hub framework towards greater satisfaction. Thus, Yala Hub Framework enhanced

PARAMETER	SCORE 1-10 1-lowest and 10 highest level of effectiveness before Yala modified Framework *(average score from the FGDs)*	GRADING	SCORE 1-10 1-lowest and 10 highest level of effectiveness After Yala modified Framework *(average score from the FGDs)*	GRADING
Objective of participation	5/10 *(50%)*		7/10 *(70%)*	
Contexts for the participation	4/10 *(40%)*		7/10 *(70%)*	
Levels of involvement	3/10 *(30%)*		6/10 *(60%)*	
People involved- Who was involved?	5/10 *(50%)*		8/10 *(80%)*	
Methods used	4/10 *(40%)*		7/10 *(70%)*	
Commitment	3/10 *(30%)*		6/10 *(60%)*	
Inputs	4/10 *(40%)*		7/10 *(70%)*	
Innovation	4/10 *(40%)*		6/10 *(60%)*	
Outputs	4/10 *(40%)*		7/10 *(70%)*	
Outcome	5/10 *(50%)*		8/10 *(80%)*	

KEY

VERY POOR	(1-16%)	SATISFACTORY	(51-67%)
POOR	(17-33%)	GOOD	(68-100%)
UNSATISFACTORY	(34-50%)		

Figure 4. Effectiveness of YPAC and Yala Hub Frameworks.

effectiveness of the Yala wetland community participation in SEA and LUP processes and outcomes.

This is further confirmed with spectrum of participation at inform and consult levels in draft 1 SEA and LUP reports. Yet, early people involvement and commitment are key to the outcome of the participation process. These weaknesses had to be rectified very urgently if the process was to achieve desired outcome with the communities' meaningful participation. Thus, another mechanism to specifically deal with these weaknesses was required thus paving way for the improved Yala Community Participation framework. This result shows that community participation in LUP and SEA processes is 'alive' process that requires constant checking and modification to respond to the emerging issues on the content of the plan and the community involvement processes in the plan development.

The assessment level of community participation using Spectrum of Public Participation Model and the effectiveness using 10 Indicators of Public Participation show that YPAC framework was poor and unsatisfactory in providing meaningful participation for communities in the development of Yala wetland land use and ecosystem management plan. Likewise, the analysis revealed the need to use different models which triangulate the information but also complement each other for any model's inherent weakness. Thus, a combination of Spectrum of Public Participation Model and 10 Indicators of Public Participation effectiveness was good for Yala wetland ecosystem management context. The areas of underperformance based on these assessments are the basis for an improved community participation framework presented in below.

The Limitations and challenges of YPAC Framework- the rationale for designing an addendum mechanism to Optimize Community Participation

The results revealed strengths and challenges of the YPAC participation framework which needed to be addressed to ensure effective community participation in Yala LUP. The limitations and challenges of YPAC included narrow YPAC membership, quality of participation concerns by YPAC members (capacity issues); inadequate points of community participation 6

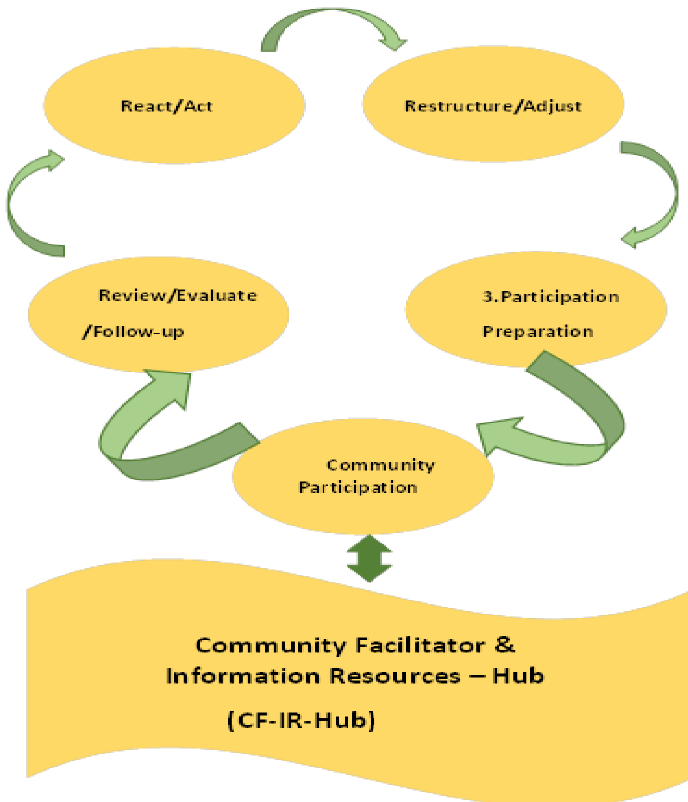

Figure 5. The YALA RAPPEF-CF-IR-HUB framework for Optimizing Community Participation in Yala LUP.

out of 11 steps in LUP process (2, 4, 5, 7, 9 and 10); low level of community involvement (spectrum levels); unsatisfactory participation (10 indicators evaluation results); challenge of communicating scientific and technical information to communities; dominant fixed and negative mindsets about the wetland; lack of methodology for integration of indigenous knowledge with scientific information; disconnect between the wetland decision making and provision of adequate scientific and technical evidence/or information; absence of governance framework with communities strong representation; lack of transformational and value driven leadership at the community level, and absence of comprehensive wetland wide information system (rather ad hoc and scattered pieces of data and information). These 12 limitations as an outcome of the analysis of SEA and LUP processes compromised the ability of YPAC to represent wetland communities meaningfully and effectively in SEA/LUP process, thus the basis for designing framework to optimize the given framework.

The Yala RAPPEF-CF-IR-Hub framework (The Yala Hub framework)

This is a framework designed to optimize community participation in Yala Wetland planning and ecosystem management. The framework sought to remedy the weaknesses of the original YPAC mechanism as well as tap opportunities presented as an outcome of the action research. The framework is called Yala RAPPEF-CF-IR Hub Framework based on the various steps on using it and shall be referred to in short form as the Yala Hub Community Framework. The five steps are 1. React/Act. 2. Restructure/Adjust the participation framework based on the reactions. 3. Participation Preparations. 4. Community Participation and 5: Review, Evaluate and Follow-up and these are supported by a base of a Community Facilitator (CF) with a supportive Information Resources Hub (IR-Hub) to support its execution as presented in Figure 5. The details of how this framework works are discussed subsequently.

Step 1: React/Act.

The first thing is to gain entry to participate in the process with a high degree of acceptance if the process is already ongoing. The intervener has to find appropriate entry point which depends on the context and how the facilitator positions self (e.g. researcher with their interest at heart, their own representative with technical expertise in the process, known conservationist of good reputation with community) and also application of emotional intelligence to penetrate the ongoing process (e.g. understand their areas of greatest need to participate in the process).

If the process is starting, then conduct stakeholder analysis to check on representation particularly of the local wetland communities. If it is in progress then conduct stakeholder analysis tier two, which reviews existing stakeholders and their level of participation, and special preference for local communities. The key guiding question is how effective the processes in representing the local communities (their interests, sharing wetland accrued benefits).

The guiding questions for this step are:

1. What does this community regard highly that can lead to high degree of acceptance of an outsider/ a facilitator?
2. Who is participating in this process? Who is missing on the decision-making table? Which other important voices are not being heard on this planning agenda? Are the divergent voices included in this process? Does participation ensure fair geographic representation? The process facilitator should identify these and ensure their inclusion.
3. What are the strengths and challenges of the existing community participation framework currently being implemented? In the three phases baseline, scenario building and alternative land use options and preparation of final plan; the 11-steps SEA/LUP processes and on spectrum of public participation (informing, consulting, involving, collaborating to empowering levels).
4. Using the 10 indicators for public participation effectiveness, what are strengths and weaknesses of the current community participation framework in the SEA and LUP processes? How do you ensure the weaknesses are mitigated going forward? The 10 indicators are Objective of participation; Contexts for the participation; Levels of Involvement; Who was involved**,** how were they chosen and by who? What methods were used (maps, interviews), if they did, they work? Innovation of the methods used; Commitment to community participation; Inputs (time, money etc. and results in relation to those inputs); Outputs (hard outputs, reports, posters, press, completed survey forms); and Outcome**.**

Step 2: Restructure/adjust the participation framework based on the feedback step

The outcome of step one forms the basis for adjustment and restructuring at this stage. In the SEA and LUP processes the researcher adjusted the participation process by bringing to the decision-making table very important stakeholders who were not initially left out. It expanded the representation of local communities to include community formations/organizations and learning institutions at their bases in addition to YPAC. Both preparations and actual implementation methodologies were modified, and new ones added based on step one feedback. If the project or program is new, then it moves from step 1 to step 3 bypassing step 2.

Guiding questions were:

1. Who needs to be added to the participation processes? What uniqueness do they bring on board?
2. How can one ensure meaningful participation from the people joining an ongoing process (i.e. language, facilitation, logistics and associated costs) without feeling they are joining the process late?
3. How are the elements that were hampering community participation effectiveness being tackled in the adjusted mechanism?
4. How can one use participatory methodologies (like empathy walks) to improve participation?
5. What should one do to improve the environment for participation and harness creativity?

Step 3: Participation preparations

The third step called for thorough preparation before the actual participation. Consequently, this step evaluated participation readiness and ensured the process was ready by addressing identified concerns/feedback; identifying facilitator(s) and equipping them to manage the process effectively; practical training on facilitation skills including mock training amongst facilitators; enabling logistical support, and framing issues for discussion with the identified stakeholders in step one using appreciative lenses focusing on root causes and suggesting the possibilities of tackling them.
The guiding questions for this step were:

1. What is the community participation process in this activity? Does the process provide local communities with room to articulate their interests and concerns?
2. What are the units of participation? What is the smallest unit for participation in this case? How are they organized to enable smooth flow of information and receive timely feedback?
3. What type of persons will be required to facilitate this participation process?
4. What type of skills and training are required to equip facilitators of this process?
5. What logistical support and budget will be required to conduct this participation?
6. How does one frame issues for effective discussion with the identified stakeholders in step 1 above?
7. Which participatory methodologies (including empathy walk) and how will one use these in community

participation processes?
8. What creativity and innovations will one bring to this community participation process?

Step 4: Community participation

This step is where the wetland communities interact with the planning processes and relay the feedback to the main LUP technical team. Various methods are used for these interactions which enable the communities to express themselves holistically. For example, by empathy walks; consulting in communities' local languages; artistic works where talented community members express themselves; and cultural artifacts to express themselves. The CF manages the community participation processes using various participatory methodologies and resolves any participation challenges to ensure maximum interaction of communities in the planning process and relaying critical feedback to the technical team and other planning organs outside the formal consultation sessions.

The guiding questions were:

1. How does one conduct community consultations that will allow participation of the new groups to smoothly integrate with other existing teams?
2. Summarize the key issues about (SEA/LUP) process to date? What are the areas of convergence? What are the areas of disagreement? What other concerns about Yala wetland do the wetland communities have?
3. What participation tools are appropriate for the targeted community and why?
4. How are the processes outcomes documented, validated by the communities and relayed to the LUP technical team for inclusion?
5. What do the wetland communities' value most about the wetland and why? What are the communities' non-negotiable on the wetland ecosystem resources?
6. Identify sites of environmental significance and conduct empathy walk with communities to pool out their issues /feelings on those sites?
7. Immerse oneself in the community to experience their issues and ensure that the participation process brings out what one has experienced even if not comfortable to talk about?

Step 5: Review, evaluate and follow-up: Participants feedback about participation processes

At this stage stakeholders evaluate the participation processes and outcomes guided by the following questions:

1. Evaluate the community participation process using appreciative enquiry methodologies targeting the key groups involved in the planning process: a. with the wetland communities' b. with the researchers' c. with the technical team d. with custodians /County officials from departments of Lands e. with Professionals f. with schools.
a. What went very well? b. What could be done even better/improved next time?
2: How does one feel about the final outcome of Yala Wetland Land Use Plan and ecosystem management plan?
3. What follow-up mechanism is in place to ensure community participation issues /outcomes in the plan are later implemented?
4. How does one get the community as a key player in the implementation processes?
5. How does one ensure that the benefits from Yala wetland are shared equitably with the wetland communities and other key wetland actors with a mutual accountability system?

Community facilitator

At the core of optimizing community participation in SEA and LUP processes is the CF who helps communities navigate those five steps and is supported by an Information Resources Hub (IR-Hub). The Yala RAPPEF-CF-IR-Hub framework is a facilitative model and with the CF being key to its execution. Therefore, a dedicated community facilitator should bring certain attributes to the process that are in synch with the planning context. The attributes that were appropriate for Yala wetland were: skills and capabilities in planning and management; knowledge of environmental sciences; networking and advocacy, proximity and access to decision makers; and, community acceptance to generate a feeling that it was a safe environment of trust and mutual respect.

Effective participation demanded the commitment to implement the plan as the local communities saw themselves as co-creators. The researcher became a CF in wetland planning process thereby provided a link amongst local communities, the SEA/LUP technical team and the Inter-County Steering committee**.** The expanded community consultations feedback was then presented in YPAC meetings and at various writing stages with IMTC technical specialists by the CF.

The creation of CF in the framework served many practical concerns of the wetland communities. A key feature it provided was a safe environment of trust, inspired confidence and mutual respect for participation. This was further confirmed by top-level leadership respondents' remarks who told the CF "you are our son please tell us, will our ideas be taken seriously or they will do like what Dominion Farms did". The CF-IR-Hub component sought to reduce the disconnect between decision makers and provision of scientific and technical information for Yala wetland. The CF had access to the decision makers and was part of the technical team hence would weigh in to provide this nexus.

Among the key framework inputs taken on board in final SEA/LUP documents were: i) Historical and contextual information of Yala swamp (chapter four in SEA report titled understanding characteristics of Yala swamp and its recent history); ii) previous studies on how multipurpose water projects would affect environmental flows of the river Yala and the swamp (i.e. Identification of a Multipurpose Water Resources Development Projects in Gucha-Migori and Yala River Basins in Kenya (2011-2012) where the researcher was part of the team); iii) envisioning the future Yala Wetland and subsequent broader shared ownership of the sustainable Yala wetland vision; iv) creating a sense of urgency on the need to conserve Yala wetland and the role of local communities required to take charge (co-owners of the wetland) in line with the Indigenous Community Conservation Areas (ICCAs) management requirements rather than being bystanders (Davies et al., 2012).

Information resources hub (IR-Hub)

The IR-Hub was vital in gathering, processing and relaying timely data and information required to inform the processes. The information resources gathered included previous related studies on Yala wetland, feedback from community meetings, validation feedback of various SEA/LUP outputs and draft reports; vital networks/contact persons who were called to inform and input the various parts of the process. In the IR-Hub, facilitators used multifaceted but audience appropriate channels in communicating with them. For example, CF relayed technical process outputs through graphical images, community, storytelling, folklores, sayings, proverbs and metaphors. Constant feedback by CF using appropriate target audience information and channel was key in applying the framework. The IR-Hub should be a 'live' entity, constantly growing and replenished with current information.

The application of Yala community participation Framework in SEA/LUP process and its outcomes

The framework was applied in the then on-going SEA and LUP and the following discussion show the processes and outcomes.

Important but ignored actors brought to the decision-making table

The second stakeholders' analysis substantially brought important but initially left out actors in the SEA/LUP process to the table. Consideration here was given to subject matter representation, meaningful geographic representation/spatial spread; the first stakeholder analysis assumptions which did not hold that YPAC would represent the communities and have seamless flow of SEA/LUP information to the local communities; and empathy walk to have a feeling for the community on the Yala Wetland. These eleven additional actors were: the Luo Council of Elders (custodians of communities' heritage). Schools (nursery schools, primary, secondary and post-secondary) played catalytic role of learning and implementing, ethos for sound management of the wetlands, awareness raising about the Yala wetland sensitivity, envisioning Yala wetland future through essays, debates and artwork). Change makers in the community who brought new planning issues such preservation of herbal trees, land tenure socio-cultural dynamics and how it determines its subsequent care, as one female change maker deeply revealed on gender constraints.

"we cannot obtain land title deeds without the permission of our husbands or male guardians. Communities fear losing their land to strangers from different clans when their women are inherited upon the death of a husband or if a woman remarries from a different clan"

The professionals from the Yala Wetland (experts on land, water, environmental conservation, academia, scientists and researchers) who brought a deeper analysis of the planning issues, lessons learnt and best practices from elsewhere, interrogated drafts and gave their expert views and recommendations; The local administrators (chiefs, sub-chiefs, village elders (*mlangos)*-(current and retired) were key entry points into the communities as well as resolving communal conflicts besides providing additional historical and contextual information; The Wetland International Eastern Africa office (WI) wetland experts visiting guest in their network from various African countries on a tour of Yala swamp (unique biodiversity value and those ones under threats like globally threatened species which are endemic to the delta ecosystem); The Tourist Association of Kenya on tourism potential of the Yala swamp and its integration within the western Kenya tourism circuit; the small and medium scale investors in Yala swamp on their plans to expand their farm activities and the need to increase water abstracted from Lake Kanyaboli and the wetland. Additional NGOs giving valuable feedback to draft plans; The Motorcycles Association (*Boda boda*); and the media who covered subsequent process outcomes in their various media channels mainly newspapers, FM radios and documentaries.

Levers for increasing community participation rates

The Yala Hub framework provided events for multi-stakeholder participation and feedback which include Annual Wetland Day Events, World Migratory Birds' Day and Environment Days. Additionally, schools essay

Plate 2. Researcher, supervisor and research assistant following the proceedings of Wetland Day on February 2, 2016 and launched school's participation in LUP competition.

Plate 3. The Bridge Usenge school pupils performing at on Wetland day in Usenge Primary school extolling the benefits of Yala Wetland and call to action for conservation.

writing, debates and artworks, organized community meetings at village levels were new avenues for participation that required its own facilitation as discussed below.

Annual wetland and environmental day events

Siaya County Wetland Day of 2016 held in Usenge Primary school had schools who extolled the benefits of the Yala Wetland and the need to preserve it. The event was preceded by a bird watching exercise at Goye cause way with identification of 60 bird species while songs, poems and dramas were used to convey wetland conservation messages. The Yala Hub framework also used the occasion to update the communities on the progress with SEA and LUP and researcher launched the school's competition titled envisioning the Yala Wetland in 2063 at the event (Plate 2-3).

The 2017 World Wetland's Day was celebrated in

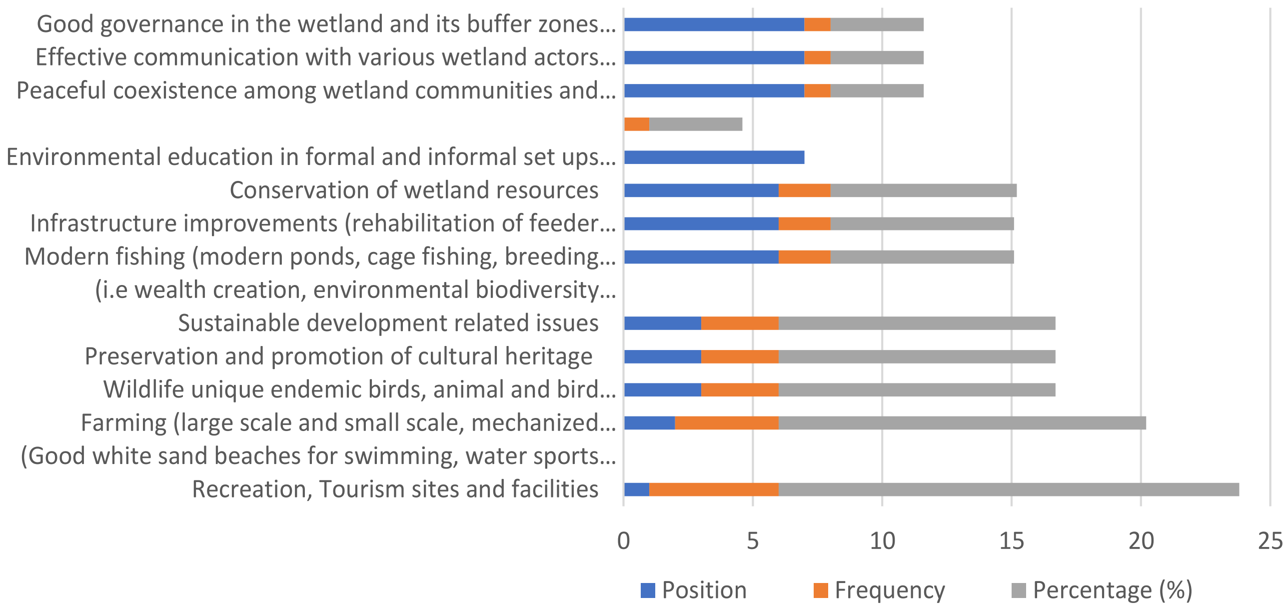

Figure 6. The dreams and aspirations ranking from students in learning institutions.

Hawinga Primary school themed: the importance of world migratory birds where the researchers seized the occasion to discuss the progress of SEA and LUP and then sought community contributions on the same. The results of these participation processes were: strengthening environmental awareness programmes in schools through clubs, tree planting and post planting care, promoting hygienic practices and protection of Lake Kanyaboli and water springs; a deeper understanding on the Yala Wetland challenges and the role of the wetland communities in solving them. Likewise, some of elders gave talks on the values the Yala communities attached to various types of birds and how they then treated them based on these understanding (indigenous knowledge and passing that to school during the event). The structured and goal oriented social interaction/active engagement amongst pupils, parents and guardians and technical staff from the government continued to offer opportunity for cross learning from all the subsets of communities represented. The continued participation of schools inculcated environmental consciousness and subsequent behavior change among the pupils at an early age.

Schools debates and artworks contribution to Yala SEA/LUP

The participation of learning institutions in SEA and LUP that came with the Yala RAPPEF-CF-IR Hub framework which was done through competitions on essay writing, debates and artworks gave the students an opportunity to focus on Yala Wetland and then contribute based on the environmental issues/challenges and their envisioned future which helped in crystalizing the vision of Yala LUP. The results on envisioning priorities are shown in Figure 6 while the artworks were creatively integrated in one mosaic shown in Figure 7.

Community meetings at village levels

Communities' participation was mostly done through community meetings at village levels facilitated by the researcher and assisted by research assistants and YPAC members. Some were done as focus group discussions for smaller groups; community open forums where researcher explained the purpose of mission, briefing on SEA/LUP status and then discussions guided by the facilitator on key themes SEA/LUP issues. To ensure high level of attendance, wetland residents from relatively far-off places were facilitated with transport and light refreshments during the meetings.

The YPAC members then got the opportunity to meet communities and discussed YPAC issues during those researcher's facilitated sessions. The process was enriched as they managed to gather from communities on their priority issues using participatory methodology tools. The feedbacks were captured and processed and the researcher feedback (as a new feedback loops) to the technical team in the form of review of drafts and commenting with input from the community. Second, during the meeting with YPAC the various members were able to bring key summaries from these meetings to the LUP technical team which they could not do before the support they got from the application of Yala Hub

Figure 7. Mosaic of students' impression of the future Yala wetland in 2063. (Mosaic by N. Anyango, 2019)

framework. Later, the researcher had the opportunity with various subject matter specialists in the technical team and would reach out to them for key inputs for incorporation the plan drafting process (community facilitator secured a place in the technical team to work with them in preparing the LUP).

Targeted sourcing for critical inputs into the SEA/LUP

The communities' feelings on participation in SEA/LUP based on the Yala RAPPEF-CF-IR-Hub framework were varied. Majority felt that this should have come at the beginning of the LUP process to allow for intense consultations with communities and solicit their critical input to inform the processes.

The pupils and students on their part while expressing gratitude for the involvement; proposed that the competition should be held annually to allow many students to get involved and steer tangible conservation action. Additionally, they suggested that environmental clubs should be actively involved in conservation activities of Yala Wetland and be recognized if they implemented their dreams as captured in the mosaic Figure 7. Furthermore, environmental conservation and education guidelines for lake and river basins and wetland should be developed to guide implementation of these activities. In the guide development, the learners stressed the use of students and young people friendly packaged information and expanding the guide to cover areas brought out in their aspirations, debates and artworks' submissions.

Community participation requires full time institutional support and commitment - Community Facilitator and Information Resources Hub

The Community Facilitator and Information Resources Hub was designed as the base of the framework to support the communities navigate the five steps processes accounting for 35% of its improved framework effectiveness.

Community facilitators

The Community Facilitator (as the researcher) formed a team and networks to enhance community participation in SEA/LUP processes. The team consisted of Research Assistants from School of Environmental Studies, University of Eldoret (for technical know-how); some members of Project Advisory Committee and Yala Site Support Group (YSSG) (for local knowledge, acceptance by community and community level meeting facilitation) and linkage with networks of professionals from and/ or with interest in Yala Wetland (technical expertise and genuine involvement in determining the development paths of their communities); Development Facilitators and partners to allow for navigation into the processes without hindrances (Nature Kenya, The IMTC and County Government Leadership). Thus, relationship building was vital aspect of increasing community participation and the Community Facilitator brought in this aspect by building a safe environment of trust, inspired confidence and mutual respect for participation.

The type of stakeholders targeted determined the type data collection tool adopted**.** For example, the youth preferred a mix of media at the same time (audiovisuals, social media whatsapp, facebook, instagram, group work sent to their phones directly), while in schools the team opted for artwork, debates, essays with queries that focused on challenges and what future they envisioned of the future Yala Wetland, for environmental events days the team choose gallery walks on artistic works display of Yala Wetland, wetland products display, live performances like poems and dramas with conservation messages, display of ecotourism sites and thematic songs delivered with aid of traditional instruments (such *nyatiti, ohangla, orutu, pekee, tung*) and talks by both government and community leaders based on the theme of the event. The CF also seized those occasions to update wetland communities on SEA/LUP progress, key planning issues and obtained their feedback on the updates.

In addition, the steps intentionally involved the use of local leaders to co-facilitate the meetings with the researchers after being trained on SEA/LUP specific issues. This gave them the opportunity to relay SEA/LUP updates from Inter-county steering committee and technical team, which had been a challenge before. Each team was also provided with latest copies of SEA and LUP and YPAC meeting minutes to equip them while conducting community meetings.

The CF became a lever for increasing participation rates and new feedback loop for the SEA/LUP processes. Consequently, to perform these functions, the CF needed to be somebody whom they respected, trusted and had the power to engage at main stages and structures of SEA/LUP processes (ICSC, YPAC, Technical team, Learning and Research institutions, various players of policymakers). The CF brought certain attributes to the process that were harmonious with Yala wetland context. The skills and capabilities in planning and management; environmental sciences knowledge; networking and advocacy, proximity and access to decision makers and community acceptance.

Information resources Hub for accessing relevant information to make informed decisions that is evidence and outcome based

There was a gap of Yala Wetland Information System to collate existing relevant information, information generated by the SEA/LUP studies and processes; and others to increase the quality of community participation in managing Yala Wetland ecosystem. During the process the SEA/LUP secretariat and the researcher carried out some of those tasks. The information resources gathered related to studies on Yala swamp, feedback from community meetings, validation feedback of various SEA/LUP outputs and draft reports; vital networks or contact to review the various parts of the process. For example, CF relayed technical process outputs to the wetland communities through graphical images, storytelling, folklores, sayings, proverbs and metaphors. In repackaging technical information, the communities required less text and tables but rather more visuals, graphics and intuitive information delivered mostly in consultative and experiential processes with adequate time for questioning, reflection and responding. Therefore, IR-Hub enabled communities and their agents to access relevant, timely and repackaged information to facilitate their participation in SEA/LUP processes. The IR-Hub operations thus entailed sourcing, processing, repackaging, storing, retrieving, targeted dissemination, and receiving and acting on feedback. In the IR-Hub, facilitators used multiple audience appropriate channels in communicating with them. Also, there were constant feedback by CF using appropriate target audience information and channel.

On framing issues, the team used appreciative words, that is, positive, optimistic and desired result focus to guide the information gathering for some respondents. For community organizations to elicit feedback, the researcher framed guiding questions for each category.

For the students, the essay topic was “what is your dream for the future of Yala Wetland in 50 years’ time if money is not a problem?; the religious leaders, they were asked to reflect with their leadership teams and thereafter prepare a compelling God inspired sermon on the theme of a better Yala Wetland; and the professionals, they were asked to give back to their communities their expertise in developing the Yala wetland land use plan, to which some responded by reviewing the SEA/LUP drafts.

The researchers used empathy walks shown in Plate 5 as he moved into the Yala Wetland with inhabitants who narrated their issues (e.g. an elderly woman showing the graveyard of her husband and reasserting her unwillingness to leave the grave in Yala Wetland if the residents are to be relocated; mini-boarding school in the swamp where pupils return home over the weekends to replenish food supplies (Plate 4) and in those situations researchers just engaged in deep listening to derive deeper meanings which they reflected in their journals allowing new forms of information to flow into the process and was key in designing the logical steps of the Yala RAPPEF-CF-IR Hub framework. Therefore, the IR-Hub became a ‘live’ entity, constantly growing and replenished with current information.

The researchers lived with the communities during the study period which extended for over one year (2016-2018) since the LUP processes delayed. This gave them opportunity to immerse themselves into the communities to experience their lives firsthand, obtain people issues very deeply, and to infuse creativity in the participation process based on those experiences. Some communities (especially in Usonga) very hostile to the LUP but through participatory processes the researcher was able to get their inputs and concerns. They did not welcome the creation of Lake Kanyaboli Game Reserve which they considered would take away some portion of Yala Wetland hence not available for their use (farming, accessing wetland resources) and they had fear of having the KWS staff around that will control their activities in the wetland including poaching. The researchers accessed some insiders among them to get limited entry and their fears and strong opinions over the wetland management. They also felt that the wetland was part of their ancestral land hence could not be taken away.

Overall, IR-Hub subcomponent of the Yala Hub framework provided timely access to relevant, repackaged information and kept new forms information flowing into the process thus evidence and outcome-based decision making.

Community conservation champions to provide transformative leadership in the wetland

During the study, some individuals were found to be active and pursued Yala Wetland conservation matters passionately. Some had been trained by conservation agencies on bird watching, on conservation of fragile wetland ecosystems and while some were change makers who in their respective undertakings brought positive changes in their localities and had earned communities’ respect. The change makers have been profiled in a database and remained strategic community pointers for LUP implementation and ecosystem

Plate 4. Pupils from Maduwa primary school in Maduwa island returning to school after collecting food. The school had to make boarding provision to manage the challenge of daily commute by pupils on the manual boats.

Plate 5. Researcher and Research Assistants travelling to Yala wetland islands for community meeting. Empathy walk entailed experiencing what the respondents go through by walking with them and feeling that.

management in the IR-Hub. More change makers would be required to provide authentic and transformative leadership to champion wetland conservation at community level.

Shamir and Eilam (2005) defined authentic leaders as genuine, principled, and original. George (2003) presented five characteristics of authentic leadership that are especially relevant to Yala swamp ICCA leadership: (1) having a clear purpose, (2) having strong ethical values, (3) establishing trusting relationships, (4) demonstrating self-discipline and action, and (5) having passion. These values are key in implementing the Yala Wetland conservation plans and conservation champions will require retooling on these to meet the conservation demands for a sustainable Yala Wetland.

Learning institutions active involvement, changing mindsets and updating environmental education curriculum

The Learning Institutions in Yala wetland who were involved in expanded LUP development consultations were very positive on the essays, debates and artworks competitions on Yala wetland and proposed that those should be done annually. Intrinsically, a mechanism for yearly competition, participation on key environmental events like Wetland days and strengthening environmental groups in school should be prioritized in the implementation phase. This will require wetland customized environmental education guide.

The substantial involvement of learning institutions in SEA/LUP processes revealed weakness in the existing Education for Sustainable Development for Schools in Lake Victoria Basin region given to participating schools as incentive for participation. The submissions and analysis of the current wetland challenges and their propositions for a sustainable wetland called for expanding the curriculum to incorporate the following aspects: mindsets and mindsets for planning conservation, integration local communities knowledge with sustainability ethos and values for managing the wetland ecosystem that provide for required deep changes; transformative leadership Yala wetland conservation, transformational learning methodologies (appreciative inquiry and applying Theory- U for leading deep changes); incentivizing participation in wetlands conservation, the student, the teacher and parent nexus for sound conservation; innovative avenues mobilizing local communities to participate in wetland's management such as the Wetlands Day Celebrations, Environment day and World Migratory Birds. The upgraded curriculum should aim at instilling higher level environmental consciousness and stewardship among the learners in Yala wetland. This is in line with recommendations of learning and equipping students for 21st century by embracing innovative pedagogies, tailored to particular education settings; hybrid learning environments, which blend formal and nonformal schooling, and; promoting the pivotal role of the "missing middle," or "meso," layer of education-consisting of networks, chains of schools, and communities of practice-to scale deep change (Istance and Paniagua, 2019).

Information access and seeking behavior and opportunities for optimizing participation

The information access and seeking behaviors of the wetland community leaders was diverse. The common approaches they use to get information included peer talks, authoritative policy orders and regulations from administrators. Further, all the leaders had mobile phones and in some groups all the members also had telephone connectivity thereby providing greatest opportunity for telephone communication. The telephone was both a tool for communication and money transaction. The analysis revealed that various group had their different and unique information seeking behaviours and had different interactions among these categories and how they influenced one another.

The wetland school children were found to be highly influential on their parents and guardians with conservation messages shared in schools like tree planting and wetland conservation. When pupils were made to plant trees in schools and given seedlings to plant at home, they reported that their guardians helped them to care for them while they were in school (e.g. watering and preventing domestic animals from damaging them). The different information seeking behaviours and outcomes of interactions among wetland communities offer opportunity on what factors and nuances are key in ensuring effective community participation. The further stakeholder analysis tier two revealed primary influencers of decision makers as an avenue of participation which was pivotal to information transmission at both community and government leadership levels and should be utilized as an additional entry points but cautiously since they are not official channels.

Local community ownership of Yala LUP and ecosystem management plan

The local communities felt valued through their involvement in LUP preparation using Yala Hub framework. As such they committed to implement LUP and Yala management plans recommendations. Similarly, the technical team embraced the application of Yala Hub framework in thinking through methodically and identifying weak points in community participation and took on board some of practical ways of improving community participation in the remaining LUP steps. The technical team and the secretariat were also flexible to take in inputs from these communities' consultations thus underscoring the transformative learning application in the framework. The final land use plan with it recommended land uses which benefited from the application of Yala Hub framework is shown on the map in Figure 8.

Creating incentives for participants

Students looked forward to giving their best with a view to winning the prizes announced in the competition advertisement which were Polo T-shirts and certificates of recognition. Therefore, creating incentives for participants contributed to enabling them to focus and give their best during the exercise. As a reward for participation, schools were given booklets for Environmental Studies Curriculum for upper primary and secondary schools developed by Retouch Africa Consulting (RAI) done for World-Wide Fund (WWF) for Lake Victoria Basin Environment Programme. This needs to been updated to respond to some of the research finding and inputs. The schools were also given Model Schools Best Practices on Education for Sustainable Development, Income Generating Activities (IGA) and Education for Sustainable Development (ESD) village

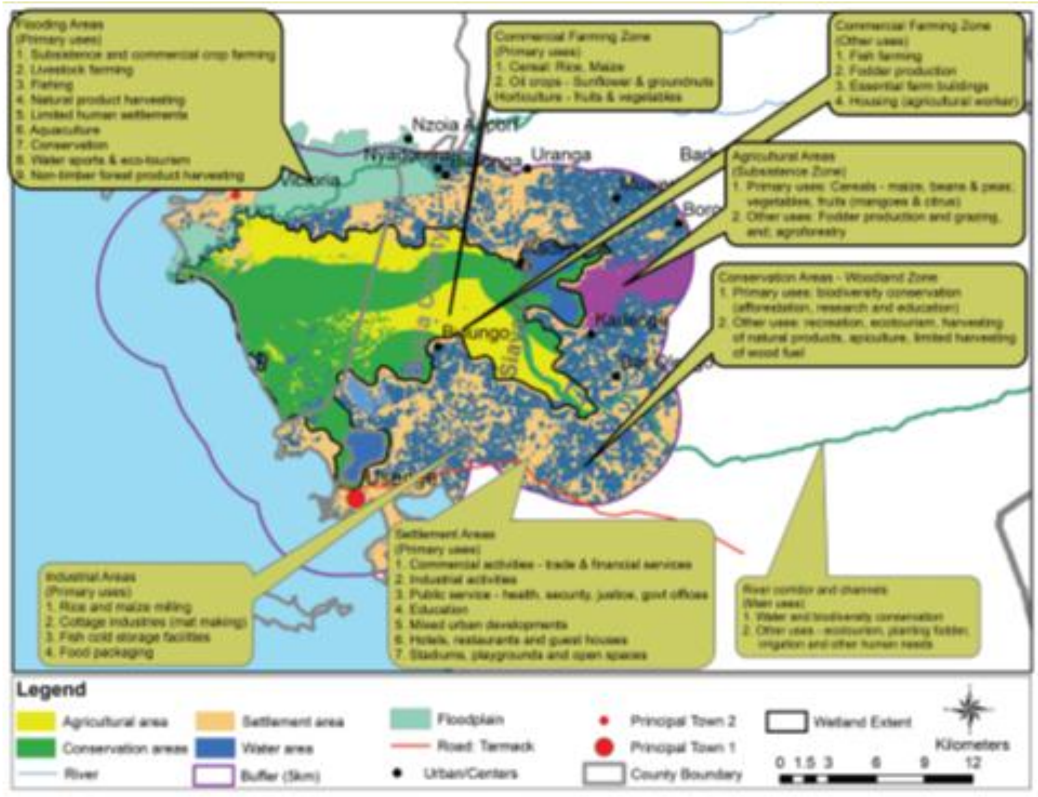

Figure 8. Yala Land Use Plan – Recommended Land Uses.
Source : Odhengo et al. (2018b).

concept in project areas. The students were awarded certificates of participation while the winners got Polo T-shirts with wetland conservation messages. This triggered further demand for the annual competition to give others a chance to participate.

Substantial application of participatory methodologies in community participation processes

The process incorporated deeper interaction participatory community participatory tools like empathy walks, focus group discussions, community maps, pair-wise ranking and appreciative enquiry methodologies to gather expanded stakeholders' inputs from different shades of local communities: young and the old, males and females; persons living with disabilities, poorest of the poor into planning process.

During an empathy walk with an old lady in Buhuma Village Island, she said. "I cannot leave the body of my husband here due to the fear of being submerged by floods". Other instance include: while moving into and from the swamp with YPAC representative Gladys we experienced what islanders go through to participate in one day meeting in Siaya but takes a total five days detailed as leaving the island in the afternoon to spend the night in the mainland on the Lake Victoria shore (day one), then start the journey to Siaya the following day where spends the night in readiness for the meeting the following day (day two); one day meeting (day three); journey back to shores in Osieko where she spends the night (day four), crossing back to the island (day five). Other examples include talking to school girls and boys paddling a canoe to go home over the weekend to get food supplies, observing a boy playing with snake on the shore of the island at the entry to their school; and going for data collection in the Buhuma island village and on return at night the boat running out of fuel on the lake, seeking help from Uganda fisherfolk who did not help and finally Osieko chief mobilized rescue team from Obaro village island to bring fuel to the research team in the lake at night. Going to the gravesite of a respondent's grandfather with his grandmother and attending a meeting with the assistant chief when village elder's path had been blocked by a rival subclan.

The study also identified other participatory methodologies and situations where they are best applicable that would be useful in optimizing communities' participation in various development interventions. These include the watering plants and circles and stars tools for financial data and services; the extension river tool for community advisory services; the food diary tool for dietary diversity; the ideal job tool for youth job opportunities, the land access and control matrix tool for women empowerment; and the social protection traffic light tool for community social protection.

Repackaging information

This is providing feedback in ways that communities could understand the information easily. The community focused facilitation helped with simplifying the SEA/LUP processes, languages, and simulations of the issues at community meeting. Likewise, local communities were able to draw simple maps to give their inputs, used their proverbs and sayings to pass their concerns on the LUP which were then repackaged by the researcher and relayed to the technical team. Thus, repackaging SEA/LUP information this way for communities helped to educate them and then sharpened their contribution in LUP remaining phases using different channels namely: community channels, radio, music, religious leader sermon, local administration *barazas*, funerals, special community events, special events such as World Wetlands Days, Environment Days, and Partners Field days, competition in learning institutions through essays, debates, performances such dramas, songs, and artwork among others. Thus, Yala Hub framework hence responded the study call on public participation during EIA in Kenya's recommended that EIA study reports should not only be widely available but also translated into indigenous languages with simple explanations and illustrations (Okello et al., 2009).

The Yala RAPPEF-CF-IR-Hub Framework as a system

The Yala RAPPEF-CF-IR-Hub framework is a system and the relative weights of its subsystems are step 1. React/Act; (10%) step 2. Restructure/Adjust the participation framework based on the reactions of step 1 (7%); step 3. Participation Preparations (20%), step 4. Community Participation (16%) step 5: Review, evaluation and follow-up (12%) and the base CF-IR-HUB (35%). This proposition is supported by the works of Dr. Brent Peterson of Columbia University (2004) who found that learning effectiveness is a product of three subsystems namely pre- work (26%); learning event (24%) and follow-up/post learning event (50%), thus pre-course work and post-event follow-up contributes a combined total of 86% of learning effectiveness. However, the application of Yala RAPPEF-CF-IR-Hub Framework requires a mindset shift among the local communities, technical teams and county government staff; and requisite resources to be operationalized optimally.

CONCLUSION AND RECOMMENDATIONS

The under representation of local communities in Yala wetland management prompted the formation YPAC to remedy this in the development of its SEA/LUP. However, analysis of YPAC using Spectrum of Public Participation Model and 10 Indicators of public participation revealed that YPAC framework had 12 limitations, that compromised its ability to represent wetland communities meaningfully and effectively in SEA/LUP process. As such, Yala RAPPEF-CF-IR-Hub Framework (Yala Hub Framework) was developed and applied in the remainder of SEA/LUP processes to overcome these limitations and eventually optimize community participation. The Yala Hub Framework is a 5-steps process with a Community Facilitator and an Information Resources Hub at its base and has guiding questions for every step in applying it. The Yala Hub was applied in Yala LUP occasioning significant improvements of community participation in levels and effectiveness of participation of Yala wetland communities. They moved to Consult (80%) and Collaborate (20%) levels of the spectrum, while effectiveness moved to satisfactory (3 indicators) and good (7 indicators). Besides, it induced sustainability through ownership of the land use and ecosystem management plans; empowered the stakeholders to take responsibility for sustainable management of Yala Wetland ecosystem; minimized conflicts during plan preparations; and increased transparency, inclusivity and accountability in Yala Wetland ecosystem management decision making process. The Framework was further deployed in Siaya County CIDP 2018-2022, where it also occasioned a significant improvement in public participation processes through a creation of a public participation directorate.

From the foregoing study, it is evident that effective community participation determines and influences effective implementation of decisions made therein; and that increased participation through deliberate intervention by Yala Hub Framework, as an optimizer and a diagnostic tool, will eventually increase the effectiveness of community development. However, the application of Yala Hub Framework requires a mindset shift among the local communities, technical teams and county government staff; and requisite resources to be operationalized optimally. Implementation of this framework is recommended for the success of the Yala Wetland Land Use Plan and in other LUP processes to wetlands with "similar challenges" as Yala and in community development.

Research Implications

The systematic process of the Yala Hub framework underpins the action, reflection, refining aspects of public participations, and calls for learning, applying and modifying as one moves along with participation. A static procedure hampers effective community participation.

Instead, procedures for public participation that factor in frameworks providing fluidity is demonstrated by the Yala RAPPEF-CF-IR-Hub as an optimizer and a diagnostic tool community development. Further, community participation requires resources (technical and financial resources including facilitations, incentivization, room for learning/making mistakes and learning from them) and a mindset shift among the local communities. Multiple layers of participation with various actors and feedback loops requires availing expertise to explain community inputs and concerns and relay the same to the participation model used in the development intervention being undertaken.

Suggestion for future research

Future research needs to be directed at community organizing for effective participation of wetland ecosystems management, sensitive spaces, and other development interventions. Development of an ICT based application for the Yala RAPPEF-CF-IR-Hub (named I-Yala Hub) and linkage with E-Riparian application currently being tested for providing information about the wetlands in Kenya. Conduct mapping, documentation and repackaging of indigenous knowledge and innovations systems for managing the Yala wetland systems; and, integrate with planning knowledge systems. Further studies on Ornithological investigation targeting both migratory and resident species; models for sustainable conservation enterprises identified in Yala wetland, conflict resolution and management options for human wildlife conflicts; capacity assessment and targeted strengthening of community governance and codifying the emerging Yala wetland lessons and resource use efficiency modelling for Yala wetland natural resources.

CONFLICT OF INTERESTS

The authors have not declared any conflict of interests.

ACKNOWLEDGMENTS

The authors are grateful to the Yala Delta Land Use Plan Team, the University academics who contributed to this research and finally to the Yala wetland communities who were part of this action research. The authors appreciate Retouch Africa Consulting (RAI) for financially supporting the research.

REFERENCES

Aloo PA (2003). Biological Diversity of the Yala Swamp Lakes, with special emphasis on fish species composition in relation to change in L. Victoria Basin: Threats and conservation measures. Biodiversity and Conservation 12(5):905-920.

Ampofo S, Ampadu B, Abanyie SK (2015). Landcover Change Patterns in the Volta Gorge Area, Ghana: Interpretations from Satellite Imagery. Journal of Natural Sciences Research 5(4):2224-3186.

Anyango NO (2019). Mosaic of students' impression of the future Yala wetland in 2063.

Arnstein SR (1969). A ladder of citizen participation. Journal of the American Institute of Planners 35(4):216-224.

Awange JL, Ogalo L, Bae KH, Were P, Omondi P, Omute P, Omullo M (2008). Falling Lake Victoria water levels: Is climate a contributing factor?. Climatic Change 89(3):281-297.

Babbie ER (2015). The practice of social research: Nelson Education. Boston, MA Cengage Learning (14th Edition). USA.

Birldlife International (2018). Important Bird Areas Factsheet.Yala swamp complex. Retrieved January 22, 2018, from http://www.birdlife.org

Bond I, Davis A, Nott C, Nott K, Stuart-Hill G (2006). Community-based natural resource management manual. WWF-World Wide Fund pp. 23-35.

Chambers R (2006). Participatory Mapping and Geographic Information Systems: Whose Map? Who is Empowered and Who Disempowered? Who Gains and Who Loses? Electronic Journal of Information Systems in Developing Countries 25(2): 1-11. Retrieved May 20, 2018 from http://www.ejisdc.org/ojs/include/getdoc.php?id=247&article=264&mode=pdf

Corbin JM, Strauss A (1990). Grounded theory research: Procedures, canons, and evaluative criteria. Qualitative Sociology 13(1):3-21.

Cooke B, Kothari U (Eds.) (2001). The Case for Participation as Tyranny. Participation: The New Tyranny? London: Zed Books.

Cooperrider DL, Leslie S (2006). "Toward a theory of positive organizational change." Organization development: A Jossey-Bass reader pp. 223-238.

Davidson S (1998). Spinning the wheel of participation. Planning, 1262(1415.15).

Davies J, Hill R, Walsh FJ, Sandford M, Smyth D, Holmes MC (2012). Innovation in management plans for community conserved areas: experiences from Australian indigenous protected areas. Ecology and Society 18(2):14.

Dawson S, Manderson L, Tallo V (1993). A manual for the use of focus groups. International Nutrition Foundation for Developing Countries: Boston.

Department of the Environment, Transport and Regions (DETR) (2000). Public Participation in making local environmental decisions. The Aarhus Convention Newcastle Workshop Good Practice Handbook, London. Retrieved May 3, 2018. from www.unece.org/env/pp/enaces/handbook.pdf

Dobiesz NE, Lester NP (2009). Changes in mid-summer water temperature and clarity across the Great Lakes between 1968 and 2002. Great Lakes Resources 35(3):371-384.

Doelle M, Sinclair J (2005).Time for a new approach to public participation in EIA: Promoting cooperation and consensus for sustainability. Environmental Impact Assessment Review 26:185-205.

Dominion Farms (2003). The Environmental Impact Assessment Study Report. Siaya. Dominions Farms Limited.

Dugan P (1992). Wetlands in the 21st Century: The challenge to Conservation Science. In: Mitsch, J.W. (Ed) Global Wetlands: Old World and New World pp. 75-87. Elsevier, Amsterdam

Dweck CS (2008). Mindset: the new psychology of success. New York: Ballantine Books.

Envertek Africa Consult Limited (EACL) (2015). Proposed sugarcane plantation and processing mill for dominion farms limited in Siaya county location: reclaimed section of Yala swamp on longitude 34.171380 east and latitude 0.022992 north in the flood plain of river Yala in Siaya and Bondo sub counties in Siaya county, Kenya. Environmental and social impact assessment (esia) study report. Dominion farms limited (DFL).

East Africa Natural History Society (EANHS) (2018). Balancing Conservation and Development in Yala Swamp. Posted on January 30, 2018.

Ekirapa AE, Kinyanjui HCK (1987). The Kenya soil survey. Ministry of Agriculture, National Soil Laboratories.

Friis-Hansen E, Duveskog D (2012). The Empowerment Route to Well-

being: An Analysis of Farmer Field Schools in East Africa, World Development.
Gaventa J (2004). Representation, community leadership and participation: citizen involvement in neighbourhood renewal and local governance. Report, Neighbourhood Renewal Unit, Office of Deputy Prime Minister, July, 04. https://opendocs.ids.ac.uk/opendocs/bitstream/handle/20.500.12413/12494/Gaventa_2004_representation.pdf?sequence=1
Gichuki J, Maithya J, Masai DM (2005). Recent ecological changes in of Lake Sare, Western Kenya. In: (eds). Odada EO, Olago DO, Ochola W, Ntiba M, Wandiga S, Gichuki N, Oyieke H Proceedings of the 11th World Lakes Conference, Nairobi, Kenya. Vol II. Ministry of Water and Irrigation; International Lake Environment Committee (ILEC).
Government of Kenya (GoK) (1987). Yala Swamp Reclamation and Development Project: Inception Report'. The Government of Kenya and the Government of Netherlands. Lake Basin Development Authority.
Government of Kenya (GoK) (2010a). Constitution of Kenya, 2010. Retrieved May 10, 2015, from http://www.kenyalaw.org:8181/exist/kenyalex/actview.xql?actid=const2010
Government of Kenya (GoK) (2010b). Schedule-Lake Kanyaboli National Reserve,Government Printer, Nairobi.
Government of Kenya (GoK) (2012a). The National Land Commission Act, 2012. Nairobi. Government Printer. http://extwprlegs1.fao.org/docs/pdf/ken112132.pdf
Government of Kenya (GoK) (2012b). The County Governments (Amendment) Act, 2012. http://www.parliament.go.ke/sites/default/files/2017-05/CountyGovernmentsAct_No17of2012_1.pdf
Government of Kenya (GoK) (2012c). The Intergovernmental Relations Act, 2012. Retrieved May 20, 2015, from http://www.parliament.go.ke/sites/default/files/2017-05/IntergovernmentalRelationActNo2of2012.pdf
Government of Kenya (GoK) (2012d) Physical Planning Act, 2012. www. kenyalaw.org.
Government of Kenya (GoK) (2015a). The Environmental Management and Co-ordination Amendment) Act, EMCA (2015). Retrieved May 10, 2015, from http://extwprlegs1.fao.org/docs/pdf/ken41653.pdf
Government of Kenya (GoK) (2018). Siaya County Integrated Development Plan 2018-2022. Nairobi. Government Printer. https://cog.go.ke/media-multimedia/reportss/category/106-county-integrated-development-plans-2018-2022?download=345:siaya-county-integrated-development-plan-2018-2022
Greene M (1995). Releasing the imagination: Essays on education, the arts, and social change. Jossey-Bass.
Hardin G (1968). The tragedy of the commons: the population problem has no technical solution; it requires a fundamental extension in morality. Science 162(3859):1243-1248.
Harrison A, Schmidt G, Avis C, Hauser R (2001). WWF's preliminary comments on Public Participation in the context of the Water Framework Directive and Integrated River Basin Management. Copenhagen: WWF European Freshwater Programme.
Hartley N, Wood C (2005). Public participation in environmental impact assessment: implementing the Aarhus Convention. Environmental Impact Assessment Review 25: 319-340. http://www.cickenya.org/index.php/legislation/acts/item/227-the-intergovernmental-relations-act-2012
IAP2 (2008). International Association of Public Participation; Public Participation Spectrum. Retrieved March 6, 2018 from, http://www.iap2.org/associations/4748/files/spectrum.pdf.
International Union for Conservation of Nature (IUCN). (2009). Indigenous and community conserved areas: The Legal Framework in India. a bold https://www.iucn.org/downloads/india_3.pdf
International Union for Conservation of Nature (IUCN) (2018). Protected Planet Report. IUCN, Geneva, Switzerland. https://www.iucn.org/news/aires-prot%C3%A9g%C3%A9es/201801/analysis-non-state-protected-area-governance-kenya
International Water Management Institute (IWMI) (2014). Wetlands and people. Colombo: IWMI.
Istance D, Paniagua A (2019). Learning to Leapfrog: Innovative Pedagogies to Transform Education. Center for Universal Education at The Brookings Institution.
International Yearbook of Soil Law and Policy (IYSLP) (2017). International Yearbook of Soil Law and Policy 2016. Springer Science and Business Media LLC. https://link.springer.com/book/10.1007/978-3-319-42508-5
Johnson RA (1976). Management, systems, and society: an introduction. California: Goodyear Publication Company.
Japan International Cooperation Agency (JICA) (1987). The Study of Integrated Regional Development Master Plan for the Lake Basin Development Area.
Kansiime F, Saunders MJ, Loiselle SA (2007). Functioning and dynamics of wetland vegetation of Lake Victoria: an overview. Wetlands Ecology and Management 15(6):443-451.
Kenya National Bureau of Statistics (KNBS) (2009). 2009 Population and Housing Census.
Kenyan Wetlands Forum (2006) Rapid assessment of the YalaSwamp wetland. East African Wildlife Society, Nairobi. https://na.unep.net/siouxfalls/publications/Kenya_Wetlands.pdf
Kenya Wildlife Service (KWS) (2010). Resource Mapping Lake Kanyaboli Ecosystem.
Krueger R, Casey M (2009). Focus groups: A practical guide for applied research (4th edition). Thousand Oaks, CA: Sage Publications.
Lake Basin Development Authority (LBDA) (1989). Reclaiming the Yala Swamp. Resources 1(1):9-11.
Lee N (2000). Reviewing the quality of environmental assessments. Environmental assessment in developing and transitional countries: principles, methods and practice pp. 137-148.
Lewin K (1946). Action Research and Minority Problems. Journal of Social Issues 2(4):34-46.
Lihanda M, Aseto O, Atera F (2003). Environmental Assessment Study Report of the Proposed Rice Irrigation Scheme at Yala Swamp – Socio-cultural and Economics Survey, Volume III.
Lillesand TM, Kiefer RW (1987). Remote sensing image interpretation. 2nd edition. Chichester and New York: John Wiley.
Liverman D, Moran EF, Rindfuss R, Stern PC (2000). People and Pixels: Linking Remote Sensing and Social Science (Book Review). The Geographical Bulletin 42(1):61.
Lockie S, Sonnenfeld DA (2008). Communities, natural resources, and environments: African and Asian experiences. Local Environment 13(5):385-391.
Luedeling E (2011). Climate change impacts on crop production in Busia and Homa Bay Counties, Kenya. Nairobi, Kenya: World Agroforestry Centre.
Maclean IMD, Tinch R, Hassal M, Boar R (2003). Social and economic use of wetland resources: A case study from Lake Bunyonyi, Uganda. Centre for Social and Economic Research on the Global Environment, University of East Anglia (CSERGE), Working Paper ECM 03-09.
Michener V (1998). The Participatory Approach: Contradictions and co-option in Burkina Faso. World Development 26(12):2105-2118.
Mills GE (2000). Action research: A guide for the teacher researcher. Prentice-Hall, Incorporated. One Lake Street, Upper Saddle River, New Jersey 07458.
Muoria P, Field R, Matiku P, Munguti S, Mateche E, Shati S, Odeny D (2015). Yala Swamp Ecosystem Service Assessment Report. Nairobi, Kenya. http://www.birdlife.org/sites/default/files/attachments/yalaecosystemerviceassessmentreport_-20_july_2015_subimitted_to_prepared_1.pdf
Nasongo AAS, Zaal F, Dietz T, Okeyo-Owuor JB (2015). Institutional Pluralism, access and use of wetland resources in Nyando papyrus, Kenya. Journal of Ecology and the Natural Environment 7(3): 56-71.
Natasha M, Cynthia W, Family Health International (FHI), United States. Agency for International Development (USAID) (2005). Qualitative research methods: a data collector's field guide. North Carolina.
NEMA (2016). Yala Swamp Integrated Management Plan (2016-2026): Enhancing Environmental Management through Devolved Governance. Nairobi: NEMA.
Neuman WL (1997). Social Research Methods: Quantitative and Qualitative Approaches, 3rd ed. Boston. MA: Allyn and Bacon. New frontier for conservation. IUCN, Geneva, Switzerland. Retrieved June

2018, from www.iucn.org/about/union/commissions/ceesp/topics/governance/icca/
Odero DO (2015a). Promoting Community Participation in Transboundary Natural Resource Management in Mt Elgon Ecosystem using Geographic Information Systems: Case study of Mount Elgon Regional Ecosystem Conservation Programme. Graduate Seminar Paper, University of Eldoret.
Odero DO (2015b). The Application of Remote Sensing in Community Participation for Managing Mt Elgon Transboundary Natural Resources: Case study of Mount Elgon Regional Ecosystem Conservation Programme. Graduate Seminar Paper, University of Eldoret.
Odero DO (2021). Integrated Community and Participatory GIS in Management of Yala Wetland Ecosystem, Lake Victoria Basin, Kenya. Doctoral Dissertation, University of Eldoret, Eldoret, Kenya.
Odhengo P, Matiku P, Muoria JK, Nyangena J, Wawereu P, Mnyamwezi E, Munguti S, Odeny D, King'uru W, Ashitiva D, Nelson P (2018a). Yala Delta Strategic Environmental Assessment. Siaya and Busia County Governments, Siaya and Busia.
Odhengo P, Matiku P, Muoria JK, Nyangena J, Wawereu P, Mnyamwezi E, Munguti S, Odeny D, King'uru W, Ashitiva D, Nelson P (2018b). Yala Delta Land use Plan. Siaya and Busia County Governments, Siaya and Busia of land use change. International Journal of Science Arts and Commerce 2(3):12-38.
Ogutu MA (1987a). Fisheries and fishing. Siaya District Socio-Cultural Profile. Ministry of Planning and National.
Ogutu M A (1987b). Fisheries and fishing. Republic of Kenya. Pages 86-105. In: Republic of Kenya (1987) Siaya District Socio-cultural Profile. Ministry of Planning and National Development and Institute of Agricultural Studies, University of Nairobi, Kenya.
Okello N, Beevers L, Douven W, Leentvaar J (2009). The doing and un-doing of public participation during environmental impact assessments in Kenya. Impact Assessment and Project Appraisal Journal 27(3)217-226.
Okungu JO, Sangale FD (2003). Water quality and hydrology of Yala wetlands. ECOTOOLS Scientific Workshop on Yala Swamp. Switel Hotel, Bondo, Kenya. 9th–10th December.
Olson M (1965). The Logic of Collective Action: Public Goods and the Theory of Groups. Havard Economic Studies 124. Cambridge, M.A. Havard University Press.
Ondere LA (2016) Spatial-temporal changes of landcover types in response to anthropogenic dynamics in Yala Swamp, Siaya County, Kenya. https://ir-library.ku.ac.ke/handle/123456789/14945
Onywere SM, Getenga ZM, Mwakalila SS, Twesigy CK, Nakiranda JK (2011). Assessing the Challenge of Settlement in Budalangi and Yala Swamp Area in Western Kenya Using Landsat Satellite Imagery. The Open Environmental Engineering Journal 4:97-104.
Ostrom E (1990). The evolution of institutions for collective action. Spanish edition: Fondo de Cultura Económica, Mexico.
Otieno MN, Odenyo VOA, Okeyo JB (2005). The capabilities of Multispectral Landsat TM for mapping spatial landscape characteristics of a tropical wetland. The case of Yala Swamp, Kenya. Knowledge and Experiences gained from Managing the Lake Victoria Ecosystem pp. 118-124.
Owiyo P, Kiprono B E, Sutter P (2014). The Effect of Dominion Irrigation Project on Environmental Conservation in Yala Swamp, Siaya District, Kenya. Proceedings of the National Academy of Sciences 101(39):13976-13981.
Panayotou T (1994). The economics of environmental degradation: Problems, causes and responses. In: Pattanayak, S. & Kramer, R. A. Pricing ecological services: Willingness to pay for drought mitigation in eastern Indonesia. Land Economics.
Raburu PO (2012). Conservation and rehabilitation of Kanyaboli wetland, Kenya. In: Streever W J (EDs). An International Perspective on Wetland Rehabilitation. Springer Science and Business Media, 6 December 2012 - Technology and Engineering pp. 167-172.
Sandelowski M (1995). Sample size in qualitative research. Journal of Research in Nursing and Health 18(2):179-183.
Sangale F, Okungu J, Opango P (2012). Variation of flow of water from Rivers Nzoia, Yala and Sio into Lake Victoria. Ministry of Environment and Natural Resources (LVEMP).
Semenov MA (2008). Simulation of extreme weather events by a stochastic weather generator. Climate Resources 35(3):203-212.
Shamir B, Eilam G (2005). “What's your story?” A life-stories approach to authentic leadership development. The leadership quarterly 16(3):395-417.
Simonit S, Perrings C (2011). Sustainability and the value of the 'regulating' services: Wetlands and water quality in Lake Victoria. Ecological Economics 70:1189-1199.
Springate-Baginski O, Allen D, Darwall WRT (2009). An Integrated Wetland Assessment Toolkit: A guide to good practice. Gland, Switzerland: IUCN and Cambridge, UK: IUCN Species Programme xv.
Stec S, Casey-Lefkowitz S, Jendroska J (2000). The Aarhus Convention: An implementation guide.Geneva:United Nations Economic Commission for Europe. Retrieved April 20, 2018, from http://www.unece.org/env/pp/acig.pdf>
Stringer ET (1999). Action research second edition. Thousand Oaks, CA: Sage.
Stuart G (2017). What is the Spectrum of Public Participation? Sustaining Community.
Thenya T, Ngecu WM (2017). Indigenous strategies and dynamics of resource utilization in tropical wetland. A case study of Yala swamp, Lake Victoria Basin, Kenya. International Journal of Arts and Commerce 6:21-39.
Thomas D, Kariuki M, Magero C, Schenk A (2016). Local people and Tool for Action, Results and Learning prepared for Annie E. Casey Foundation (www.aecf.org and www.organizationalresearch.com)
Turner BL II (1998). Frontiers of Exploration: Remote Sensing and Social Science Research., Pecora 13 Symposium, Human interaction with the Environment: Perspectives from Space (August 20-22, 1996, Souix Falls, SD) pp. 15-19.
Van Dam AA, Kipkemboi J, Mazvimavi D, Irvine K (2014). A synthesis of past, current and future research for protection and management of papyrus (*Cyperus papyrus* L.) wetlands in Africa. Wetlands Ecology and Management 22(2):99-114.
Van Heukelom ST (2013). Security: The controversy of foreign agricultural investment in the Yala Swamp, Kenya. Doctoral Thesis. Centre for International Security Studies, Business School University of Sydney. Wetland Rehabilitation. Springer Science & Business Media, 6 December 2012 - Technology & Engineering pp. 167-172.
White SC (1996). Depoliticising development: the uses and abuses of participation. Development in practice 6(1):6-15.
WWF (2006). Community-based Natural Resource Management Manual. WWF.
Yala Wetland ICCA (2020). The Yala Wetland ICCA Management Plan 2019-2029. ICCA.

Vol. 16(1), pp. 37-70, January 2022
DOI: 10.5897/AJEST2021.3065
Article Number: AD6D22D68508
ISSN: 1996-0786

http://www.academicjournals.org/AJEST

ACADEMIC JOURNALS
expand your knowledge

African Journal of Environmental Science and Technology

Full Length Research Paper

Isotherms, kinetic and thermodynamic studies of methylene blue adsorption on chitosan flakes derived from African giant snail shell

Olaosebikan Abidoye Olafadehan[1*], Victor Ehigimetor Bello[1], Kehinde Olawale Amoo[2] and Adebukola Morufat Bello[1]

[1]Department of Chemical and Petroleum Engineering, University of Lagos, Akoka-Yaba, Lagos 101017, Nigeria.
[2]Department of Chemical Engineering, Lagos State University, Epe, Lagos State, Nigeria.

Received 6 September, 2021; Accepted 7 January, 2022

In the present study, modeling of 19 adsorption isotherms, 8 kinetic models and thermodynamics of methylene blue (MB) adsorption on chitosan flakes synthesized using *Archachatina marginata* shell wastes was investigated in a batch mode. The operational parameters' effects on the MB adsorption were studied. The model parameters were statistically analyzed using 10 error functions. The choices of the best fitted adsorption and kinetic models were based on the comparison of the sum of normalized error (SNE) and two statistical tools of information-based criteria. The 5-p Fritz-Schlüender isotherm best fitted the experimental adsorption data of MB on chitosan flakes based on SNE whereby maximum adsorption capacity, q_{max}, of 143.6660 mg/g was obtained. The adsorption rate of MB on chitosan flakes was kinetically described by pseudo second-order model at all initial concentrations of MB investigated, with film diffusion being the rate-controlling step and the adsorption process chemisorption-influenced. The calculated thermodynamic parameters, ΔH^0 = 4.23 kJ/mol, ΔS^0 = 0.4563 kJ/(mol K), negative ΔG^0 values revealed that the adsorption of MB onto chitosan flakes was physical, endothermic, spontaneous, energetically favorable and exergonic. The reaction mechanism of the adsorption of MB onto chitosan flakes was proposed taking cognizance of the electrostatic force of attraction between the negatively charged surface of the chitosan (biosorbent) and the positively charged MB.

Key words: chitosan, dye adsorption, isotherm, kinetics, thermodynamics, information-based criteria.

INTRODUCTION

The use of dyes in dyeing and printing processes is quite enormous, which is evident in many industries globally (Afroze et al., 2015). The perennial discharges of wastewater containing dyes from textile, dyeing, pharmaceutical, food, cosmetics and healthcare, paper and leather industries, amongst others, into the water

*Corresponding author. E-mail: oolafadehan@unilag.edu.ng.

bodies are worrisome and of great concern (Derakhshan et al., 2013) owing to their potent obstinately color and great amount of biochemical oxygen demand that is non-aesthetical to the environment (Annadurai and Krishnan, 1997). Many of these dye wastes pose serious hazards to aquatic living organisms for reason of their toxicity and even carcinogenicity and mutagenic influence on human beings. Equally, there is a reduced penetration of light as a result of their presence in water bodies thereby preventing the aqueous fauna and flora photosynthesis (Elizalde-González and Hernández-Montoya, 2009). A typical example of such dyes is methylene blue (a heterocyclic aromatic chemical compound), which is reported to be responsible for a number of health issues such as eye burn, regurgitation, shock, blue discoloration of the skin (that is, cyanosis), yellowness of the eyes, skin and urine (that is, icterus), high heart rate, among others, with much acute exposure. Consequently, environmental regulations have been enacted by many governments concerning the quality of colored effluents and thus the dye-industries have been compelled to decolorize these colored effluents before they are being discharged into the environment. Hence, much attention should be given to the treatment of dyes before discharge. However, dye producers and users generate dyestuff that is somewhat not easy to degrade after utilization. Attempt to remove them from industrial wastewater by employing the conventional treatment technologies such as trickling filter, liquid-liquid extraction, membrane filtration, chemical coagulation, activated sludge, carbon adsorption and photodegradation, whose extensive review has been provided by Vandevivere et al. (1998), is financially demanding due to their resistant biodegradable complex structure (Afroze et al., 2015; Khodaie et al., 2013). Among these treatment techniques, adsorption is highly employed owing to its flexibility, ease of operation, high performance and relatively inexpensive use, efficient regeneration and eco-friendly operating system (Vakili et al., 2014). It can equally manage quite high flow rates. Hence, during the photodegradation of wastewater-containing dyes using ultra-violet light, the generation of obnoxious substances, such as free radicals and ozone, is mitigated so that high-quality effluent results (Wang et al., 2013). Moreover, adsorption process is still a relevant and comparatively simple, viable and less expensive among other unit operations. However, its effectiveness depends largely on the adsorbents applied and the operating conditions of the process.

Many investigators have reported dyes adsorption on different adsorbents such as peat (Poots et al., 1976), wood (Poots et al., 1976; Asfour et al., 1985a; 1985b; El-Geundi, 1991), pith (McKay, 1987), activated carbon (Walker and Weatherley, 1997; Namasivayam et al., 2001a; Namasivayam and Kavitha, 2002), waste red mud (Namasivayam and Arasi, 1997; Namasivayam et al., 2001b; Namasivayam et al., 2002), fuller's earth (Atun et al., 2003), bottom ash and de-oiled soya (Mittal et al., 2010), copper oxide nanoparticle-modified activated carbon (Nekouei et al., 2015), and synthesized novel adsorbent of ZnO-NR-activated carbon (Dil et al., 2016). Other commercially-potentially adsorbents employed to treat industrial wastewater containing dyes are agricultural byproducts (Namasivayam and Kavitha, 2002; Marshall and Champagne, 1995; Marshall and Johns, 1996), miswak leaves (Elmorsi, 2011), titanium (IV) oxide surface (Gupta et al., 2011), multi-walled carbon nanotubes and titanium (IV) oxide (Saleh and Gupta, 2014). Equally, mercury-doped zinc (II) oxide nanorods (Saravanan et al., 2013a), ZnO/CuO nanocomposites (Saravanan et al., 2013b), CeO_2, V_2O_5, CuO and nanocomposite of CeO_2/V_2O_5 and CeO_2/Cu (Saravanan et al., 2013c) and zinc (II) oxide/silver nanocomposite (Saravanan et al., 2013d) have been applied for the adsorption of dyes. Also, adsorbents for the treatment of dye contaminated aqueous solution include Fe_3O_4 nanoparticles (Ghaedi et al., 2015), zinc (II) oxide/silver/Mn_2O_5 nanocomposite (Saravanan et al., 2015), carbonaceous material (Gupta et al., 2016), ZnO/CeO_2 nanoparticles (Saravanam et al., 2016), commercially used bast fibers under the names of flax, ramie and kenaf (Kyzas et al., 2018) and activated carbon coated with zinc oxide (Pourali et al., 2020). In particular, adsorbents that have been utilized for methylene blue adsorption from aqueous solution include jute fiber carbon (Senthilkumaar et al., 2005), unburned carbon (Wang et al., 2005), cedar sawdust and crushed brick (Hamdaoui, 2006), bamboo activated carbon (Hameed et al., 2007), garlic peel (Hameed and Ahmad, 2009), bentonite (Hong et al., 2009) and carbon nanotube (Yao et al., 2010). Nevertheless, some of these adsorbents showed a low-level property of methylene adsorption and have the drawbacks of inefficacious extraction of MB (Sun et al., 2011). Moreover, almost all of them become problematic with regard to recycling and reuse. Thus, a high-performance, inexpensive and easily-regenerated adsorbent is highly preferred.

In general, non-synthetic and sustainable materials are being used as cost-effective adsorbents in the process of adsorption. Biosorbents have gained wide attention owing to their somewhat plenteousness and non-toxic nature (Tran et al., 2015). Natural polymer biosorbents (such as polysaccharides, that is, chitosan and its precursor, chitin) have been favorably utilized in adsorption studies (Sarode et al., 2019). The second naturally available biopolymer after cellulose is chitin. The application of chitosan typically those derived from crustacean sources are presently considered as a good replacement for charcoal due to their high adsorption capacities under favorable conditions. However, the application of chitin on a commercial scale is limited owing to its poor solubility. Hence, soluble chitosan has been obtained from chitin by an alkaline deacetylation process (Hamed et al., 2016; Muxika et al., 2017). Chitosan is an efficacious biosorbent for the removal of a number of contaminants owing to its reactive functional groups, amine and hydroxyl groups, enriched-structure (Sharififard et al., 2018). Thus, for reason of their intrinsic characteristics, the non-synthetic polymers are usually deployed as effective biosorbents for the removal or the recovery of hazardous dyes, proteins, heavy metals, amongst others (Fan et al., 2012). So, the evaluation of adsorption capacity of chitosan from diverse sources is an area of great interest to many researchers. Chitosan has been applied in the literature (Annadurai et al., 1999; Hu et al., 2006; Annadurai et al., 2008; Hasan, 2008; Wan Ngaha et al., 2011; Fan et al., 2013; Periolatto and Ferrero, 2013; Li et al., 2014; Sheshmani et al., 2014; Shajahan et al., 2017; Ahmed et al., 2020; da Silva Alves et al., 2021) as an adsorbent for the removal of dyes from aqueous solution. However, to the best of our knowledge, none of these studies carried out an extensive investigation on the modeling of the equilibrium data of the adsorption of methylene blue on chitosan flakes from *Archachatina marginata* shell powder using 19 isotherms and 8 kinetic models coupled with statistical criteria and sum of normalized error (SNE) to select the best models. Hence, the present study reports comprehensively the adsorption of methylene blue (MB) on the prepared chitosan from *A. marginata* shell powder. The effects of operational parameters such as adsorbent dosage, pH of methylene blue solution, initial concentration of MB solution, contact time and temperature on the % removal of MB and adsorption capacity of the chitosan flakes were investigated. The fit of the experimental equilibrium adsorption data of MB to seven 2-p, eight 3-p, three 4-p and one 5-p isotherms were exhaustively carried out in this study, wherein the inherent parameters in the 19 isotherms were evaluated using linear and non-linear methods, as the case may be, to convincingly reflect the surface properties and by extension the adsorption capacity of the chitosan flakes from *A. marginata* shell powder. The kinetics of the adsorption of MB on chitosan flakes was investigated using 8 kinetic models. Moreover, sum of normalized error (*SNE*) was used to opt the most superior models amongst the isotherms and kinetic models for the adsorption of MB on chitosan flakes since *SNE* has been reported as a way or criterion for selecting the best fitted isotherm/kinetic model (Anirudhan and Radhakrishnan, 2009; Yanev et al., 2013; Popoola, 2019). Equally, in this study, Akaike information criteria (*AIC*) and model selection criterion (*MSC*) were used to select the best fitted isotherm and kinetic models for the MB adsorption on the prepared chitosan flakes. Thermodynamic parameters such as activation energy, E_a, changes in enthalpy, ∆H°, entropy, ∆s° and Gibbs free energy, ∆G°, were evaluated. The data reported in this study can be of beneficial use for the design and fabrication of an economically viable treatment process using batch reactor for MB adsorption on a biosorbent and for diluting industrial effluents.

MATERIALS AND METHODS

The analytical grade chemical reagents used in this study included NaOH pellet (99.8% purity), obtained from Merck, India and methylene blue ($C_{16}H_{18}N_3SCl$), whose molecular weight and purity are 319.85 g/mol and 98.7%, respectively, procured from Loba Chemie PVT Limited, India, ethanol (absolute 98%), hydrochloric acid (36.5-38%, specific gravity=1.18) and acetone, $CH_3C{=}O$ ($\geq$99.5% ACS), which were procured from BDH Laboratories Supplies, England. These chemicals were used without additional treatment.

Production of biosorbent

The production of the biosorbent (chitosan) used in this study from the shell wastes of *A. marginata* (African giant snail) was performed by washing the shell, drying, pulverization and following the processes of demineralization, deproteinization, deacetylation and decolorization as detailed in the works of Amoo et al. (2019), Olafadehan et al. (2020; 2021) and Bello and Olafadehan (2021).

Characterization of biosorbent

The characterization of the resulting flakes of chitosan was extensively carried out and reported elsewhere (Bello and Olafadehan, 2021). In this study, the surface point of zero charge of the prepared chitosan flakes from *A. marginata* shell was performed using the pH drift method as adopted by Banerjee and Chattopadhyaya (2013) with slight modification. 0.1 M NaCl solution was freshly prepared and 50 mL was placed in a series of 250 mL Erlenmeyer flasks and various values of pH between 2 and 12 were initiated using 0.1 M HCl and 0.1 M NaOH solutions monitored by a sensitive pH meter. 0.1 g of the chitosan flakes was discharged into the solution, which was allowed to reach equilibrium in 24 h. The solutions were filtered and the difference between the initial pH values $(pH)_i$ and final pH values, $(pH)_f$ was evaluated to obtain change in pH values, $\Delta(pH)$. The $\Delta(pH)$ values were plotted against $(pH)_i$ values. The point of intersection of the curve with the abscissa, $(pH)_i$, gives the zero-point charge value, pH_{zpc}.

Preparation of methylene blue solution

A stock solution of 1000 mg/L of methylene blue (MB) was prepared by dissolving a weighed portion of 1 g of it in 1000 cm^3 (or 1 L), from which various concentrations were obtained by serial dilution.

Batch adsorption experiment

The batch adsorption experiment considered the operational effects of adsorbent dosage, pH of MB solution, initial concentration of MB solution, contact time and temperature on the methylene blue adsorption on the prepared chitosan flakes. Each 50 mL sample of methylene blue solution was put in 250 mL capacity of Erlenmeyer flasks at specific or certain conditions. The effect of adsorbent dosage on the % removal of MB and adsorption capacity of the chitosan was studied by using the mass of the biosorbent between 0.1 and 2 g. The influence of pH was investigated in acidic and alkaline medium by varying pH values using 0.1 M HCl and 0.1 M NaOH measured by a pH meter. The effect of initial concentration of MB solution on the % removal of methylene blue (MB) was investigated by using 10 to 60 mL with a fixed amount of 0.1 g of biosorbent (chitosan) at contact time of 30 min, agitated using a mechanical orbit shaker set at 120 rev/min and ambient temperature of 30 $\pm$ 2°C. The impact of contact time was carried out within 4 h durations at a fixed mass of 0.1 g chitosan and room temperature of 30 $\pm$ 2°C. The thermodynamics study, which is hinged on the effect of variation of temperature, was carried out in water bath within the temperature ranges of 30 to 90°C at a fixed adsorbent amount of 0.1 g.

At the end of each adsorption operational batch experiments, chitosan flake particles were filtered from the suspension and the final concentration was measured by ultra-visible spectrophotometer at maximum wavelength of 650 nm.

Adsorption equilibrium isotherms

An adsorption isotherm is an empirical equation that solely gives an insight of the mechanism or phenomenon that revolves round the retention or release of a liquid phase (adsorbate) on a solid phase (adsorbent) at constant temperature (Deng and Chen, 2019). The adsorption process is said to have attained equilibrium when the adsorbate and adsorbent have been sufficiently contacted and adsorbate concentration in the bulk solution is in a dynamic balance with the interface concentration (Magdy et al., 2018). This present study uses two-, three-, four- and five- parameter isotherms to model the equilibrium sorption data of methylene blue on chitosan flakes using linear and non-linear regression methods, where appropriate.

2-p Freundlich isotherm

The 2-p Freundlich isotherm assumes a reversible adsorption that is not limited to the formation of monolayer, non-uniform distribution of heat of adsorption, heterogeneous adsorbate surface without lateral interaction and initial stronger binding sites, which reduce with increase of coverage. The empirical equation of Freundlich isotherm is of the form (Freundlich, 1906):

$$q_e = k_F c_e^{1/N} \quad (1)$$

where q_e is the weight of adsorbate adsorbed per unit weight of adsorbent at equilibrium (mg/g), c_e the residual concentration of the solute (mg/L) and k_F is a constant depending on the adsorbate and the adsorbent: it indicates the Freundlich adsorption capacity (Benzaoui et al., 2018) and the parameter, N, characterizes the homogeneity of the system (that is, the favorability of adsorption). A larger *N* value is an indication that that the system is more heterogeneous that usually results in the non-linearity of the adsorption isotherm.

Taking natural logarithms of Equation 1, we have:

$$In\ q_e = In\ k_F + \frac{1}{N} In\ c_e \quad (2)$$

The linear plot of $In\ q_e$ against $In\ c_e$ is used to test the fitness of equilibrium data to the Freundlich isotherm provided $N > 1$ and a high correlation coefficient, R^2, close to unity is obtained. Thus, the Freundlich isotherm parameters, N and k_F, can be determined from the slope $\left(= 1/N\right)$ and intercept on $In\ q_e$ axis $\left(= In\ k_F\right)$, respectively. The values of *N* between 1 and 10 are used to assess the adsorbent-adsorbate interaction (Kumar et al., 2012). The magnitude of the exponent, 1/*N*, is a measure of the nature of the adsorption process. When $1/N = 0$, the adsorption is irreversible. The adsorption is favorable (that is, indicative of chemisorption) when $0 < 1/N < 1$. It is also indicative of chemisorption and unfavourability when $1/N > 1$. Hence, if $1 < N$, favorable (or cooperative) adsorption results (Pandey and Mishra, 2011). The empirical constant, *N*, which indicates adsorption intensity, depends on the temperature and properties of the adsorbate and the adsorbent.

2-p Langmuir isotherm

Langmuir (1918) proposed an empirical model, which assumes complete monolayer adsorption, limited number of active sites, voidance of lateral interaction, homogeneous adsorbent surface with identical adsorption sites and constant heat of adsorption for all sites. The 2-p Langmuir isotherm, when applied to liquid phase adsorption, is given by:

$$q_e = \frac{q_{max} K_L c_e}{1 + K_L c_e} \quad (3)$$

where q_{max} is the Langmuir constant related to the adsorption capacity (that is, maximum adsorption capacity for the solid phase loading) (mg/g) and K_L the energy constant related to the heat of adsorption (L/mg). q_{max} can be correlated with the variation of the suitable area and porosity of the adsorbent. Hence, large surface area and pore volume result in higher adsorption capacity of the adsorbent (Olafadehan, 2021).

Five different linear forms can result from Equation 3. One of such forms used in this study is given by:

$$\frac{c_e}{q_e} = \frac{1}{q_{max}} c_e + \frac{1}{q_{max} K_L} \quad (4)$$

The linear plot of $\left(c_e/q_e\right)$ against c_e should yield a straight line with a high coefficient of regression, R^2, being close to unity if the adsorption process was described by the model. The inherent parameters, q_{max} and K_L, in the 2-p Langmuir isotherm can thus be determined from the slope $\left(= 1/q_{max}\right)$ and intercept on $\left(c_e/q_e\right)$ axis $\left(= 1/\left(q_{max} K_L\right)\right)$ respectively.

Hall et al. (1966), Weber and Chakkravortic (1974) and Malik (2004) described the essential attributes of the Langmuir model using a dimensionless constant referred to as separation factor or equilibrium parameter, R_L, given by Mahmoud et al. (2016) thus:

$$R_L = \frac{1}{1 + K_L c_0} \quad (5)$$

The factor, R_L, describes the nature of adsorption within a certain limit as either irreversible for $R_L < 1$, favorable for $0 < R_L < 1$, linear for $R_L = 1$ and unfavorable for $R_L > 1$ (Zhai et al., 2004).

2-p Temkin isotherm

The Temkin isotherm assumes that the heat of adsorption, ΔH_{ads}, of the molecules at the surface of the adsorbent decreases linearly rather than logarithmically with coverage θ, that is, $\Delta H_{ads} = (\Delta H_{ads})_0 (1 - \theta)$; homogeneous distribution of binding energies of the adsorbent surface and it takes cognizance of the adsorbate-adsorbent surface interaction (Temkin and Pyzhev, 1940). The 2-p Temkin isotherm is given by:

$$q_e = \frac{RT}{b_T} In(A_T c_e) = \frac{RT}{b_T}(In A_T + In c_e) \quad (6)$$

where b_T is Temkin constant, which is related to the heat of adsorption (J/mol) and A_T the Temkin isotherm constant (L/g). A plot of q_e against $In c_e$ should be a straight line with slope equals RT/b_T and intercept on q_e axis = $RT \, In A_T / b_T$. Hence, the two parameters, b_T and A_T, of the isotherm can be determined at the temperature of adsorption.

2-p Dubinin-Radushkevich (D-R) isotherm

The mechanism for adsorption can be expressed with a Gaussian energy distribution onto a heterogeneous surface using the 2-p Dubinin-Radushkevich model (Celebi et al., 2007; Gunay et al., 2007). It assumes a multilayer physical adsorption process that involves van der Waal's forces and is a fundamental equation that is used qualitatively for the description of the adsorption of gases and vapors onto microporous sorbents (Israel and Eduok, 2012). The 2-p Dubinin-Radushkevish isotherm is expressed as:

$$q_e = q_{DR} \exp(-\beta \varepsilon^2) \quad (7)$$

In linear form, Equation 7 becomes:

$$In q_e = In q_{DR} - \beta \varepsilon^2 \quad (8)$$

The approach was often applied to distinguish between the physisorption and chemisorption of metal ions (Dubinin, 1960; Vijayaraghavan et al., 2006), with its mean free energy, *E*, per molecule of adsorbate (for removing a molecule from its location in the adsorption space to infinity) given by:

$$E = 1 / \sqrt{2\beta} \quad (9)$$

The Polanyi potential, ε, is given by:

$$\varepsilon = RT \, In(1 + c_e^{-1}) \quad (10)$$

Using Equation 10 in Equation 8, a linear plot can be made to determine the relevant constants inherent in Dubinin-Radushkevich isotherm.

2-p Harkins-Jura (H-J) isotherm

The 2-p Harkins-Jura model accounts for the adsorption of multilayer on the surface of adsorbents having heterogeneous pore distribution. The non-linear relationship of Harkins-Jura isotherm is given by:

$$q_e = \sqrt{\frac{A_{HJ}}{B_{HJ} - \log c_e}} \quad (11)$$

where A_{HJ} and B_{HJ} are the isotherm constant parameters. On linearization of Equation 11, we have:

$$\frac{1}{q_e^2} = \frac{B_{HJ}}{A_{HJ}} - \frac{1}{A_{HJ}} \log c_e \quad (12)$$

Therefore, a straight line should be obtained from the plot of $1/q_e^2$ against $\log c_e$, which is adequate to determine the isotherm parameters, A_{HJ} and B_{HJ}, from slope $= 1/A_{HJ}$ and intercept on vertical axis = B_{HJ} / A_{HJ}.

2-p Frenkel-Halsey-Hill (F-H-H) isotherm

The 2-p Frenkel-Halsey-Hill assumes a multilayer adsorption on a heterogonous adsorbent surface. Its non-linear form is expressed as:

$$q_e = exp\left(\frac{In K_{FHH} - In c_e}{n_{FHH}}\right) \quad (13)$$

whose linear form is given by:

$$In q_e = \frac{1}{n_{FHH}} In K_{FHH} - \frac{1}{n_{FHH}} In c_e \quad (14)$$

Therefore, a straight line should be obtained from the plot of $In q_e$ against $In \, c_e$, which suffices to determine the isotherm parameters, n_{FH} and K_{FH}, from slope $= 1/n_{FHH}$ and intercept on the vertical axis = $In K_{FHH} / n_{FHH}$.

Brunauer-Emmett-Teller (BET) isotherm

The Brunauer-Emmett-Teller (BET) model is a notable representation of multilayer adsorption. It assumes that the adsorbate-adsorbent surface interaction is much larger than between neighboring molecules, the possession of homogeneous chemical properties by the adsorbent and it is applied generally for estimating the surface area of porous media (Chen et al., 2017). The non-linear form of BET isotherm is expressed as (Olafadehan, 2021):

$$q_e = \frac{q_s c_{BET} c_e}{(c_s - c_e)\left[1 + (c_{BET} - 1)\left(\frac{c_e}{c_s}\right)\right]} \quad (15)$$

where c_s is the adsorbate monolayer saturation concentration, q_s the amount of solute adsorbed in forming a complete monolayer (mg/g) and c_{BET} indicates a constant that explains the energy of interaction with the surface.

The linearized form of Equation 15 is given thus:

$$\frac{c_e}{q_e(c_s - c_e)} = \frac{1}{q_s c_{BET}} + \frac{(c_{BET} - 1)}{q_s c_{BET}}\left(\frac{c_e}{c_s}\right) \quad (16)$$

Equation 16 serves as a two-parameter BET isotherm (designated as BET1 in this current study) if the monolayer saturation concentration, c_s, was considered as a constant value (Agarwal et al., 2014; Rahmi et al., 2018; Gupta and Kumar, 2019; Sabar et al., 2020) and a three-parameter BET isotherm as a curve fitting value (designated as BET2 in this study). According to Ebadi et al. (2009), to eliminate the discrepancies associated with the value of monolayer saturation concentration widely reported, a new or modified 3-parameter BET equation was developed (designated as BET3 in this study), represented as:

$$q_e = \frac{q_m K_s c_e}{(1 - K_L c_e)(1 - K_L c_e + K_s c_e)} \quad (17)$$

where K_L is the equilibrium constant of adsorption of upper layers in BET3 isotherm (L/mg) and K_s the equilibrium constant of adsorption for the first layer in Langmuir and BET isotherms (L/mg).

3-p Redlich-Peterson isotherm

The 3-p Redlich-Peterson isotherm, given in Equation 18, fuses the Langmuir and Freundlich isotherms into a single equation (Redlich and Peterson, 1959).

$$q_e = \frac{k_{RP} c_e}{1 + \alpha_{RP} c_e^{\beta_{RP}}} \quad (18)$$

where k_{RP} and α_{RP} are the Redlich-Peterson isotherm constant parameters of units L/g and L/mg, respectively and $0 < \beta_{RP} < 1$. For $\beta_{RP} = 0$ and $\beta_{RP} = 1$, Equation 18 reduces to Henry's law (or linear adsorption) and Langmuir isotherm, respectively.

Rearranging and linearizing Equation 18, we have:]

$$\frac{c_e}{q_e} = \frac{1}{k_{RP}} + \left(\frac{\alpha_{RP}}{k_{RP}}\right) c_e^{\beta_{RP}} \quad (19)$$

The inherent parameters in the Redlich-Peterson isotherm are determined by minimizing the sum of squares of errors between the $(q_e)_{expt}$ and $(q_e)_{pred}$ values using $0 < \beta_{RP} < 1$ when a plot of (c_e/q_e) versus c_e is made with slope $[= (\alpha_{RP}/k_{RP})]$ and intercept on vertical axis $[= (1/k_{RP})]$.

3-p Tóth isotherm

The 3-p Tóth model arises from the potential theory and is mainly appropriate to describe heterogeneous adsorption systems that satisfy both low- and high-end boundaries of adsorbate concentration (Padder and Majumder, 2016). It is hinged on the presupposition of possession of a quasi-Gaussian energy distribution of the adsorbent sites, that is, the sites predominantly have adsorption energies lower than the maximum adsorption (Tóth, 1971; Padmesh et al., 2006). The non-linear form of Tóth isotherm is represented thus:

$$q_e = \frac{q_m K_T c_e}{\left[1 + (K_T c_e)^{\beta_T}\right]^{1/\beta_T}} \quad (20)$$

where K_T and β_T are the Tóth isotherm constants, which are both expressed in (mg/g). The heterogeneity of the adsorption system is characterized by the parameter, β_T (Behbahani and Behbahani, 2014). The adsorption system is said to be heterogeneous if β_T is not close to 1. The parameters, q_m, K_T and β_T, of the Tóth isotherm can be estimated by non-linear regression analysis.

3-Sips isotherm

The 3-p Sips isotherm model assumes localized adsorption void of interactions between adsorbates and fuses the Langmuir and Freundlich expressions patterned to predict the behavior of heterogeneous adsorption systems. This model eradicates the Freundlich model limitation at high concentration of adsorbate but rather gives the prediction of a monomolecular layer adsorption capacity of Langmuir isotherm and is uniquely transformed to the isotherm of Freundlich at low adsorbate concentration. The non-linear Sips isotherm is expressed thus:

$$q_e = \frac{q_{SP} K_{SP} c_e^{\beta_s}}{1 + K_{SP} c_e^{\beta_s}} \quad (21)$$

where q_{SP} and K_{SP} are the Sips isotherm model constant and $\beta_S\ (= 1/N)$ is the Sips isotherm exponent. These isotherm parameters are determined using non-linear regression analysis.

3-p Khan isotherm

The 3-p Khan model, which was developed originally for biadsorbate from simulated or pure dilute solutions, combines the features of Langmuir and Freundlich isotherms. The non-linear Khan isotherm is given by (Amrhar et al., 2015a, b):

$$q_e = \frac{q_{max} b_K c_e}{a_K \left(1 + b_K c_e\right)} \tag{22}$$

where q_{max} is the Khan isotherm maximum adsorption capacity (mg/g), a_K the Kahn isotherm exponent and b_K the Khan isotherm constant.

Linearizing Equation 22, we have:

$$\frac{1}{q_e} = \left(\frac{a_K}{q_{max} b_K}\right) \frac{1}{c_e} + \frac{a_K}{q_{max}} \tag{23}$$

Therefore, a straight line should be obtained from the plot of $1/q_e$ against $1/c_e$, with slope $= a_K / \left(q_{max} b_K\right)$ and intercept on vertical axis $= a_K / q_{max}$. Thus, the general expression for the Kahn isotherm can be obtained using Equation 22. However, non-linear regression method is employed to determine the three Khan isotherm model parameters, q_{max}, a_K and b_K.

3-p Radke-Prausnitz isotherm

The 3-p Radke-Prausnitz model is basically applied for broad range of concentration and is widely used for adsorption systems at low concentration (Ramadoss and Subramaniam, 2018). It is expressed as:

$$q_e = \frac{q_{max} K_{RPI} c_e}{\left(1 + K_{RPI} c_e\right)^{\alpha_{RPI}}} \tag{24}$$

where q_{max} is the Radke-Prausnitz maximum adsorption capacity (mg/g), K_{RPI} the Radke-Prausnitz equilibrium constant and α_{RPI} the Radke-Prausnitz model exponent. The Radke-Prausnitz model parameters, q_{max}, K_{RPI} and α_{RPI} can be obtained by non-linear statistical fit of experimental data.

3-p Fritz-Schlüender isotherm

The 3-p Fritz-Schlüender isotherm is a model that incorporates the features of Langmuir and Freundlich isotherms and it utilizes three parameters that fit a wide range of experimental data. It is expressed as (Ramadoss and Subramaniam, 2018):

$$q_e = \frac{\left(q_m\right)_{FS} K_{FS} c_e}{1 + \left(K_{FS} c_e\right)^{\alpha_{FS}}} \tag{25}$$

where $\left(q_m\right)_{FS}$ is Fritz-Schlüender maximum adsorption capacity, K_{FS} the Fritz-Schlüender equilibrium constant and α_{FS} the Fritz-Schlüender isotherm exponent. The 3-p Fritz-Schlüender isotherm parameters can be determined by non-linear regression analysis.

4-p Fritz-Schlüender isotherm

The 4-p Fritz-Schlüender is an empirical model that integrates the Langmuir and Freundlich isotherms and is given thus (Hamdaoui and Naffrechoux, 2007):

$$q_e = \frac{A_{FS} c_e^{\Phi_{FS}}}{1 + B_{FS} c_e^{\beta_{FS}}} \tag{26}$$

The model is valid only when Φ_{FS} and $\beta_{FS} \leq 1$. The 4-p Fritz-Schlüender isotherm parameters can be determined by non-linear regression analysis.

4-p Bauder isotherm

The 4-p Bauder model was borne out of the need to accurately account for the differences in the course of calculating Langmuir constant and coefficient over a wide range of certain specifications linked to its parameters. It is given by:

$$q_e = \frac{\left(q_m\right)_B b_0 c_e^{1+x+y}}{1 + b_0 c_e^{1+x}} \tag{27}$$

where $\left(q_m\right)_B$ is Bauder maximum adsorption capacity, b_0 the Bauder equilibrium constant, *x* and *y* are the Bauder isotherm parameters. Owing to the inherent bias resulting from linearization, the 4-p Bauder isotherm parameters can be obtained by non-linear regression analysis. However, its application must satisfy the conditions of $\left(1 + x + y\right) < 1$ and $\left(1 + x\right) < 1$.

4-p Marczewski-Jaroniec isotherm

The 4-p Marczewski-Jaroniec model considers the local Langmuir isotherm and takes into cognizance the distribution of adsorption energies associated with the active sites of adsorbent for low and high value cases of the process. It is expressed as (Ayawei et al., 2017):

$$q_e = \left(q_m\right)_{MJ} \left[\frac{\left(K_{MJ} c_e\right)^{\alpha_{MJ}}}{1 + \left(K_{MJ} c_e\right)^{\alpha_{MJ}}}\right]^{\beta_{MJ}/\alpha_{MJ}} \tag{28}$$

where $\left(q_m\right)_{MJ}$ is Marczewski-Jaroniec maximum adsorption capacity, K_{MJ} the Marczewski-Jaroniec equilibrium constant, the heterogeneity of the adsorbent surface is characterized by the Marczewski-Jaroniec isotherm parameters, α_{MJ} and β_{MJ} : α_{MJ} and β_{MJ} give the description of the spreading of distribution in the path of less and higher adsorption energies respectively. The 4-p Marczewski-Jaroniec isotherm parameters, $\left(q_m\right)_{MJ}$, K_{MJ}, α_{MJ}

and β_{MJ} , are obtained by non-linear regression analysis.

5-p Fritz-Schlüender isotherm

The 5-p Fritz-Schlüender isotherm was proposed to simulate accurately variations in isothermic model such that it can be applied over a large range of equilibrium data. It is given by:

$$q_e = \frac{(q_m)_{FS5} K_{FS5} c_e^{\alpha_{FS5}}}{1 + \Phi_{FS5} c_e^{\beta_{FS5}}} \quad (29)$$

where $(q_m)_{FS5}$ is Fritz-Schlüender maximum adsorption capacity. The 5-p Fritz-Schlüender isotherm parameters, $(q_m)_{FS5}$, K_{FS5} , Φ_{FS5} , α_{FS5} and β_{FS5} , are estimated by non-linear regression analysis.

Batch reactor design

The aim of the prototype is to determine the mass of the prepared chitosan flakes (adsorbent), *m*, required to remove the adsorbate (methylene blue) from solution of volume, *V*, at near real environmental initial concentration of c_0 to relatively allowable levels of concentration, c_e . However, the design of single solute batch adsorption systems can be facilitated by adsorption isotherms and equilibrium data. Based on the applicable adsorption isotherm, the mass of adsorbent required to realize specified percentage removal efficiency, *R*, from aqueous solution of volume *V* for a known initial concentration of the adsorbate, except for 100% removal efficiency, is derived in this study. The adsorption percentage, R , adsorption capacity values at equilibrium, q_e , and at time *t*, q_t , are determined using Equations 30 to 32, respectively:

$$R = \left(\frac{c_0 - c_e}{c_0} \right) \times 100 \quad (30)$$

where c_0 is initial concentration of methylene blue solution (adsorbate), and c_e the concentration of adsorbate at equilibrium, both of units, mg/L.

$$q_e = \left(\frac{c_0 - c_e}{m} \right) V \quad (31)$$

$$q_t = \left(\frac{c_0 - c_t}{m} \right) V \quad (32)$$

where c_t is the concentration of adsorbate at time *t*, expressed in mg/L, *m* the mass of adsorbent (g), V volume of aqueous solution in contact with the adsorbent (L).

From Equation 30, we obtain:

$$c_e = c_0 (1 - R/100) \quad (33)$$

Combining Equations 30 and 31, we have:

$$q_e = RVc_0 / 100m \quad (34)$$

Equations 33 and 34 can now be used in the isotherm that correlates the equilibrium adsorption data to determine the mass of adsorbent required to achieve certain percentage removal of adsorbate from solutions of varied volumes (say, 1-20 L) at ambient temperature in a mono-solute batch reactor system. Olafadehan (2021) obtained Equation 35 assuming the adsorption equilibrium data are correlated using Langmuir isotherm.

$$m = \frac{V \times R \times c_0 \{1 + K_L \{c_0 [1 - (R/100)]\}\}}{100 q_{max} K_L \{c_0 [1 - (R/100)]\}} \quad (35)$$

Adsorption kinetics

The adsorption kinetics describes rate of uptake of the solute, which, in turn, influences the residence time of the uptake of the adsorbate at the solid-solution interface. Thus, it is imperative to understand the reaction mechanism for the sorption process in a bid to design appropriately the sorption treatment plants. So, the adsorption kinetics is a major issue in the design of a treatment system using adsorbent. Moreover, it is used to establish the controlling step in an adsorption process. Adsorption kinetics provides information to relational industry operators and planners that can be used to effectively treat the contaminated wastewater by adsorption since rapid adsorption of the solute in an adsorption system is desirable and beneficial for actual or industrial applications. The kinetic parameter, which aids the prediction of the rate of adsorption and equilibrium time, gives significant information for designing and modeling the adsorption processes (Sivarajasekar and Baskar, 2014). The adsorption kinetics investigated in this study are illustrated in the following.

Fractional power model

The fractional power model can be expressed in the form of Freundlich equation, which indicates that the uptake of the adsorbate (or solute) increases exponentially with time. It is given by:

$$q_t = k_f t^v \quad (36)$$

where q_t is the amount of solute adsorbed per weight of adsorbent at time *t* (mg/g); v the fractional order, k_f is the fractional power kinetic model constant (mg/(g min^v)) and *t* time of adsorption (min).

Taking natural logarithms of Equation 36 gives:

$$In\, q_t = In\, k_f + v\, Int \quad (37)$$

Therefore, a plot of $In\ q_t$ against $In\ t$ can be made to determine the parameters, v and k_f , from the slope and intercept on the vertical axis, respectively.

Lagergren pseudo first-order kinetic model

The Lagergren pseudo first-order kinetic model, expressed in Equation 38, describes the adsorption of solutes onto adsorbents following the first-order mechanism (Ho, 2004):

$$\frac{dq_t}{dt}=k_1(q_e-q_t) \tag{38}$$

where k_1 the Lagergren pseudo first-order rate constant (min^{-1}).

The integral of Equation 38 from $t=0$, $q_t=0$ to $t=t$, $q_t=q_t$ yields the non-linear form:

$$q_t=q_e\left(1-e^{-k_1t}\right) \tag{39}$$

The linearized form of Equation 39 is:

$$In(q_e-q_t)=In\,q_e-k_1t \tag{40}$$

Therefore, a straight line should be obtained from the plot of $In(q_e-q_t)$ against t, which is adequate to determine k_1.

Pseudo second-order kinetic model

The pseudo second-order kinetic model assumes the adsorption of solutes onto adsorbents follows the second-order mechanism and is given by:

$$\frac{dq_t}{dt}=k_2(q_e-q_t)^2 \tag{41}$$

where k_2 is the specific reaction rate constant for the pseudo second-order kinetics (g/(mg min)), which can be used to calculate the initial sorption rate, h, [=] mg/(g min) thus:

$$h=k_2q_e^2 \tag{42}$$

When integrated, Equation 41 yields:

$$q_t=\frac{k_2q_e^2t}{1+k_2q_et} \tag{43}$$

Linearization of Equation 43 yields different forms. One of such linear forms employed in this study is:

$$\frac{t}{q_t}=\frac{1}{k_2q_e^2}+\frac{t}{q_e} \tag{44}$$

Therefore, a straight line should be obtained from the plot of (t/q_t) against *t*, which is adequate to determine k_2.

Elovich kinetic model

The Elovich kinetic model describes adsorption process in a non-ideal state and on chemisorption phenomena (Gupta and Kumar, 2019) and is given by:

$$\frac{dq_t}{dt}=\alpha\exp(-\beta q_t) \tag{45}$$

where α and β are constants during an experiment. As $q_t\rightarrow 0,\ dq_t/dt\rightarrow\alpha$. Hence, α is regarded as the initial rate of adsorption. Equation 45, when integrated using the conditions $t=0,\ q_t=0$ and $t=t,\ q_t=q_t$, yields:

$$q_t=\frac{1}{\beta}\left[In(t+\Phi)-In\,\Phi\right] \tag{46}$$

where $\Phi=1/(\alpha\beta)$. If $t>>\Phi$, Equation 46 simplifies to:

$$q_t=\frac{1}{\beta}In(\alpha\beta)+\frac{1}{\beta}In\,t \tag{47}$$

Therefore, a straight line should be obtained from the plot of q_t against $In\,t$ to check if $t>>\Phi$ for the coefficient of determination, R^2, should be greater than 1. This allows the determination of β (g/mg) and α (mg/(g min)) from the slope and intercept on vertical axis respectively.

Avrami kinetic model

The Avrami kinetic model, also known as the Johnson-Mehl-Avrami-Kolmogorov (JMAK) model, was first derived by Kolmogorov et al. (1937) and popularized by Avrami (1939, 1940, 1941). The Avrami kinetic model assumes random nucleation sites across the reaction surface of the adsorbent and it evaluates changes in kinetic parameters as function of reaction time and temperature. The non-linear form of the expression is given as (Ahmad et al., 2014; Yoro et al., 2017):

$$q_t=q_e\left[1-\exp\left(-k_{AV}t^{n_{AV}}\right)\right] \tag{48}$$

where k_{AV} is the Avrami rate constant ($\min^{-n_{AV}}$) and n_{AV} is a dimensionless constant related to the mechanism of adsorption with regard to temperature and contact time.

Taking the natural logarithms of Equation 48, we have:

$$-In\left(1-\frac{q_t}{q_e}\right)=k_{AV}t^{n_{AV}} \tag{49}$$

To enable determination of the inherent kinetic parameters in the Avrami kinetic model, another natural logarithmic approach is applied to Equation 49 to yield:

$$In\left[-In\left(1-\frac{q_t}{q_e}\right)\right]=In\,k_{AV}+n_{AV}In\,t \tag{50}$$

which allows the determination of the constants, n_{AV} and k_{AV}, from a plot of $In\left[-In\left(1-\frac{q_t}{q_e}\right)\right]$ against Int. If the transformation followed the Avrami equation, this yields a straight line with slope = n_{AV} and intercept on vertical axis $= In\,k_{AV}$, from which k_{AV} can be determined.

Adsorption is largely over when (q_t/q_e) reaches values close to 1, which will be at an adsorption time, t_a, defined by $k_{AV}(t_a)^{n_{AV}} \approx 1$ as then the exponential term in the above expression for (q_t/q_e) will be small. Thus, adsorption takes a time of order:

$$t_a = 1.0116 \Big/ \left(k_{AV}\right)^{1/n_{AV}} \quad (51)$$

Therefore, adsorption takes a time that decreases as one over the one-quarter power of k_{AV}.

Intraparticle diffusion (IPD) (or Weber-Morris) model

The intraparticle diffusion (IPD) (or Weber and Morris) model, given in Equation 51, is employed to establish the diffusion mechanism involved in the adsorption process.

$$q_t = k_{IPD}\sqrt{t} + C \quad (52)$$

where k_{IPD} is the intraparticle diffusion rate constant (mg/(g min^{½})) and *C* is a constant (mg/g). The intraparticle diffusion rate constant, k_{IPD}, can be estimated from the slope of q_t - $\sqrt{t}$ plot, which ought to be a straight line passing through the origin $(C=0)$ if IPD model could be employed to describe the kinetics of the adsorption process.

The intraparticle diffusion model has attracted many researchers because of the multi-linearity the plot of Equation 52 gives. Malash and El-Khaiary (2010) suggested the use of piecewise regression in expressing adequately the model. The piecewise regression is a special type of linear regression that is used when a single line is insufficient to model a data set marked with multi-linearity. It allows multiple linear models to be fitted to the data for different independent variables. For a two-segment form, the expression is given as:

$$y_i = \beta_0 + \beta_1 x_{i1} + \beta_2\left(x_{i1} - x^{(k)}\right)x_k \quad (53)$$

where x_{i1} is the independent variable value, $x^{(k)}$ the knot value and x_k the knot dummy variable is expressed as:

$$x_k = \begin{cases} 0 & if \;\; x_{i1} \le x^{(k)} \\ 1 & if \;\; x_{i1} > x^{(k)} \end{cases} \quad (54)$$

In this investigation, Equation 52 is tagged IPD-1 segment and Equation 53 is named IPD-2 segment.

Boyd model

Though the Boyd et al. (1947) diffusion model was developed theoretically for ion-exchange kinetics, it had been applied successfully to adsorption studies (Morrison and Boyd, 2004; Castillejos et al., 2011; El-Khaiary and Malash, 2011; Olafadehan et al., 2018) to establish the exact rate-limiting step involved in the adsorption process due to the two-mass transfer processes of solute, which are film and pore diffusion. The Boyd model assumes that the boundary layer surrounding the adsorbent has a greater effect on the diffusion of solute. The Boyd's model is given by:

$$F_B(t) = \frac{q_t}{q_e} = 1 - \frac{6}{\pi^2}\sum_{n=1}^{\infty}\frac{1}{n^2}\exp\left(-n^2 Bt\right) \quad (55)$$

where $F_B(t)$ is dimensionless fraction of solute adsorbed at time *t*, $B = \pi^2 D \big/ R_p^2$: D the effective intraparticle diffusion coefficient (m^2/s) and R_p radius of adsorbent particle (m).

If intraparticle diffusion was the rate-controlling step in the adsorption process, Equation 52 is valid with $C=0$. Reichenberg (1953) obtained approximate expressions given by Equations 56 and 58 via the application of Fourier transform and then integration of Equation 55:

$$F_B(t) = 1 - \frac{6}{\pi^2}\exp\left(-Bt\right),\; F_B(t) > 0.85 \quad (56)$$

That is,

$$Bt = -In\left[1 - F_B(t)\right] - 0.4977,\; F_B(t) > 0.85 \quad (57)$$

$$Bt = \left(\sqrt{\pi} - \sqrt{\pi - \frac{\pi^2 F_B(t)}{3}}\right)^2,\; F_B(t) \le 0.85 \quad (58)$$

The value of B can be determined using Equation 57 or 58 for each and every value of $F_B(t)$, depending on the conditions given and the Boyd plots (*B*–*t*) constructed (Olafadehan et al., 2018; Ho et al., 2002). The distinction between intraparticle transport-controlled rates of adsorption and the film diffusion (external transport) is revealed by the linearity of the *B*–*t* plots (Olafadehan et al., 2018; Wang et al., 2006). If the adsorption process was controlled by intraparticle diffusion, a straight line passing through the origin would be obtained; otherwise, film diffusion governs the adsorption process (El-Khaiary and Malash, 2011; Olafadehan et al., 2018; Mohan and Singh, 2002; Sharma and Das, 2012).

Diffusion-chemisorption model

The diffusion-chemisorption model assumes that the adsorption or uptake of adsorbate is under the influences of both diffusion and chemisorption. This model was originally used for the uptake of heavy metals on heterogeneous surface (Sutherland and

Venkobachar, 2010). The non-linear form of the diffusion-chemisorption model is given by:

$$\frac{q_e^2}{(q_e - q_t)} = k_{DC}\sqrt{t} + q_e \quad (59)$$

where k_{DC} (mg/(g min$^{-0.5}$)) is the diffusion-chemisorption parameter related to the initial sorption rate, k_i (mg/(g min)) by assuming a linear region as $t \rightarrow 0$ using the empirical relationship:

$$k_i = \frac{k_{DC}^2}{q_e} \quad (60)$$

The linear form of Equation 59 amenable for the determination of k_{DC} and q_e by plotting $\sqrt{t}/q_t$ against $\sqrt{t}$ is expressed in Equation 61:

$$\frac{\sqrt{t}}{q_t} = \frac{1}{q_e}\sqrt{t} + \frac{1}{k_{DC}} \quad (61)$$

Error functions

The minimization of the error distribution between the experimental equilibrium data and the predicted isotherms/adsorption kinetics can be determined via error functions' values. Depending on definition of the error function, the error distribution between the experimental equilibrium data and the predicted values is minimized either by the minimization or maximization of the error function. Thus far, no detailed studies are available to compare the accuracy of the error functions in predicting the isotherm/kinetic parameters and also the optimum isotherm/kinetics. The various error functions used in this study for the comparison of the experimental and predicted equilibrium adsorption data are shown in Table 1 where $Q_{k,expt}$ [= $(q_e)_{k,expt}$ or $(q_t)_{k,expt}$] is the measured adsorption data for run *k*, $Q_{k,pred}$ [= $(q_e)_{k,pred}$ or $(q_t)_{k,pred}$] the predicted (or calculated) adsorption data for run *k*, N_e the number of experimental data points and N_p the number of model parameters.

Information-based criteria

The information-based criteria (IC) are criteria for selecting the best fitted isotherm and kinetic model through the use of statistical tools such as Akaike Information Criterion (AIC), Schwarz Bayesian Information Criterion (SBIC), Khinchin's law of Iterated Logarithm Criterion (KLILC), among others (Dávila-Jiménez et al., 2014). The model selection depends on the sample size. The criteria estimate loss of information that a model records as a measure of distance from the true model (Alston et al., 2015). The SBIC and KLILC are usually used for large sample data while AIC are used for both large and small sample data. In the present work, only AIC are employed for both the adsorption isotherm and the kinetic studies.

Akaike information criteria

The *AIC* were developed by Akaike (1974). They are statistical tools that have been adopted for selecting the most fitted model amongst competing models with a varying number of parameters (Akpa and Unuabonah, 2011; Turner et al., 2015; Nayak and Pal, 2019). According to Nayak and Pal (2019), with the assumption of independent model errors and normal error distribution, the equation for using *AIC* is expressed as follows:

$$A_{IC} = 2N_p - N_e \, In\left(\frac{ERRSQ}{N_e}\right) \quad (62)$$

Sugiura (1978) and Hurvich and Tsai (1989) modified and advanced the model for a small data in which $(N_e/N_p) < 40$ as follows (Nayak and Pal, 2019):

$$(A_{IC})_{mod} = A_{IC} + \left[\frac{2N_p(N_p+1)}{N_e - N_p - 1}\right] \quad (63)$$

The use of Akaike weights, λ_i, and strength of evidence, *ER*, gives one greater insight into the relative merits of the competing models (Turner et al., 2015; Wagenmakers and Farrell, 2004; Ibrahim et al., 2018). The Akaike weight, λ_i, is expressed as:

$$\lambda_i = \frac{\exp(-0.5\Delta A_{IC})}{\sum_{k=1}^{n}\left[\exp - 0.5(\Delta A_{IC})_k\right]} \quad (64)$$

$$(\Delta A_{IC})_k = (A_{IC})_k - (A'_{IC})_k \quad (65)$$

$$ER = \frac{1}{\exp\left[-0.5(\Delta A_{IC})_k\right]} \quad (66)$$

where $(\Delta A_{IC})_k$ denotes the differences between the value of $(A_{IC})_k$ for the *kth* model and the minimum $(A_{IC})_k$ value of the best ranked model, denoted by $(\Delta A'_{IC})_k$.

Model selection criterion

The model selection criterion is a statistic that expresses a function for assessing competing models vying for the best fitted model and it is expressed as (Adekunbi et al., 2019):

$$MSC = In\left(\frac{ESS}{SSE}\right) - \frac{2P}{N} \quad (67)$$

$$ESS = \sum_{k=1}^{N_e}\left(Q_{k,pred} - \overline{Q}_{k,pred}\right)^2 \quad (68)$$

where *MSC* is the model selection criterion, *ESS* the sum of squares

Table 1. Mathematical expressions for error functions.

S/N	Error functions	Model	Reference
1	Coefficient of determination, R^2	$R^2 = 1 - \frac{\sum_{k=1}^{N_e}\left(Q_{k,expt} - Q_{k,pred}\right)^2}{\sum_{k=1}^{N_e}\left(Q_{k,pred} - Q_e\right)^2}$	Olafadehan (2021)
2	Average relative error, *ARE*	$ARE = \frac{100}{N_e}\sum_{k=1}^{N_e}\left\lvert\frac{Q_{k,expt} - Q_{k,pred}}{Q_{k,expt}}\right\rvert$	Chan et al. (2012)
3	Standard deviation of relative errors, *SRE*	$SRE = \sqrt{\frac{1}{N_e}\sum_{k=1}^{N_e}\left[\left(Q_{k,expt} - Q_{k,pred}\right) - ARE\right]^2}$	Popoola (2019)
4	Marquardt's percent standard deviation, *MPSD*	$MPSD = 100\sqrt{\frac{1}{N_e - N_p}\sum_{k=1}^{N_e}\left(1 - \frac{Q_{k,pred}}{Q_{k,expt}}\right)^2}$	Chan et al. (2012)
5	Normalized standard deviation, *NSD*	$NSD = 100\sqrt{\frac{1}{N_e - 1}\sum_{k=1}^{N_e}\left(\frac{Q_{k,expt} - Q_{k,pred}}{Q_{k,expt}}\right)^2}$	Ahmad et al. (2014)
6	Residual Root Mean Square Error, *RMSE*	$RMSE = \frac{1}{N_e - 2}\sqrt{\sum_{k=1}^{N_e}\left(Q_{k,expt} - Q_{k,pred}\right)^2}$	Alston et al. (2015)
7	Normalized chi-square test, χ^2	$\chi^2 = \sum_{k=1}^{N}\left[\frac{\left(Q_{k,expt} - Q_{k,pred}\right)^2}{Q_{k,expt}}\right]$	Amrhar et al. (2015a, b)
8	Sum of squares of the errors, *ERRSQ*	$ERRSQ = \frac{1}{N_e}\sum_{k=1}^{N_e}\left(Q_{k,expt} - Q_{k,pred}\right)^2$	Amrhar et al. (2015a, b)

Table 1. Contd.

9	Sum of absolute error, *EABS*	$EABS=\sum_{k=1}^{N_p}\left(Q_{k,expt}-Q_{k,pred}\right)$	Chan et al. (2012)
10	Hybrid functional error, *HYBRID*	$HYBRID=\frac{100}{N_e-N_p}\sum_{k=1}^{N_e}\left[\frac{\left(Q_{k,expt}-Q_{k,pred}\right)^2}{Q_{k,expt}}\right]$	Olafadehan (2021)

due to regression, that is, the sum of the squares of the difference of the predicted values and the mean value of the response variable and $\overline{Q}_{k,pred}$ is the mean of the predicted values.

Thermodynamics studies

The thermodynamic features and parameters (such as change in Gibbs free energy, ΔG^0, enthalpy change, ΔH^0, entropy change, ΔS^0) of the adsorption of methylene blue on chitosan flakes were determined using Equations 69 and 70 (Erdem et al., 2004; He et al., 2010; Hefni et al., 2019):

$$K_d=\left(\frac{c_0-c_e}{c_e}\right)\times\frac{V}{M} \quad (69)$$

$$\Delta G^0=\Delta H^0-T\Delta S^0=-RT\,In\,K_d \quad (70)$$

where K_d is the distribution coefficient (mL/g) and $c_d\left(=c_0-c_e\right)$ the concentration of MB on chitosan flakes (mg/L). From Equation 70, the linear plot of $In\,K_d$ against T^{-1} enables ΔH^0 and ΔS^0 to be obtained from the slope $\left[=\left(-\Delta H^0/R\right)\right]$ and intercept on vertical axis $\left[=\left(\Delta S^0/R\right)\right]$, respectively.

The modified Arrhenius type equation is used to relate the sticking probability, S^*, to surface coverage, θ, thus (Najim et al., 2010):

$$S^*=(1-\theta)\exp\left(-\frac{E_a}{RT}\right) \quad (71)$$

Where

$$\theta=1-\frac{c_e}{c_0} \quad (72)$$

The linearized form of Equation 71 is given as:

$$In(1-\theta)=\frac{E_a}{RT}+In\,S^* \quad (73)$$

Hence, the linear plot of $In(1-\theta)$ against T^{-1} enables the activation energy, E_a, and S^* to be obtained from the slope and intercept on vertical axis, respectively.

RESULTS AND DISCUSSION

Characterization of chitosan flake

The physicochemical properties of the prepared chitosan flakes from *A. marginata* shell powder, which included moisture, ash, fiber and protein contents, average molecular weight and apparent viscosity, were reported in our recent work to be 5.5%, 0.25%, 2.70, (0.85 ± 0.27%), 220 kDa and (85.20 cP at 20°C), respectively (Bello and Olafadehan, 2021). Other properties of the chitosan flakes obtained in this study are particle size =150 µm, bulk density = 0.9 g/cm^3, pH = 7.3 and pHpzc = 7.8. Equally, the morphological features of the chitosan flakes were assessed using Scanning Electronic Morphology (SEM) at 10,000 and 11,000 magnifications in our investigation (Bello and Olafadehan, 2021). It was revealed in Bello and Olafadehan (2021) that the surfaces of the shell of *A. marginata* and the chitosan flakes possessed cavities, pores and rough surfaces, which are viable characteristics of a typical adsorbent such as chitosan flakes. Also, the Electron Dispersive X-ray Spectroscopy (EDS) spectrum and the distribution of chemical elements in the grated *A. marginata* shell waste revealed that the precursor contained the highest weight % of calcium (53.35) and least weight % of iron (0.52) with weight % of oxygen, silica, sodium, magnesium, phosphorus and carbon being 3.20, 1.72, 2.24, 3.32, 13.10 and 2.45, respectively (Bello and Olafadehan, 2021). The X-ray diffraction (XRD) of the prepared chitosan

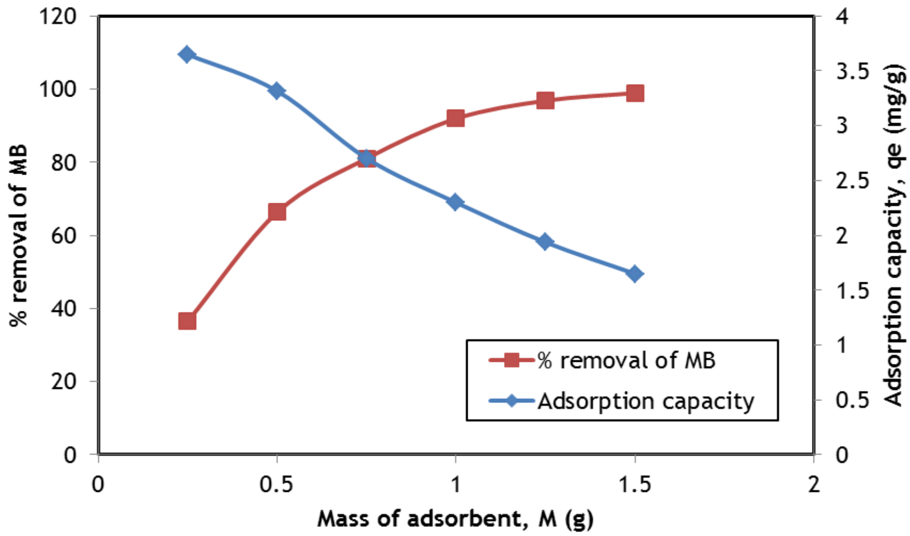

Figure 1. Effect of adsorbent dosage on removal efficiency and adsorption amount.

flakes indicated the crystalline natures of the biopolymer, where well-defined peaks, conspicuously among others at 2θ = 20 and 26°, were obtained (Bello and Olafadehan, 2021). In addition, the Fourier transform infrared spectroscopy (FT-IR) spectrophotometer (IS10, Thermo Nicolet, USA) in the wave number range of 4000-400 cm^{-1} with KBr pellet was used to determine the absorption bands and subsequent functional groups for *A. marginata* shell and the chitosan flakes before and after adsorption of methylene blue (Bello and Olafadehan, 2021). We showed that there was an interaction between methylene blue (MB) and the chitosan flakes and the adsorption was accomplished for reason of the significant differences in absorbance wavelength coupled with an increase in the absorbance wavelength of the amide and hydroxyl groups being responsible for the efficacious adsorption of methylene blue on the prepared chitosan flakes from *A. marginata* shell powder.

Effects of operational parameters on MB adsorption

Effect of adsorbent dosage

Figure 1 depicts the respective effects of the mass of adsorbent (chitosan flakes), *M*, on the removal efficiency of the chitosan flakes and the equilibrium adsorption capacity, q_e. It is revealed in the figure that the percentage removal of MB increases appreciably with increase in adsorbent mass owing to the fact that an increase in adsorbent mass leads to an increase in the number of active sites, except for cases of overlapping of adsorption sites or due to the screening effect occasioned by overcrowding of adsorbent where the percentage removal of the target pollutant shows no further increase (Benzaoui et al., 2018).

It was observed in Figure 1 that the adsorption capacity decreases with a corresponding increase in the dosage of the adsorbent. This is as a result of entire exposure of the actives sites at low amount of adsorbent dose while a few fractions were exposed at higher dose of the chitosan flakes (Alghamdi et al., 2019).

Effect of solution pH

The influence of pH of methylene blue solution on adsorption capacity, q_e, of the chitosan flakes and % removal of MB was investigated by varying the solution pH values for an initial concentration of MB of 100 mg/L at 303 K. Figure 2 reveals that the pH of solution influences appreciably the percentage of MB molecules adsorbed on the chitosan flakes and the adsorption capacity of the chitosan flakes within a pH range of 2 to 12 considered. The percentage removal of MB increases from 49.82 to 98.95 at solution pHs of 2.4 and 11.8, respectively largely due to the pH of zero point charge (pHzpc) of the adsorbent measured at 7.3. At a solution pH lower than zero-point charge $(pH < pH_{zpc})$, the surface charge of the adsorbent becomes positively charged and initiates the presence of hydrogen ions, which heightened the competition between the MB cations and the hydrogen ions on the active site of the adsorbent. Thus, % removal of MB as well as the adsorption capacity is low. Conversely, at higher solution pH, the surface charge of the adsorbent becomes negatively charged owing to the large presence of hydroxyl ions, which eventually paved way for less competition and facilitates the electrostatic forces of attraction between the cations of MB on the much available actives sites (Bernal et al., 2017; Boumediene

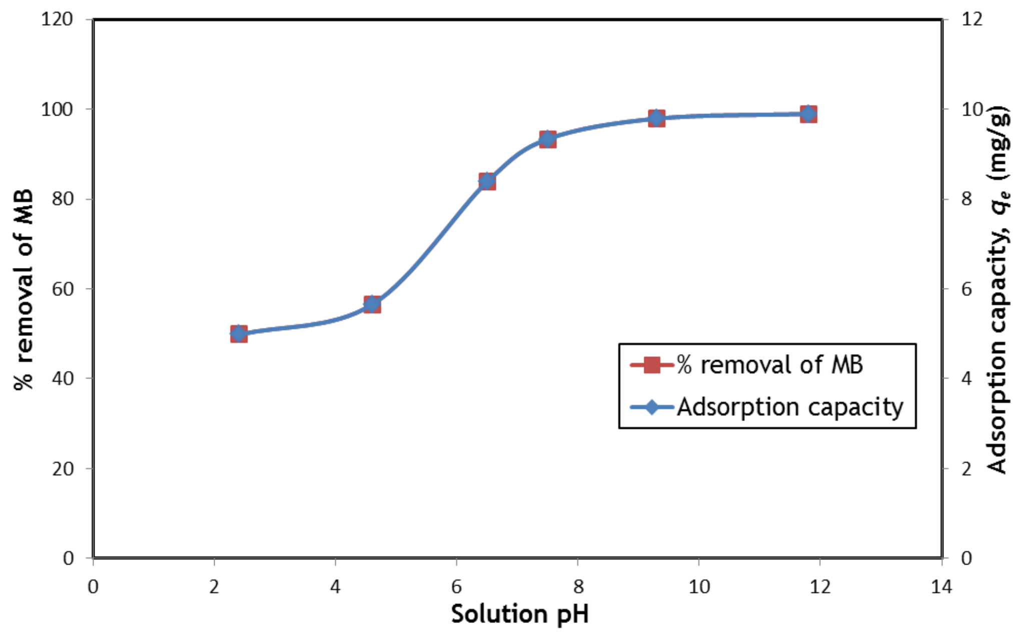

Figure 2. Effect of solution pH on removal of MB on chitosan flakes and adsorption capacity.

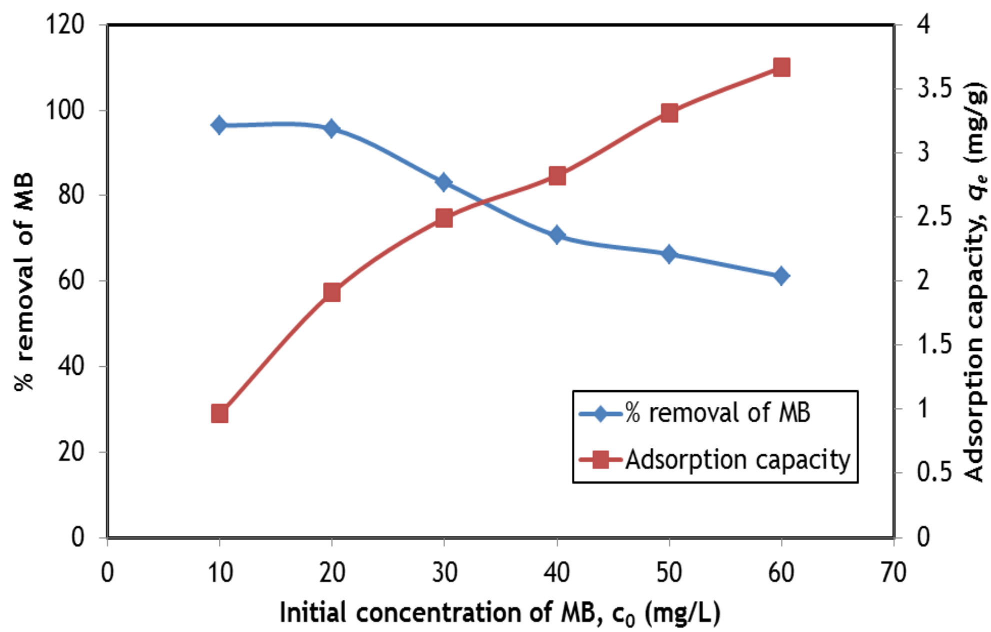

Figure 3. Effect of initial concentration of MB on adsorption capacity and % removal of MB.

et al., 2018). Thus, a relatively high amount of MB adsorbed on the chitosan flakes as well as adsorption capacity was achieved.

Effect of initial MB concentration

The respective effects of the initial methylene blue concentrations on the % removal of MB and adsorption capacity of the chitosan flakes were shown in Figure 3. The percentage removal of MB decreases from 96.49 to 61.11 as the initial concentration of MB increases from 10to 60 mg/L while the amount of MB adsorbed per unit mass of chitosan flakes increases significantly from 0.9641 to 3.67 mg/L as the initial MB concentration increases from 10 to 60 mg/L as a result of the

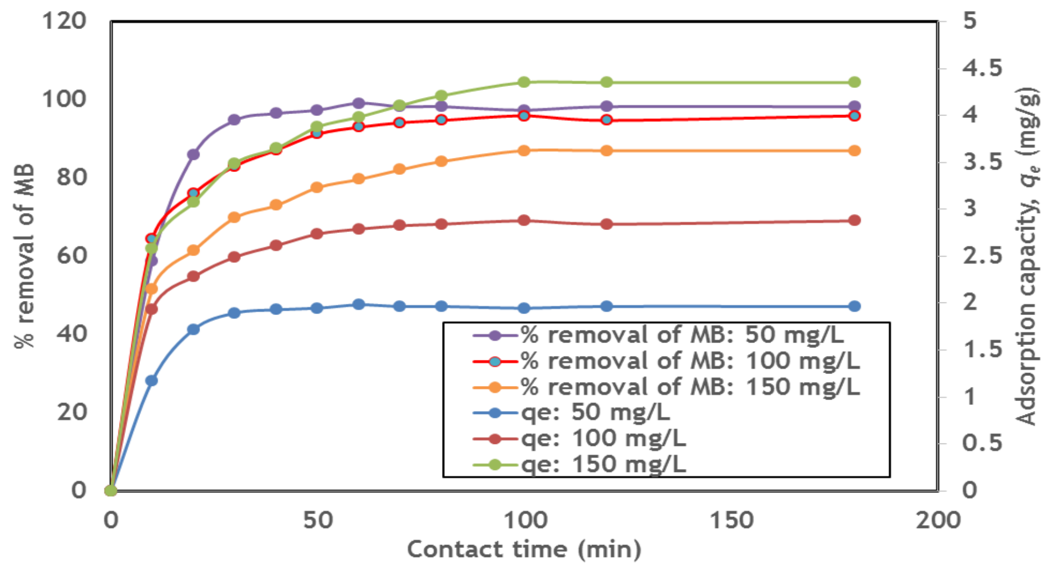

Figure 4. Effect of contact time on the adsorption amount and removal efficiency of MB using chitosan flakes at pH = 8.2, adsorbent dose of 0.1 g and varying initial concentrations, c_0, of 50, 100 and 150 mg/L.

unavailable requisite number of active sites to cater for the increased initial concentration of MB (Edet and Ifelebuegu, 2020).

Effect of contact time

The contact time is an influential factor and a key parameter for design, management and operation of wastewater treatment. Figure 4 shows the amount of MB adsorbed per unit mass of chitosan flakes and percentage removal of MB against contact time at a temperature of 30°C, pH of 8.2, adsorbent dose of 0.1 g and varying initial MB concentrations, c_0, of 50 mg, 100 mg/L and 150 mg/L. It was observed that the first phase of adsorption of MB on the chitosan flakes, which is characterized by a steeper gradient, depicts an increment in the percentage removal of MB and the amount of MB adsorbed per unit mass of the chitosan flakes as the contact time increases until the second phase, which is recognized as the equilibrium stage, was attained. During the first phase, the enormous number of vacant active sites is available for the adsorption of MB molecules on the chitosan flakes. However, at the second stage in the adsorption process characterized with a plateau, there are no significant observable changes in both the % removal of MB and the adsorption capacity of the chitosan flakes due to the few available sites and possible repulsive forces between MB molecules adsorbed on the chitosan flakes and the solution phase ((Edet and Ifelebuegu, 2020; Slimani et al., 2011). Equilibrium times were established at 70, 80 and 100 min with % removal of MB of 98.2, 94.7 and 87 at initial concentrations of MB of 50, 100 and 150 mg/L respectively. In a similar fashion, the amount of MB molecules adsorbed per unit mass of the chitosan flakes at the respective established equilibrium times was obtained as 1.96, 2.84 and 4.35 mg/g for 50, 100 and 150 mg/L. These results imply that the higher the initial concentration of MB, the higher the equilibrium time and conversely (Kuang et al., 2020).

Effect of temperature

The respective effects of temperature on the percentage adsorption of MB ions and the adsorption capacity of the chitosan flakes are depicted in Figure 5. It was observed that the percentage removal of MB and adsorption capacity of the chitosan flakes reduce as the temperature increases. These obvious trends lend credence to the fact that the adsorption process is favored at low temperature and inimical at high temperature. From literature, this equally inferred that the process of adsorption is an exothermic one, which is in consonance with the thermodynamics parameters estimated (Edet and Ifelebuegu, 2020; Horsfall and Spiff, 2005).

Analysis of 2-p adsorption isotherms

The Gill isotherm classification enables an insight to the specific adsorption process. Figure 6 shows the relationship between q_e and c_e, wherein an "L" shape is

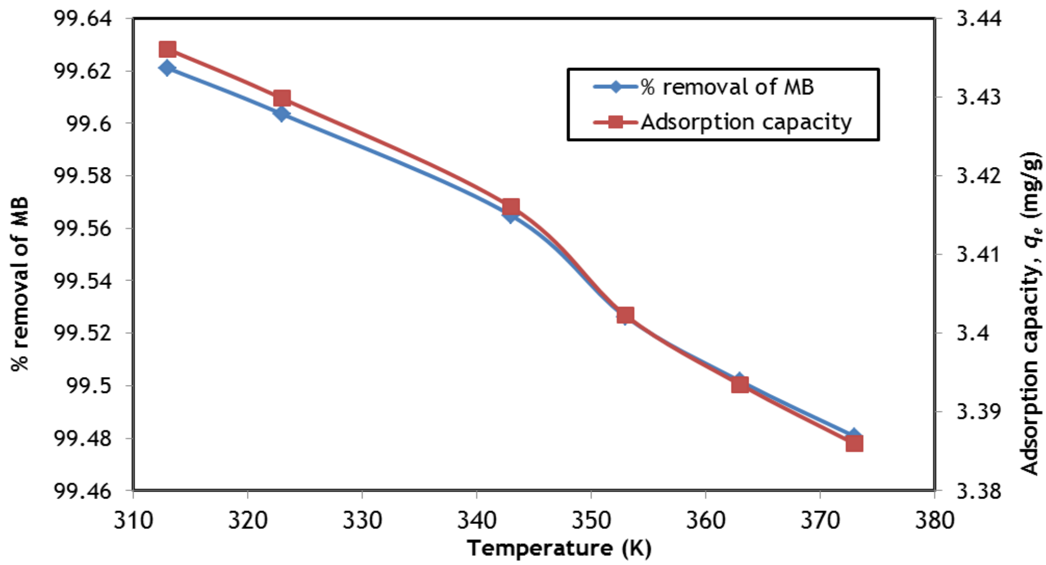

Figure 5. Effect of temperature on adsorption capacity and % removal of MB.

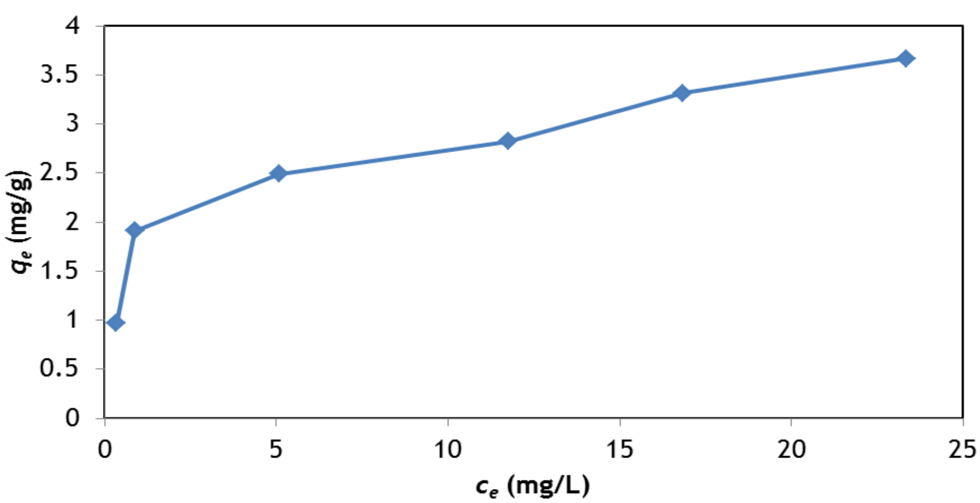

Figure 6. q_e against C_e.

obtained. This implies that there is no strong competition between the solvent and the adsorbate vying for the occupation of the adsorbent surface sites. It can equally be inferred that the methylene blue molecules are adsorbed flat on the surface of the chitosan flakes because the longitudinal axes of the adsorbed MB molecules are parallel to the adsorbent surface (Hamdaoui and Naffrechoux, 2007).

All the isotherms investigated in this study were attempted to be fitted to the batch equilibrium data of MB adsorption on chitosan flakes as adsorbent at pH=8.2, temperature of 30°C, agitation speed=150 rpm and adsorbent dose of 0.1 g.

From the linear plot of 2-p Freundlich isotherm, expressed in Equation 2, the estimated R^2 value is 0.914, the adsorption intensity, *N*, is 3.663 and the measure of adsorption capacity, k_F = 1.5516. The calculated value of $1/N$ (= 0.273) is within the range of 0.1 to 1.0. Thus, the adsorption of MB on the prepared chitosan flakes is adjudged to be a good adsorption process (Kuang et al., 2020). From the literature, it was reported that adsorption process is good for $2 \leq N < 10$, moderate difficult for $1 \leq N < 2$ and poor for $N < 1$ (Olafadehan et al., 2018; Razavi et al., 2013; Húmpola et al., 2013; Chen et al., 2010; Tahir and Rauf, 2006). Hence, the 2-p Freundlich isotherm obtained for the

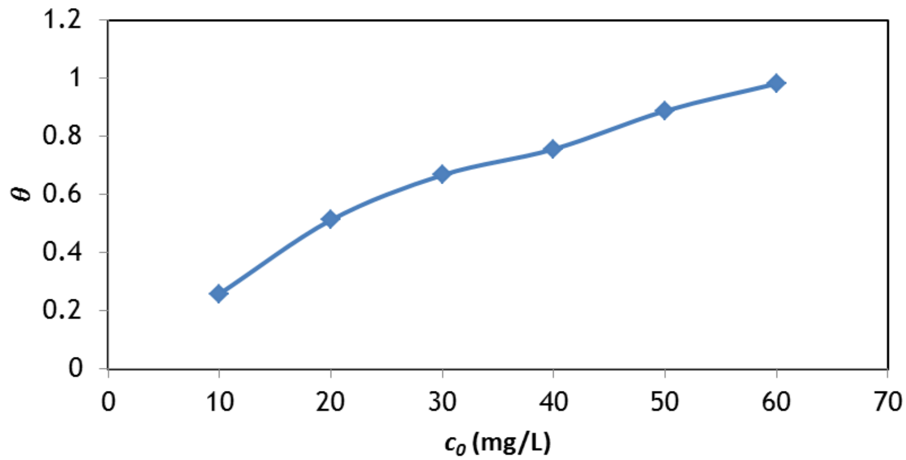

Figure 7. Surface coverage against initial concentration of methylene blue.

removal of MB using chitosan flakes from *A. marginata* shell powder is given by $q_e = 1.5516 c_e^{0.273}$.

From the linear plot of 2-p Langmuir isotherm, expressed in Equation 4, q_{max} and K_L were obtained to be 3.7327 mg/g and 0.5615 L/mg, respectively with the coefficient of determination, R^2 = 0.9816, which gives an impression of a better fit to the adsorption of MB on chitosan flakes than the 2-p Freundlich isotherm. The essential attributes of the model regarded as separation factor, R_L, was evaluated to be in the range $0 < R_L < 1$ for c_0 = 10 to 60 mg/L. Hence, the adsorption process is adjudged to be favorable. Figure **7** shows the variation of surface coverage, θ, with initial concentration, c_0, of methylene blue solution. It is revealed that a rapid succession of chitosan flakes surface coverage fraction increases as the initial concentration of MB increases till θ is close to unity, which is in consonance with the underlying assumptions of Langmuir isotherm.

From the linear plot of 2-p Temkin isotherm, expressed in Equation 6, the isotherm constants, b_T and A_T were evaluated to be 4481.6616 J/mol and 20.4606 L/h respectively with the coefficient of determination, R^2 =0.9533, which gives an impression of a better fit to the adsorption data of MB on chitosan flakes than the 2-p Freundlich isotherm but otherwise for the 2-p Langmuir isotherm. The positive value of b_T, which is related to the variation of the adsorption energy, indicated that the adsorption process was endothermic (Ghogomu et al., 2013; Inam et al., 2016).

From the linear plot of the 2-p Dubinin-Radushkevish isotherm, expressed in Equation 8, the isotherm constants, β and q_{DR} were evaluated to be 1.0×10^{-7} $(mol/J)^2$ and 3.0213 mg/g respectively with R^2 = 0.9254. The mean energy of adsorption, *E* was calculated to be 2.2361 kJ/mol. From the literature, the mean energy of adsorption value indicates physical adsorption for values of 1–8 kJ/mol; ion-exchange for values of 8-16 kJ/mol and 20-40 kJ/mol for chemisorption (Chen et al., 2010; Tahir and Rauf, 2006). This result clearly reflects a physical adsorption process of MB adsorption on chitosan flakes from *A. marginata* shell powder.

From the linear plot of 2-p Harkins-Jura isotherm, expressed in Equation 12, the isotherm constants, A_{HJ} and B_{HJ} were evaluated to be 2.2894 and 1.3299 g/mg^2, respectively with a relatively poor regression coefficient, R^2 =0.7044.

From the linear plot of 2-p Frenkel-Halsey-Hill isotherm, expressed in Equation (14), the isotherm constants, n_{FHH} and K_{FHH} were evaluated to be -3.6630 and 0.2, respectively with regression coefficient, R^2 =0.914.

From the linear plot of 2-p Brunauer-Emmett-Teller isotherm, expressed in Equation 16, which is designated as BET1 isotherm in this study, the isotherm constants, q_S and c_{BET} were evaluated to be 99.99 mg/L and 1.00, respectively with a significant high regression coefficient, R^2 =0.9816 for the saturated concentration, c_S, of MB used = 43210 mg/L (Salimi and Roosta, 2019).

The estimated parameter values of the 2-p isotherms using linear regression methods are shown in Table 2.

The decreasing order of the fit of the isotherms to the equilibrium adsorption data of MB on chitosan flakes, as shown in Table 2, is 2-p Langmuir isotherm, 2-p BET1 isotherm > 2-p Temkin isotherm > 2-p Dubinin-Radushkevish isotherm > 2-p Frenkel-Halsey-Hill isotherm > 2-p Harkins-Jura isotherm, 2-p Freundlich isotherm. Hence, 2-p Langmuir and 2-p BET1 isotherms are adjudged to correlate best the adsorption of MB on chitosan flakes.

Table 2. Comparison of linear and non-linear adsorption isotherm parameters.

Isotherm	Parameter	Estimated values using linear form	Estimated values using non-linear form
2-p Freundlich	N	3.6630	1.6310
	k_f (mg/g)	1.5516	3.9800
	R^2	0.9140	1.0
2-p Langmuir	q_{max} (mg/g)	3.7327	3.4824
	K_L (L/mg)	0.5615	1.1818
	R^2	0.9816	1.0
	R_L	$0 < R_L < 1$	$0 < R_L < 1$
2-p Temkin	b_T (J/mol)	4481.6616	4439.68
	A_T (L/g)	20.4606	20.4870
	R^2	0.9533	1.0
2-p Dubinin-Radushkevish	β (mol/J)^2	1.0×10^{-7}	7.0×10^{-8}
	q_{DR} (mg/g)	3.0213	3.3109
	R^2	0.9254	0.8331
	E (kJ/mol)	2.2361	2.6726
2-p Harkins-Jura	A_{HJ}	2.2894	2.3008
	B_{HJ} (g/mg)^2	1.3299	1.7079
	R^2	0.7044	1.0
2-p Frenkel-Halsey-Hill	n_{FHH}	-3.6630	-3.9763
	K_{FHH}	0.2	0.1433
	R^2	0.914	1.0
2-p BET1	q_S (mg/L)	99.99	3.6313
	c_{BET}	1.00	26832
	R^2	0.9816	1.0

Analysis of adsorption isotherms using non-linear regression analysis

For the purpose of adequate modeling of the adsorption process of MB on chitosan flakes and to evaluate the affinity of MB on the chitosan flakes, nineteen different adsorption isotherms were investigated using non-linear method characterized by trial-and error-procedure aided by the SOLVER ADD-IN obtained in MICROSOFT EXCEL SPREADSHEET and guided by 9 different error functions aside the R^2 function shown in Table 1. These involve seven two-parameter isotherms, eight three-parameter isotherms, three four-parameter and one five-parameter isotherms. The algorithm adopted in this work for non-linear evaluation of isotherm and kinetic models' parameters is the one given by Popoola (2019) with slight modification of the inclusion of statistical evaluation as another criterion for model selection amongst competing models and the process for evaluating sum of normalized errors (SNE) adopted for the isotherm and kinetic models' parameters is given by Amrhar et al. (2015a, b).

The estimated parameter values of the 3-p, 4-p and 5-p isotherms using non-linear regression methods are summarized in Table 3.

Table 3. Values of three, four and five-parameter isotherms using non-linear method.

Isotherm	Parameter	Estimated value using non-linear method
3-p BET2	q_s	2.6489
	c_{BET}	160.5411
	c_s	77.0698
	R^2	1.0
3-p BET3	q_m	2.6496
	K_s	2.0696
	K_L	0.0130
	R^2	1.0
3-p Redlich-Peterson	k_{RP}	11.7778
	α_{RP}	6.0082
	β_{RP}	0.8079
	R^2	1.0
3-p Toth	q_m	3.4824
	K_T	1.1818
	β_T	1.0
	R^2	0.9149
3-p Sips	q_{SP}	14.4412
	K_{SP}	0.1277
	β_S	3.3306
	R^2	1.0
3-Khan	q_{max}	1.3364
	b_K	6.1178
	a_K	0.8023
	R^2	1.0
3-p Radke-Prausnitz	q_{max}	1.3363
	K_{RPI}	6.1174
	α_{RPI}	0.8023
	R^2	1.0

Table 3. Contd.

3-p Fritz-Schlüender	$(q_m)_{FS}$	6.0236
	K_{FS}	1.9582
	α_{FS}	0.8075
	R^2	1.0
4-p Fritz-Schlüender	A_{FS}	4.8087
	Φ_{FS}	1.5489
	B_{FS}	3.1480
	β_{FS}	0.8541
	R^2	1.0
4-p Bauder	$(q_m)_B$	2.0254
	b_0	1190.71
	x	5.3247
	y	0.1884
	R^2	1.0
4-p Marczewski-Jaroniec	$(q_m)_{MJ}$	4.3910
	K_{MJ}	0.02
	α_{MJ}	6.3960
	β_{MJ}	0.2410
	R^2	1.0
5-p Fritz-Schlüender	$(q_m)_{FS5}$	143.6660
	K_{FS5}	3.9303
	α_{FS5}	0.2060
	Φ_{FS5}	306.3960
	β_{FS5}	0.00035
	R^2	1.0

A closer examination of the results in Tables 2 and 3 depicts that the non-linear method gives the better fit of the isotherms to the adsorption data of MB on chitosan flakes than the linear method on the basis of high regression coefficient, R^2, which almost gave a value of 1 in all cases, except for 2-p Dubinin-Radushkevich and 3-p Toth isotherms with R^2 values of 0.8331 and 0.9149, respectively.

Kinetic study

Linearized kinetic models

The necessary linear plot for each of the adsorption kinetics investigated in the current study for the adsorption of MB on chitosan flakes was made to determine the kinetic parameters inherent in it. Table 4 presents the values of the kinetic parameters in each of the 8 kinetic models investigated for the adsorption of MB on chitosan flakes using the linearized kinetic models.

For the fractional power kinetic model, the exponent, v, at all initial MB concentrations was found to be less than unity with a good correlation value at initial methylene blue concentrations of 100 and 150 mg/L shown in Table 4. This validates the time-dependence behavior during the adsorption of MB on the chitosan flakes (El-Khaiary and Malash, 2011).

At concentrations of MB of 50, 100 and 150 mg/L initially, high regression coefficients, R^2, of 0.9529, 0.9726 and 0.9894 were obtained respectively using the Lagergren pseudo first-order kinetic model. As presented in Table 4, higher values of regression coefficient were marginally obtained for the pseudo second-order kinetic model than for the Lagergren pseudo first-order kinetic model and any other kinetic models at all the initial concentrations of MB investigated. It was thus observed that R^2 values of 0.9924, 0.9996, 0.9984 at initial MB concentrations of 50, 100 and 150 mg/L, respectively are good representations of the experimental kinetic data of MB adsorption on chitosan flakes.

In Table 4, the Elovich kinetic model equally gave high regression coefficient values, which are good enough to fit the experimental kinetic data of the adsorption of MB on chitosan flakes but not as high as the R^2 values obtained using the pseudo second-order model.

For the intra-particle diffusion (IPD) model, reasonably good R^2 values were obtained, with straight line not passing through the origin at all initial concentrations of MB considered, as shown in Figure 8. Consequently, the intraparticle diffusion was not the rate-limiting step in the adsorption of MB on the chitosan flakes. The plots of the model had intercepts for all initial concentrations of MB of 50, 100 and 150 mg/L. The value of the intercept increases significantly with initial MB concentrations of 50 to 100 mg/L and then decreases slightly at 150 mg/L. This gives the impression that the boundary layer linked to the intercepts may likely increase with increase in initial concentrations of MB in the range 50 to 100 mg/L.

A closer observation of the graphs in Figure 8 shows a multi-linear one of three distinct phases, especially for the initial concentrations of MB solution under study. The first phase was observed to be relatively fast due to boundary layer or strong electrostatic attraction of MB on the external surface of the chitosan flakes. The second observable phase is a palpable gradual adsorption stage suggested to be influenced or occasioned by intraparticle as the rate-limiting step at this stage, which culminated to the equilibrium phase (that is, the third phase) with high affinity to the chitosan flakes surface active sites (Zbair et al., 2018).

The estimated intra-particle diffusion rate constant, k_{IPD}, shows a gradually retrogression from the slopes values of the multi-lines under study. The intercept values, *C*, for each observed stage shows progressive increment in value as the initial concentration of MB increases. This presupposes the boundary effect is taking a toll on the adsorption process. Such increase in boundary layer thickness would pave way for low external mass transfer and high chances of internal mass transfer.

The Boyd model plot in Figure 9 confirms that the intra-particle diffusion step is not the rate-controlling step in the adsorption of MB on chitosan flakes but rather film diffusion (external diffusion) due to the linearity observed to be away from the origin.

In Table 4, the diffusion-chemisorption model equally gave high regression coefficient values, which are good enough to fit the experimental kinetic data but not as high as the pseudo second-order model. Using the diffusion-chemisorption model, the resulting straight line, coupled with high regression coefficient values, shows that the sorption process is under the influences of both diffusion and chemisorption.

Results from non-linear kinetic model

The estimated kinetic parameters for the non-linea kinetic models using non-linear regression method subjected to the error functions used previously are shown in Table 5. Using the values of the coefficient of determination, the non-linear method gave a better fit than the linear method. With the various error functions employed, for MB concentration of 150 mg/L, *NSD* function fitted 4 kinetic models (fractional power model, pseudo second-order model, Elovich model, intraparticle diffusion, IPD (or Weber-Morris) model); *EABS* fitted 1 model (Lagergren pseudo first-order model); *ARE* fitted 1 model (Avrami model) and *RSME* fitted 1 model (diffusion-chemisorption model). For MB concentration of 100 mg/L, *NSD* fitted 4 models (fractional power model, Lagergren pseudo first-order, Elovich and IPD models); *ARE* fitted 1 model (pseudo second-order model); *RSME* fitted the diffusion-chemisorption model and *HYBRID* function fitted 1 model (Elovich model). For the case of initial concentration of MB of 50 mg/L, *NSD* function fitted 3 models (Lagergren pseudo first-order, pseudo second-order and Elovich models); *SSE* fitted 1 model (IPD model); *HYBRID* fitted 1 model (Avrami model); *RSME* fitted 1 model (fractional power law) and *SRE* function fitted 1 model (diffusion-chemisorption model).

Isotherm and kinetic models' selection

Since the sum of normalized error (*SNE*) has been reported as a way or criterion for selecting the best fitted isotherm/kinetic model (Anirudhan and Radhakrishnan, 2009; Yanev et al., 2013; Popoola, 2019), the *SNE* value was used as a yardstick for the model selection in this

Table 4. Values of the parameters in the linearized kinetic models for the adsorption of MB on chitosan flakes.

Kinetic model	Parameter	Values of the parameters at initial MB concentration		
		50 mg/L	100 mg/L	150 mg/L
Fractional power	v	0.135	0.1637	0.2363
	k_f	1.1632	1.6900	1.5186
	R^2	0.8760	0.9873	0.9918
Lagergren pseudo first-order kinetic model	k_1 (min^{-1})	0.0788	0.0635	0.0345
	q_e (mg/g)	1.3620	2.150	2.5870
	R^2	0.9529	0.9726	0.9894
Pseudo second-order kinetic model	k_2 (g/(mg min))	0.0550	0.0520	0.0220
	q_e (mg/g)	2.3030	3.5740	4.6707
	h (mg/(g min))	0.2917	0.6642	0.4799
	R^2	0.9924	0.9996	0.9984
Elovich kinetic model	α (mg/(g min))	0.5224	8.5724	0.6032
	β (g/mg)	2.0593	2.1240	0.7955
	R^2	0.9941	0.9970	0.9029
Avrami kinetic model	n_{AV}	0.3300	-0.7476	-0.6277
	k_{AV} ($\min^{-n_{AV}}$)	1.0932	0.1825	0.1956
	t_a (min)	0.7722	0.1040	0.0752
	R^2	0.9942	0.9592	0.9776
Intraparticle diffusion (IPD)	k_{IPD} (mg/(g min^{½}))	0.1914	0.1710	0.2773
	C (mg/g)	0.7186	1.9826	2.8335
	R^2	0.8226	0.9558	0.9724
Boyd model	D (m^2/s)	4.4911×10^{-11}	3.6191×10^{-11}	1.9663×10^{-11}
	R^2	0.9529	0.9726	0.9893
Diffusion-chemisorption model	k_{DC} (mg/(g min$^{-0.5}$))	1.2979	1.7550	1.3419
	q_e (mg/g)	2.5100	4.330	6.4800
	k_i (mg/(g min))	0.6711	0.7113	0.2779
	R^2	0.9865	0.9994	0.9980

study. The most fitted model amongst the non-linearized isotherms using the non-linear regression method is the one with the lowest value of *SNE*. The computed *SNE* values for the2-p isotherms, 3-p isotherms, 4-p isotherms

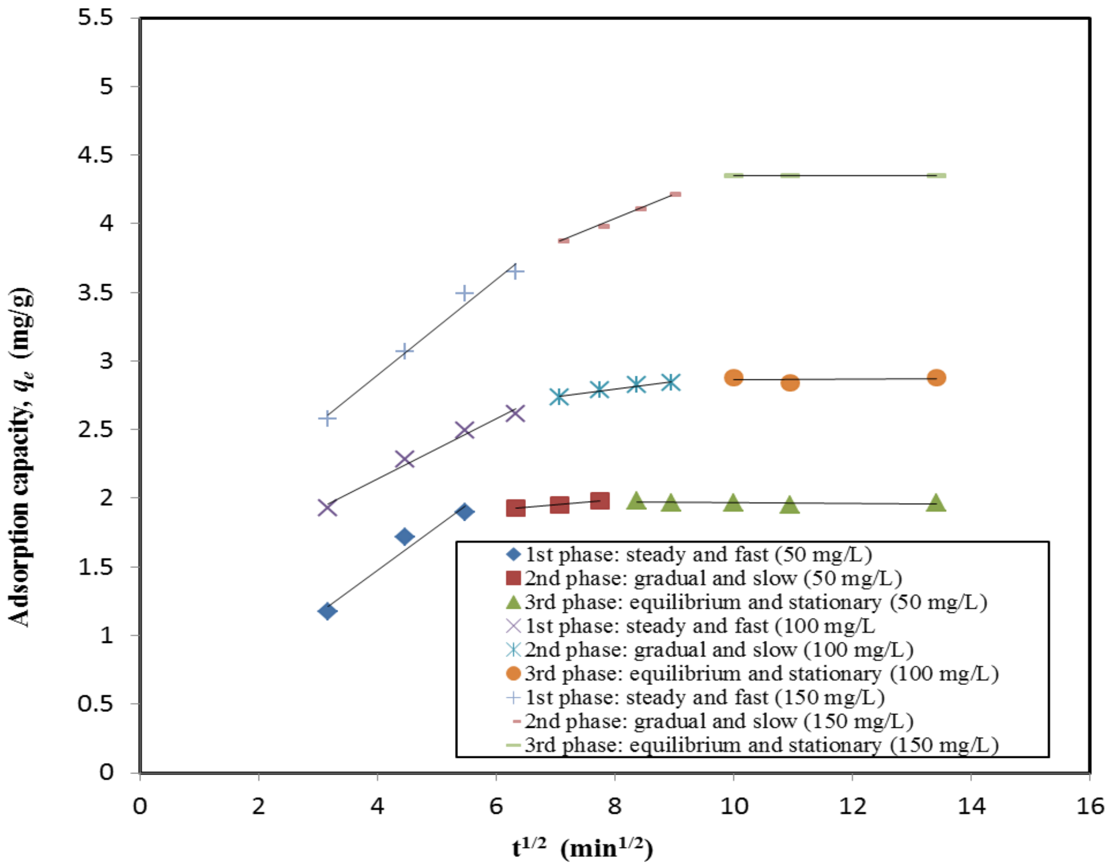

Figure 8. Variation of adsorption amount at any time *t* against *t* for intra-particle diffusion (IPD) model: mass=0.1 g; pH=8.2; agitation speed=150 rpm and temperature=30°C.

and 5-p isotherm are shown in Table 6. The 5-p Fritz-Schlüender isotherm gave the lowest *SNE* value closely followed by the 2-p Temkin isotherm. Thus, the former is the most fitted isotherm using the *SNE* value as selection. Moreover, the lowest values of Pearson's chi-squared analysis, Akaike information criterion (*AIC*), model selection criterion for isotherm models and its associated values for each of the isotherm models investigated are shown in Table 6. Using the *SNE* for the goodness-of-fit amongst the two-parameter isotherms considered, the 2-p Temkin isotherm fitted best the adsorption equlibrium data of MB on chitosan flakes having a value of 4.7721 with the *NSD* stastistical indicator. For the three-parameter isotherms, Redlish-Peterson isotherm fitted best, which recoded a value of 5.0828 with *EABS* as error function while Marczewiski-Jaroniec isotherm fitted best amongst the four-parameter isotherms having a value of 6.2345 with *MPSD* as error function. The 5-p Fritz-Schlüender isotherm fitted best overall among all other number of parameters of the isotherm considered having the least value of 4.6506 with the *NSD* error function. The lowest value of *SNE* with the corresponding error function reflect the optimum isotherm parameter for the various isotherm models considered (Ghaffari et al., 2017; Rahman et al., 2018). In all the 19 isotherm models considered, *NSD* best fitted for 12 adsorption isotherms, chi-squared best fitted for 4 isotherms while *MPSD*, *EABS* and *HYBRID* best fitted for 1 isotherm each. Also from Table 6, the Pearson's Chi-squared (χ^2) analysis carried out at the respective degree of freedom, *df*, (difference between the number of experimental data and the number of parameters) shows that all the models have a non-significant lack of normality of the residuals since the calculated value is less than the critical or table value. Statistically, it translates or reveals a high level of acceptance of the models (Mitrevski et al., 2017). In addition, the results projects Bauder isotherm as the best fitted isotherm in terms of normality of residual followed by the 3-p BET2 and 3-p BET3 isotherms in descending order.

The *AIC* function is a statistical tool well rootedas a yardstick for comparing model equations with varying number of parameters. Its principle of operation is hinged simply on the difference between calculated *AIC* values over a set of model equation with a likely product of positive or negative value. The $(A_{IC})_{mod}$ value of a model equation with the lowest value (considering the sign),

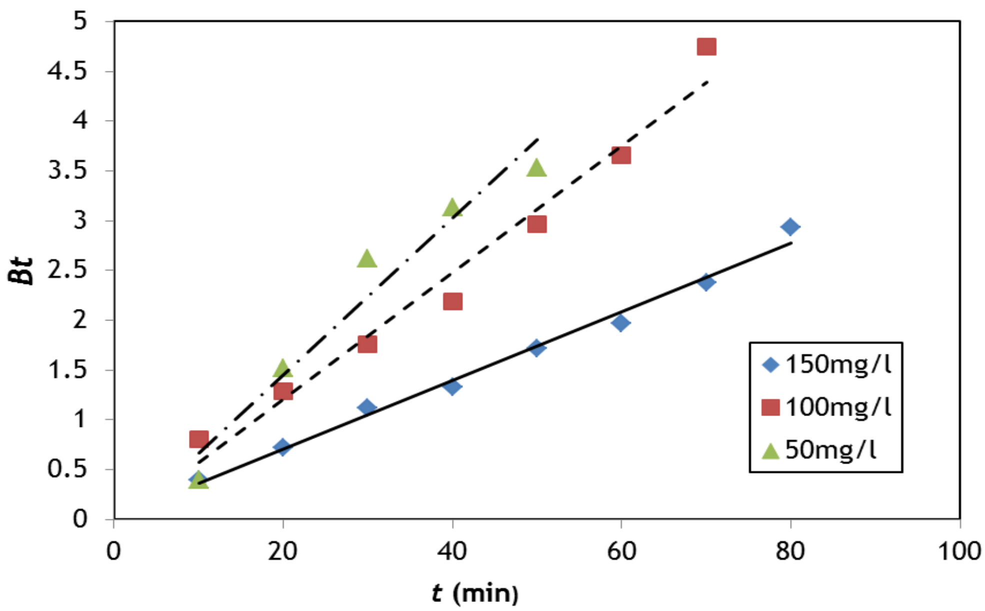

Figure 9. Boyd plot for the adsorption of MB on chitosan flakes.

lowest value of evidence ratio (*ER*) and the highest value of model selection criterion (*MSC*) amongst the competing equations is adjudged to be the superior equation over others (Akaike, 1974). From the results in Table 6, the 3-p BET2 and 3-p BET3 model equations portrayed the same lowest value of $(A_{IC})_{mod}$ = -16.2878 and evidence ratio, *ER*, of 1. With the highest value obtained for *MSC*, the 3-p BET3 isotherm is considered the most fitted model for the adsorption of MB on the synthesized chitosan flakes.

Similarly, using the information-based criteria for the selection of the best fitted kinetic models for the adsorption of MB on chitosan flakes, the pseudo second-order kinetics recorded the lowest $(A_{IC})_{mod}$, lowest evidence ratio and highest *MSC* values, amongst all the investigated kinetic models, at all initial concentrations of MB solution under this present study, as revealed in Tables 7 and 8. Hence, the adsorption rate of MB on chitosan flakes can be kinetically described by the pseudo second-order model, with the model satisfying all the criterial used in selecting the best fitted kinetic models.

In the same vein, the Pearson's chi-squared analysis carried out at the respective degree of freedom shows that all the models have a non-significant lack of normality of the residuals. The same trend was observed in all the criteria as shown in the ranking for the best fitted kinetic models.

Thermodynamics study

The effect of temperature in adsorption studies is considered as a fundamental factor in adsorption systems. It gives the thermodynamics parameters: activation energy, sticking probability and changes in entropy, enthalpy and Gibbs free energy. From the results in Table 9 and Figure 10, ΔH^0 is positive, which indicates an endothermic process of adsorption of MB on the prepared chitosan flakes from *A. marginata*. This implies that adsorption capacity of the derived chitosan flakes increases with temperature.

The value of ΔH^0 is within the range of 1-8 kJ/mol for physisorption (Zarrouk et al., 2011). Also, the positive value of ΔS^0 suggests a high degree of randomness at the chitosan-MB interface with appreciable structural changes with the adsorbate species (Saha and Chowdhury, 2011). It is also noteworthy that the negative value of the Gibbs free energy, ΔG^0, reflects a high degree of spontaneity of the adsorption process of MB on chitosan flakes and exergonic and energetically favorable adsorption process with increasing negative values occasioned by increases in temperature.

The sticking probability, S^*, known as the rate of adsorption per molecular collision with the adsorbent surface, directly expresses the difficulty encountered by a molecule in overcoming the barrier to adsorption. The calculated value of S^*, which is less than unity, indicates that the likelihood of MB ions sticking onto the chitosan surface is very high.

Batch reactor design

Figure 11 illustrates briefly the batch reactor design using

Table 5. Estimated values of the parameters in the non-linear kinetic models for the adsorption of MB on chitosan flakes using non-linear regression method.

Kinetic model	Parameter	Values of the parameters at initial MB concentration		
		50 mg/L	100 mg/L	150 mg/L
Fractional power	v	0.1095	0.1360	0.2018
	k_f	1.2886	1.5827	1.7335
	R^2	1.0	1.0	1.0
Lagergren pseudo first-order kinetic model	k_1 (min^{-1})	0.1065	0.0774	0.0910
	$(q_e)_{expt}$ (mg/g)	1.9649	2.8420	4.3509
	q_e (mg/g)	1.9575	2.7381	3.7477
	R^2	1.0	1.0	1.0
Pseudo second-order kinetic model	k_2 (g/(mg min))	0.0602	0.0287	0.0559
	q_e (mg/g)	2.2813	3.3044	4.0516
	h (mg/(g min))	0.3133	0.3134	0.9176
	R^2	1.0	1.0	1.0
Elovich kinetic model	α (mg/(g min))	3.9943	2.2664	1.4534
	β (g/mg)	13.9360	4.1265	3.4587
	R^2	1.0	1.0	1.0
Avrami kinetic model	n_{AV}	4.0761	4.0761	4.0761
	k_{AV} ($\min^{-n_{AV}}$)	2.7060	2.7060	2.7060
	q_e (mg/g)	1.9298	2.614035	3.6491
	t_a (min)	0.7924	0.7924	0.7924
	R^2	0.8534	0.8610	0.8315
Diffusion-chemisorption model	k_{DC} (mg/(g min$^{-0.5}$))	0.0990	0.2100	0.5
	q_e (mg/g)			
	k_i (mg/(g min))	0.0040	0.01432	0.0612
	R^2	1.0	1.0	1.0

Equation 35. The plots so obtained shows the mass of chitosan flakes to increase with increasing solution volume at a certain % removal of MB using the chitosan flakes prepared from *A. marginata* shell waste.

Proposed adsorption mechanism of methylene blue onto chitosan flakes

The reaction mechanism of the adsorption of MB onto chitosan (CH) was proposed by noting that the adsorption mechanism is dependent on the electrostatic attractive force between the surface of the chitosan (biosorbent) and the methylene blue, which are negatively and positively charged respectively. The electrostatic force of attraction arises as a result of the functional groups present on the surface of the chitosan and the pH dependence of MB adsorption from aqueous solution onto the chitosan flakes. The presence of hydroxyl (OH^-) and amide (NH_2^-) groups on CH was revealed

Table 6. Results of SNE, Pearson's chi-squared analysis, Akaike information criterion (AIC) and model selection criterion for isotherm models.

Isotherm	N_p	Sum of Normalized Error			χ^2 analysis (p-0.05)				Akaike Information Criteria (AIC)				Model selection criterion	
		EF	Value	RK	*df*	Calc.value	Table value	RK	$(A_{IC})_{mod}$	λ_i	*ER*	RK	Value	RK
Freundlich	2	NSD	6.3603	8	4	0.1496	9.488	8	-11.7676	0.0354	9.5843	4	2.2651	6
Langmuir	2	NSD	7.5061	18	4	0.1670	9.488	10	-7.0296	0.0033	102.4258	13	1.6383	14
Temkin	2	NSD	4.7721	2	4	0.1026	9.488	6	-12.2426	0.0448	7.5580	3	2.3683	4
D-R	2	χ^2	8.9350	19	4	0.3026	9.488	11	-2.0904	0.0003	1210.4068	15	2.0635	11
H-J	2	HYBRID	5.2870	4	4	0.3525	9.488	12	-7.4073	0.0040	84.7987	11	1.5762	17
F-H-H	2	NSD	7.1578	14	4	0.1496	9.488	8	-11.7676	0.0354	9.5843	4	2.2663	5
BET1	2	NSD	6.9096	12	4	0.1667	9.488	9	-7.0450	0.0033	101.6406	12	1.9966	13
BET 2	3	χ^2	6.8166	11	3	0.0503	7.815	2	-16.2878	0.3390	1.0000	1	3.0413	2
BET 3	3	χ^2	7.0100	13	3	0.0503	7.815	2	-16.2878	0.3390	1.0000	1	3.0448	1
Redlich-Peterson	3	EABS	5.0828	3	3	0.1009	7.815	13	-10.7609	0.0214	15.8547	7	2.1120	10
Toth	3	NSD	6.3803	9	3	0.4449	7.815	14	4.1817	1.217×10^{-5}	27855.4010	16	0.5768	19
Sips	3	NSD	6.3063	6	3	0.1296	7.815	7	0.6508	7.112×10^{-5}	4766.3842	17	0.5760	18
Khan	3	NSD	7.2572	16	3	0.0950	7.815	3	-11.0676	0.0249	13.6007	5	2.1623	8
Radke-Prausnitz	3	NSD	7.3601	17	3	0.0950	7.815	3	-11.0676	0.0249	13.6007	5	2.1624	7
Fritz-Schlüender	3	χ^2	6.3172	7	3	1.0090	7.815	4	-10.7610	0.0214	15.8537	6	2.1130	9
Fritz-Schlüender	4	NSD	7.2517	15	2	0.1020	5.991	5	-8.7610	0.0079	43.0948	9	1.8945	12
Bauder	4	NSD	6.7445	10	2	0.0340	5.991	1	-13.5762	0.0874	3.8800	2	2.6347	3
Marczewiski-Jaroniec	4	MPSD	6.2345	5	2	0.1496	5.991	8	-7.7675	0.0048	70.8233	10	1.5873	15
Fritz-Schlüender	5	NSD	4.6506	1	1	0.1604	3.841	9	-6.7246	0.0028	119.3006	14	1.5797	16

EF, RK, *df* deonte error function, ranking, degree of freedom, respectively.

Table 7. Results of SNE and criterion for kinetic models.

Kinetic models	Sum of normalized error (SNE)									χ^2 analysis (p-0.05)		
	50 mg/L			100 mg/L			150 mg/L			Average calc. value	Table value	RK
	EF	Value	RK	EF	Value	RK	EF	Value	RK			
Fractional power model	RMSE	6.3819	4	NSD	4.5572	3	NSD	3.7526	2	0.0796	21.026	4
Lagergren pseudo first-order kinetic model	NSD	4.7505	2	NSD	5.3946	4	EABS	5.0542	4	0.0632	21.026	3
Pseudo second-order model	NSD	3.9002	1	ARE	0.8418	1	NSD	1.6201	1	0.0200	21.026	1
Elovich	NSD	5.2056	3	NSD	3.0317	2	NSD	4.1980	3	0.0606	21.026	2
Avrami	HYBRID	6.7487	5	HYBRID	5.9436	5	SRE	5.06358	5	0.5376	21.026	5

Table 8. Results of Akaike information criterion (AIC) and model selection criterion for kinetic models.

Kinetic model	Akaike Information Criteria (AIC) $(A_{IC})_{mod}$			λ_i			ER				Model Selection Criterion			
	50 mg/L	100 mg/L	150 mg/L	50 mg/L	100 mg/L	15 0mg/L	50 mg/L	100 mg/L	150 mg/L	RK	50 mg/L	100 mg/L	150 mg/L	RK
Fractional Power Model	-12.2731	-17.3627	-14.2193	8.88×10^{-7}	1.131×10^{-5}	4.94×10^{-3}	1126193	88391.2551	202.3735	3	-0.1795	1.4627	-0.0704	4
Lagergren pseudo first-order	-35.4483	-17.6250	-7.0307	0.0957	1.29×10^{-5}	1.36×10^{-4}	10.4516	77527.2197	7364.1813	4	4.1554	3.2983	1.6852	3
Pseudo second-order	-35.8797	-33.9844	-22.6302	0.1187	4.60×10^{-2}	3.31×10^{-1}	8.42363	21.729588	3.0182	1	4.2616	4.3762	3.7118	1
Elovich	-13.0613	-19.2412	-17.9316	1.317×10^{-6}	2.894×10^{-5}	3.16×10^{-2}	759386	34553.8386	31.6243	2	0.1019	3.9906	2.8902	2
Avrami	-4.1626	-0.8986	28.5513	1.539×10^{-8}	3.01×10^{-9}	2.55×10^{-12}	$6.5 \times 10^{+7}$	332316707	3.92×10^{11}	5	-2.5942	-3.0839	-2.2609	5

Table 9. Thermodynamic parameters for the adsorption of MB on chitosan flakes.

T (K)	ΔG^0 (kJ/mol)	ΔH^0 (kJ/mol)	ΔS^0 (kJ/(mol K))	E_a (kJ/mol)	S^* (mg/L)
313	-10077.76	4.23	0.4563	5.1575	0.0731
323	-10514.84				
343	-11339.97				
353	-11875.64				
363	-12374.26				
373	-12804.01				

in the FTIR study at wavelengths 3419.79 and 3458.21 cm^{-1} before and after adsorption of MB respectively (Bello and Olafadehan, 2021). The ionization of these functional groups is a function of the pH of MB solution that causes the surface of CH to be electrically charged. The amide and hydroxyl groups on the surface of the biosorbent can either gain or lose a proton (that is, hydrogen ion), thereby resulting in the variation of surface charge of CH with pH of MB solution.

At low-level of pH of MB solution, protonation takes place on the active centers (that is, sites) of the chitosan flakes. Hence, the surface of the adsorbent (chitosan flakes) acquires a positive charge owing to the reactions between each of OH^- and NH_2^- functional groups on the adsorbent surface and the hydrogen ion (H^+) in solution. These reactions are represented in Equations 74 and 75, respectively:

$$CH - OH + H^+ \longrightarrow CH{-}OH_2^+ \quad (74)$$

$$CH - NH_3 + H^+ \longrightarrow CH{-}NH_4^+ \quad (75)$$

Deprotonation occurs at high pH of MB solution and the active sites on the surface of CH acquire a negative charge owing to the reactions between each of OH^- and NH_2^- functional groups on the surface of CH and the hydroxyl ion (OH^-). These reactions are represented in Equations 76 and 77, respectively:

$$CH - OH + OH^- \longrightarrow CH{-}O^- + H_2O \quad (76)$$

$$CH - NH_3 + OH^- \longrightarrow CH{-}NH_2^- + H_2O \quad (77)$$

Hence, Equations 76 and 77 reveal that electrostatic force of attraction enhances MB adsorption onto CH at high-level of MB solution pH. Thus, the reaction mechanism of MB adsorption onto the synthesized chitosan flakes from African giant snail (*A. marginata*) shell

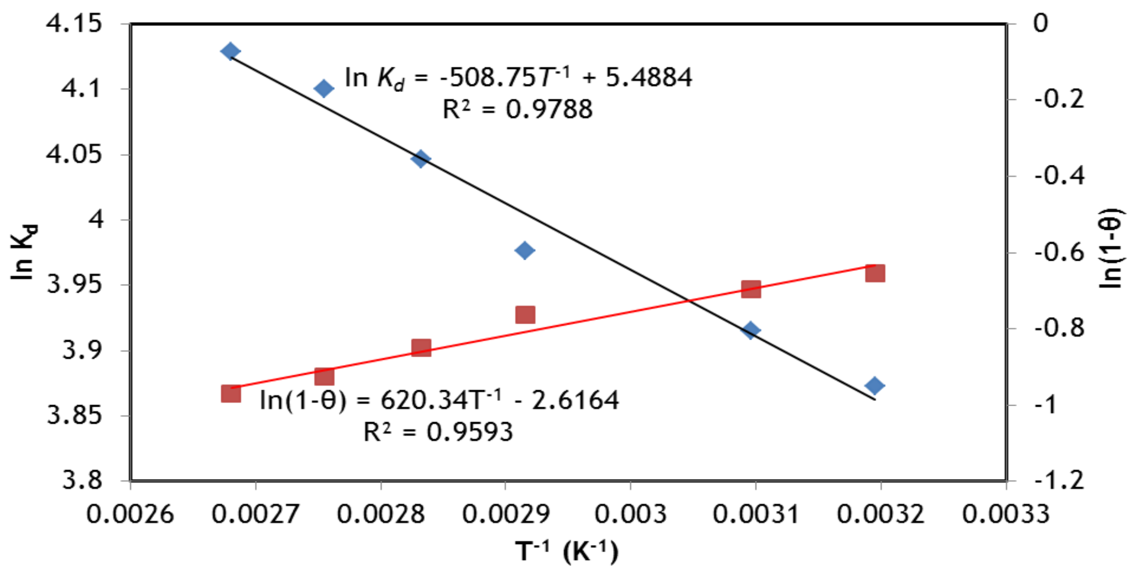

Figure 10. Variation of distribution coefficient and surface coverage with temperature.

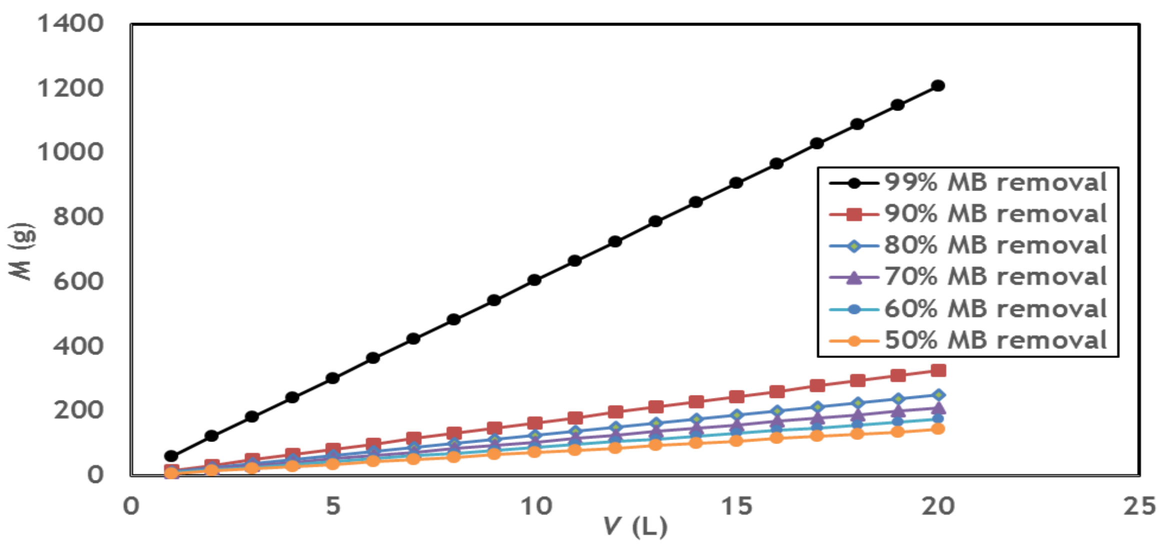

Figure 11. Variation of the theoretical mass of chitosan flakes with volume required for MB effluents to be treated for 50-99% efficiency with initial concentration of 50 mg/L at 303K.

powder is proposed thus:

$$CH - O^{-} + MB^{+} \longrightarrow CH - O^{-} \cdots MB^{+}$$

$$CH - NH_2^{-} + BGD^{+} \longrightarrow CH - COO^{-} \cdots MB^{+}$$

Conclusion

The capacity of chitosan extracted from African giant snail (*A. marginata*) shell powder in the removal of methylene blue (MB) from aqueous solution and the effects of operational parameters on its adsorption capacity in a batch system were investigated in this study. Equally, modeling of the adsorption equilibrium data using 19 isotherms and 8 kinetic models coupled with statistical criteria of Akaike information criteria (*AIC*), evidence ratio (*ER*), model selection criterion (*MSC*) and sum of normalized error (*SNE*) to select the best isotherm and kinetic models was carried out. The thermodynamic parameters such as activation energy, E_a, changes in enthalpy, ΔH^0, entropy, ΔS^0 and Gibbs free energy, ΔG^0, were evaluated. The most important conclusions from this work are summarized thus:

(1) The *A. marginata* shell waste is an abundant and cheaply available precursor for the production of chitosan.
(2) The produced chitosan flake is potentially viable as an adsorbent for the removal of MB from aqueous solution. Consequently, it may be an alternative to costly biosorbents.
(3) The 5-p Fritz-Schlüender isotherm best fitted the experimental equilibrium adsorption data of MB on chitosan flakes based on the sum of normalized error (SNE) and the 3-p BET3 isotherm is the most fitted model for the adsorption of MB on the prepared chitosan flakes based on the lowest values of AIC, lowest ER value and highest value of MSC.
(4) Kinetically, the pseudo second-order model well represented the adsorption rate of MB on chitosan flakes at all initial concentrations of MB investigated in this study.
(5) The intraparticle diffusion was not found to be the rate-limiting step for the adsorption of MB on the synthesized chitosan flakes but rather film (i.e., external) diffusion and the sorption process was chemisorption-influenced.
(6) The adsorption of MB on the prepared chitosan flakes from *A. marginata* shell powder is a physical and endothermic process with ΔH^0 = 4.23 kJ/mol, a high degree of randomness at the chitosan-MB interface (ΔS^0 = 0.4563 kJ/mol), high degree of spontaneity (negative ΔG^0 values), energetically favorable and exergonic.
(7) The data reported in this study can be of beneficial use in the conception and construction of a less-costly viable treatment process using batch reactor for MB adsorption on a biosorbent and for diluting industrial effluents.

CONFLICT OF INTERESTS

The authors have not declared any conflict of interests.

REFERENCES

Adekunbi EA, Babajide JO, Oloyede HO, Amoko JS, Obijole OA, Oke IA (2019). Evaluation of Microsoft excel solver as a tool for adsorption kinetics determination. Ife Journal of Science 21(3):169-183.

Afroze S, Sen TK, Ming A, Nishioka H (2015). Adsorption of methylene blue dye from aqueous solution by novel biomass Eucalyptus sheathiana bark: equilibrium, kinetics, thermodynamics and mechanism. Desalination and Water Treatment 57(13):5858-5878.

Agarwal AK, Kadu MS, Pandhurnekar CP, Mahendra IL (2014). Langmuir, Freundlich and BET adsorption isotherm studies for zinc ions onto coal fly ash. International Journal of Application or Innovation in Engineering Management (IJAIEM) 3(1):64-71.

Ahmad MA, Puad NAA, Bello OS (2014). Kinetic, equilibrium and thermodynamic studies of synthetic dye removal using pomegranate peel activated carbon prepared by microwave-induced KOH activation. Water Resources and Industry 6:18-35.

Ahmed MJ, Hameed BH, Hummadi EH (2020). Review on recent progress in chitosan/chitin-carbonaceous material composites for the adsorption of water pollutants. Carbohydrate Polymers 116690.

Akaike H (1974). A new look at the statistical model identification. IEEE Transactions on Automatic Control 19(6):716-723.

Akpa OM, Unuabonah EI (2011). Small-sample corrected Akaike information criterion: An appropriate statistical tool for ranking of adsorption isotherm models. Desalination 272(1-3):20-26.

Alghamdi AA, Al-Odaymi ABA, Saeed WS, Al-Kahtani A, Alharthi FA, Aouak T (2019). Efficient adsorption of lead (II) from aqueous phase solutions using polypyrole-based activated carbon. Materials. Available at: https://doi.org/10.3390/ma12122020

Alston JR, Banks DJ, McNeill CX, Mitchell JB, Popov LD, Shcherbakov IN, Poler JC (2015). Adsorption studies of divalent, dinuclear coordination complexes as molecular spacers on SWCNTs. Physical Chemistry Chemical Physics 17(44):29556-29573.

Amoo KO, Olafadehan OA, Ajayi TO (2019). Optimization studies of chitin and chitosan production from penaeus notialis shell waste. African Journal of Biotechnology 18(27):670-688.

Amrhar O, Nassali H, Elyoubi MS (2015a). Two and three-parameter isothermal modeling for adsorption of crystal violet dye onto natural illitic clay: nonlinear regression analysis. Journal of Chemical and Pharmaceutical Research 7(9):892-903.

Amrhar O, Nassali H, Elyoubi MS (2015b). Application of nonlinear regression analysis to select the optimum adsorption isotherm for methylene blue adsorption onto natural illitic clay. Bulletin de la Société Royale des Sciences de Liège 84:116-130.

Anirudhan TS, Radhakrishnan PG (2009). Kinetic and equilibrium modeling of cadmium (II) ions sorption onto polymerized tamarind fruit shell. Desalination 249(3):1298-1307.

Annadurai G, Chellapandian M, Krishnan MRV (1999). Adsorption of reactive dye on chitin. Environmental Monitoring and Assessment 59(1):111-119.

Annadurai G, Krishnan MRV (1997). Batch equilibrium adsorption of reactive dye onto natural biopolymer. Iranian Polymer Journal 6(3):169-175.

Annadurai G, Ling LY, Lee J (2008). Adsorption of reactive dye from an aqueous solution by chitosan: isotherm, kinetic and thermodynamic analysis. Journal of Hazardous Materials 152(1):337-346.

Asfour HM, Fadali OA, Nassar MM, Elgeundi MS (1985a). Equilibrium studies on adsorption of basic dyes on hardwood. Journal of Chemical Technology and Biotechnology 35(1):21-27.

Asfour HM, Nassar MM, Fadali OA, Elgeundi MS (1985b). Colour removal from textile effluents using hardwood sawdust as an absorbent. Journal of Chemical Technology and Biotechnology 35(1):28-35.

Atun G, Hisarli G, Sheldrick WS, Muhler M (2003). Adsorptive removal of methylene blue from colored effluents on fuller's earth. Journal of Colloid and Interface Science 261(1):32-39.

Avrami M (1939). Kinetics of phase change. I. General theory. The Journal of Chemical Physics 7(12):1103-1112.

Avrami M (1940). Kinetics of phase change. II. Transformation-time relations for random distribution of nuclei. The Journal of Chemical Physics 8(2):212-224.

Avrami M (1941). Kinetics of phase change. III. Granulation, phase change, and microstructure. The Journal of Chemical Physics 9(2):177-184.

Ayawei N, Ebelegi AN, Wankasi D (2017). Modelling and Interpretation of Adsorption Isotherms. Journal of Chemistry 2017:1-11.

Banerjee S, Chattopadhya MC (2013). Adsorption characteristics of modified wheat husk for the removal of a toxic dye, methylene blue, from aqueous solutions. Journal of Hazardous, Toxic, and Radioactive Waste 18(1):56-63.

Behbahani TJ, Behbahani ZJ (2014). A new study on asphaltene adsorption in porous media. Petroleum and Coal 56(5):459-466.

Bello VE, Olafadehan OA (2021). Comparative investigation of RSM and ANN for multi-response modeling and optimization studies of derived chitosan from Archachatina marginata shell. Alexandria Engineering Journal 60(4):3869-3899.

Benzaoui Z, Selatnia A, Djabali D (2018). Adsorption of copper (II) ions from aqueous solution using bottom ash of expired drugs

incineration. Adsorption Science and Technology 36(1-2):114-129.
Bernal V, Erto A, Giraldo L, Moreno-Piraján J (2017). Effect of solution pH on the adsorption of paracetamol on chemically modified activated carbons. Molecules 22(7):1032. Available at: https://doi.org/10.3390/molecules22071032
Boumediene M, Benaissa H, George B, Molina S, Merlin A (2018). Effects of pH and ionic strength on methylene blue removal four synthetic aqueous by sorption onto orange peel and desorption study. Journal of Materials and Environmental Sciences 9(6):1700-1711.
Boyd G, Adamson A, Myers L (1947). The exchange adsorption of ions from aqueous solutions by organic zeolites. II. Kinetics. Journal of the American Chemical Society 69(11):2836-2844.
Castillejos E, Rodríguez-Ramos I, Soria Sánchez M, Muñoz V, Guerrero-Ruiz A (2011). Phenol adsorption from water solutions over microporous and mesoporous carbon surfaces: A real time kinetic study. Adsorption 17(3):483-488.
Celebi O, Uzum C, Shahwan T, Erten HN (2007). A radiotracer study of the adsorption behavior of aqueous Ba^{2+} ions on nanoparticles of zero-valent iron. Journal of Hazardous Materials 148(3):761-767.
Chan LS, Cheung WH, Allen SJ, McKay G (2012). Error analysis of adsorption isotherm models for acid dyes onto bamboo derived activated carbon. Chinese Journal of Chemical Engineering 20(3):535-542.
Chen H, Zhao J, Dai G, Wu J, Yan H (2010). Adsorption characteristics of Pb(II) from aqueous solution onto a natural biosorbent, fallen Cinnamomum camphora leaves. Desalination 262(1-3):174-182.
Chen Q, Tian Y, Li P, Yan C, Pang Y, Zheng L, Meng X (2017). Study on shale adsorption equation based on monolayer adsorption, multilayer adsorption, and capillary condensation. Journal of Chemistry Article ID 1496463:1-11.
da Silva Alves DC, Healy B, de Almeida Pinto LA, Cadaval Jr TRSA, Breslin CB (2021). Recent developments in chitosan-based adsorbents for the removal of pollutants from aqueous environments, Molecules 26(3):594. Available at: https://doi.org/10.3390/molecules26030594
Dávila-Jiménez MM, Elizalde-González MP, García-Díaz E, González-Perea M, Guevara-Villa MRG (2014). Using Akaike information criterion to select the optimal isotherm equation for adsorption from solution. Adsorption Science and Technology 32(7):605-622.
Deng S, Chen Y (2019). A study by response surface methodology (RSM) on optimization of phosphorus adsorption with nano spherical calcium carbonate derived from waste. Water Science and Technology 79(1):188-197.
Derakhshan Z, Baghapour MA, Ranjbar M, Faramarzian M (2013). Adsorption of methylene blue dye from aqueous solutions by modified pumice stone: kinetics and equilibrium studies. Health Scope 2(3):136-144.
Dil EA, Ghaedi M, Asfaram A, Mehrabi F, Bazrafshan AA, Ghaedi AM (2016). Trace determination of safranin O dye using ultrasound assisted dispersive solid phase micro extraction: artificial neural network-genetic algorithm and response surface methodology. Ultrasonics Sonochemistry 33:129-140.
Dubinin MM (1960). The potential theory of adsorption of gases and vapours for adsorbents with energetically nonuniform surfaces. Chemical Reviews 60(2):235-241.
Ebadi A, Soltan Mohammadzadeh JS, Khudiev A (2009). What is the correct form of BET isotherm for modeling liquid phase adsorption? Adsorption 15(1):65-73.
Edet UA, Ifelebuegu OA (2020). Kinetics, isotherm, and thermodynamics modeling of the adsorption of phosphates from model wastewater using recycled brick waste. Processes 8(665):1-15.
El-Geundi MS (1991). Colour removal from textile effluents by adsorption techniques. Water Research 25(3):271-273.
Elizalde-González MP, Hernández-Montoya V (2009). Removal of acid orange 7 by guava seed carbon: A four parameter optimization study. Journal of Hazardous Materials 168(1):515-522.
El-Khaiary MI, Malash GF (2011). Common data analysis errors in batch adsorption studies. Hydrometallurgy 105(3-4):314-320.
Elmorsi MT (2011). Equilibrium isotherms and kinetic studies of removal of methylene blue dye by adsorption onto miswak leaves as a natural adsorbent. Journal of Environmental Protection 2(6):817-827.
Erdem E, Karapinar N, Donat R (2004). The removal of heavy metal cations by natural zeolites. Journal of Colloid and Interface Science 261(2):309-319.
Fan L, Luo C, Sun M, Qiu H, Li X (2013). Synthesis of magnetic β-cyclodextrin–chitosan/graphene oxide as nanoadsorbent and its application in dye adsorption and removal. Colloids and Surf B: Biointerf 103:601-607.
Fan L, Luo CN, Sun M, Li XJ (2012). Fabrication of magnetic chitosan nanoparticles grafted with β-cyclodextrin as effective adsorbents toward hydroquinol. Colloids and Surfaces B: Biointerfaces 95:42-49.
Freundlich HMF (1906). Uber die Adsorption in Losungen. Zeitschrift für Physikalische Chemie 57(1):385-470.
Ghaedi M, Hajjati S, Mahmudi Z, Tyagi I, Agarwal S, Maity A, Gupta VK (2015). Modeling of competitive ultrasonic assisted removal of the dyes – methylene blue and safranin-O using Fe_3O_4 nanoparticles. Chemical Engineering Journal 268:28-37.
Ghaffari HR, Pasalari H, Tajvar A, Dindarloo K, Goudarzi B, Alipour V, Ghanbarneajd A (2017). Linear and non linear two-parameter adsorption isotherm modelling: A case study. The International Journal of Engineering and Science 6(9):1-11.
Ghogomu JN, Noufame TD, Ketcha MJ, Ndi NJ (2013). Removal of Pb (II) ions from aqueous solutions by kaolinite and metakaolinite materials. British Journal of Applied Science and Technology 3(4):942-961.
Gunay A, Arslankaya E, Tosun I (2007). Lead removal from aqueous solution by natural and pretreated clinoptilolite: adsorption equilibrium and kinetics. Journal of Hazardous Materials 146(1-2):362-371.
Gupta S, Kumar A (2019). Removal of nickel (II) from aqueous solution by biosorption on A. Barbadensis miller waste leaves powder. Applied Water Science 9(96):1-11.
Gupta VK, Jain KR, Nayak A, Agarwal S, Shrivastava M (2011). Removal of the hazardous dye – Tartrazine by photodegradation on titanium dioxide surface. Materials Science and Engineering: C 31(5):1062-1067.
Gupta VK, Suhas, Tyagi I, Agarwal S, Singh R, Chaudhary M, Harit A, Kushwaha S (2016). Column operation studies for the removal of dyes and phenols using a low cost adsorbent. Global Journal of Environmental Science and Management 2(1):1-10.
Hall KR, Eagleton LC, Acrivos A, Vermeulen T (1966). Pore- and solid-diffusion kinetics in fixed-bed adsorption under constant-pattern conditions. Industrial and Engineering Chemistry Fundamentals 5(2):212-223.
Hamdaoui O (2006). Batch study of liquid-phase adsorption of methylene blue using cedar sawdust and crushed brick. Journal of Hazardous Materials B 135(1-3):264-273.
Hamdaoui O, Naffrechoux E (2007). Modeling of adsorption isotherms of phenol and chlorophenols onto granular activated carbon Part I. Two-parameter models and equations allowing determination of thermodynamic parameters. Journal of Hazardous Materials 147(1-2):381-394.
Hamed I, Özogu F, Regenstein JM (2016). Industrial applications of crustacean by-products (chitin, chitosan, and chitooligosaccharides): A review. Trends in Food Science and Technology 48:40-50.
Hameed BH, Ahmad AL (2009). Batch adsorption of methylene blue from aqueous solution by garlic peel, an agricultural waste biomass. Journal of Hazardous Materials 164(2-3):870-875.
Hameed BH, Din ATM, Ahmad AL (2007). Adsorption of methylene blue onto bamboo-based activated carbon: Kinetics and equilibrium studies. Journal of Hazardous Materials 141(3):819-825.
Hasan MB (2008). Adsorption of reactive azo dyes on chitosan/oil-palm ash composite adsorbent: batch and continuous studies. M. Sc. Thesis, Universiti Sains Malaysia.
He J, Hong S, Zhang L, Gan F, Ho YS (2010). Equilibrium and thermodynamics parameters of adsorption of methylene blue onto rectorite. Fresenius Environmental Bulletin 19(11a):2651-2656.
Hefni HHH, Nagy M, Azab MM, Hussein MHM (2019). O-acylation of chitosan by L-arginine to remove the heavy metals and total organic carbon (TOC) from wastewater. Egyptian Journal of Petroleum 29(1):31-38.
Ho YS (2004). Comments on an evaluation of copper biosorption by a brown seaweed under optimized conditions by Antunes W. M., Luna, A. S., Henriques. C. A. and da Costa, A. C. A. Electronic Journal of

Biotechnology 7(2):228-237.
Ho YS, Porter JF, Mckay G (2002). Equilibrium isotherm studies for the biosorption of divalent metal ions onto peat, copper, nickel and lead single component systems. Water, Air, and Soil Pollution 141(1):1-33.
Hong S, Wen C, He J, Gan FX, Ho YS (2009). Adsorption thermodynamics of methylene blue onto bentonite. Journal of Hazardous Materials 167(1-3):630-633.
Horsfall Jnr M, Spiff A (2005). Effects of temperature on the sorption of Pb^{2+} and Cd^{2+} from aqueous solution by Caladium bicolor (wild Cocoyam) biomass. Electronic Journal of Biotechnology 8(2):162-169.
Hu ZG, Zhang J, Chan WL, Szeto YS (2006). The sorption of acid dye onto chitosan nanoparticles. Polymer 47(16):5838-5842.
Húmpola PD, Odetti HS, Fertitta AE, Vicente JL (2013). Thermodynamic analysis of adsorption models of phenol in liquid phase on different activated carbons. Journal of the Chilean Chemical Society 58(1):1541-1544.
Hurvich CF, Tsai CL (1989). Regression and time series model selection in small samples. Biometrika 76(2):297-307.
Ibrahim HA, Abdel Moamen OA, Monem NA, Ismail IM (2018). Assessment of kinetic and isotherm models for competitive sorption of Cs^+ and Sr^{2+} from binary metal solution onto nanosized zeolite. Chemical Engineering Communication 205(9):1274-1287.
Inam E, Etim UJ, Akpabio EG, Umoren SA (2016). Process optimization for the application of carbon from plantain peels in dye abstraction. Journal of Taibah University for Science 11(1):173-185.
Israel U, Eduok UM (2012). Biosorption of zinc from aqueous solution using coconut (*Cocos nucifera* L) coirdust. Archives of Applied Science Research 4(2):809-819.
Khodaie M, Ghasemi N, Moradi B, Rahim M (2013). Removal of methylene blue from wastewater by adsorption onto $ZnCl_2$ activated corn husk carbon equilibrium studies. Journal of Chemistry. Available at: http://dx.doi.org/10.1155/2013/383985
Kolmogorov A, Petrovskii I, Piskunov N (1937). A study of the diffusion equation with increase in the amount of substance, and its application to a biological problem. Bulletin of Moscow University Mathematics and Mechanics 1(6):1-26.
Kuang Y, Zhang X, Zhou S (2020). Adsorption of methylene blue in water onto activated carbon by surfactant modification. Water 12(2):587. Available at: https://doi.org/10.3390/w12020587
Kumar ASK, Ramachandran R, Kalidhasan S, Rajesh V, Rajesh N (2012). Potential application of dodecylamine modified sodium montmorillonite as an effective adsorbent for hexavalent chromium. Chemical Engineering Journal 211:396-405.
Kyzas GZ, Christodoulou E, Bikiaris DN (2018). Basic dye removal with sorption onto low-cost natural textile fibers. Processes 6(9):166. Available at: https://doi.org/10.3390/pr6090166
Langmuir I (1918). The adsorption of gases on plane surfaces of glass, mica and platinum. Journal of the American Chemical Society 40(9):1361-1403.
Li Y, Sun J, Du Q, Zhang L, Yang X, Wu S, Xia Y, Wang Z, Xia L, Cao A (2014). Mechanical and dye adsorption properties of graphene oxide/chitosan composite fibers prepared by wet spinning. Carbohydrate Polymers 102:755-761.
Magdy YM, Altaher H, ElQada E (2018). Removal of three nitrophenols from aqueous solutions by adsorption onto char ash: equilibrium and kinetic modeling. Applied Water Science 8(1):1-15. Available at: https://doi.org/10.1007/s13201-018-0666-1
Mahmoud ME, Nabil GM, El-Mallah NM, Bassiouny HI, Kumar S, Abdel-Fattah TM (2016). Kinetics, isotherm, and thermodynamic studies of the adsorption of reactive red 195 A dye from water by modified switchgrass biochar adsorbent. Journal of Industrial and Engineering Chemistry 37:156-167.
Malash GF, El-Khaiary MI (2010). Piecewise linear regression: A statistical method for the analysis of experimental adsorption data by the intraparticle-diffusion models. Chemical Engineering Journal 163(3):256-263.
Malik PK (2004). Dye removal from wastewater using activated carbon developed from sawdust: adsorption equilibrium and kinetics. Journal of Hazardous Materials 113(1-3):81-88.
Marshall WE, Champagne ET (1995). Agricultural byproducts as adsorbents for metal ions in laboratory prepared solutions and in manufacturing wastewater. Journal of Environmental Science & Health Part A 30(2):241-261.
Marshall WE, Johns MM (1996). Agricultural by-products as metal adsorbents: Sorption properties and resistance to mechanical abrasion. Journal of Chemical Technology and Biotechnology 66(2):192-198.
McKay G, Elgeundi M, Nassar MM (1987). Equilibrium studies during the removal of dyestuffs from aqueous solutions using bagasse pith. Water Research 21(12):1513-1520.
Mitrevski V, Mitrevski C, Mijakovski V, Pavkov IS, Geramitcioski T (2017). Mathematical modelling of the sorption isotherms of Quince. Thermal Science 21(5):1965-1973.
Mittal A, Mittal J, Malviya A, Gupta VK (2010). Removal and recovery of Chrysoidine Y from aqueous solutions by waste materials. Journal of Colloid and Interface Science 344(2):497-507.
Mohan D, Singh KP (2002). Single- and multi-component adsorption of cadmium and zinc using activated carbon derived from bagasse – An agricultural waste. Water Research 36(9):2304-2315.
Morrison RT, Boyd RN (2004). Organic Chemistry, Pearson Education, Singapore.
Muxika A, Etxabide A, Uranga J, Guerrero P, de la Caba K (2017). Chitosan as a bioactive polymer: processing, properties and applications. International Journal of Biological Macromolecules 105(2):1358-1368.
Najim TS, Yassin SA, Majli AJ (2010). Poly (furfural-acetone) as new adsorbent for removal of Cu (II) from aqueous solution: Thermodynamics and kinetic studies. International Journal of Chemistry 2(2):44-53.
Namasivayam C, Arasi D (1997). Removal of Congo red from wastewater by adsorption onto waste red mud. Chemosphere 34(2):401-417.
Namasivayam C, Kavitha D (2002). Removal of Congo red from water by adsorption onto activated carbon prepared from coir pith, an agricultural solid waste. Dyes and Pigments 54(1):47-58.
Namasivayam C, Radhika R, Suba S (2001a). Uptake of dyes by a promising locally available agricultural solid waste: coir pith. Waste Management 21(4):381-387.
Namasivayam C, Yamuna RT, Arasi D (2001b). Removal of acid violet from wastewater by adsorption on waste red mud. Environmental Geology 41(3):269-273.
Namasivayam C, Yamuna RT, Arasi D (2002). Removal of procion orange from wastewater by adsorption on waste red mud. Separation Science and Technology 37(10):2421-2431.
Nayak AK, Pal A (2019). Development and validation of an adsorption kinetic model at solid-liquid interface using normalized Gudermannian function. Journal of Molecular Liquids 276:67-77.
Nekouei F, Nekouei S, Tyagi I, Gupta VK (2015). Kinetic, thermodynamic and isotherm studies for acid blue 129 removal from liquids using copper oxide nanoparticle-modified activated carbon as a novel adsorbent. Journal of Molecular Liquids 201:124-133.
Olafadehan OA (2021). Fundamentals of Adsorption Processes, ISBN: 978-620-3-30705-4, LAP Lambert Academic Publishing, OmniScriptum DUE GmbH.
Olafadehan OA, Ajayi TO, Amoo KO (2020). Optimum conditions for extraction of chitin and chitosan from callinectes amnicola shell waste. Theoretical Foundations of Chemical Engineering 54(6):1173-1194.
Olafadehan OA, Akpo OY, Enemuo O, Amoo KO, Abatan OG (2018). Equilibrium, kinetic and thermodynamic studies of biosorption of zinc ions from industrial wastewater using derived composite biosorbents from walnut shell. African Journal of Environmental Science and Technology 12(9):335-356.
Olafadehan OA, Amoo KO, Ajayi TO, Bello VE (2021). Extraction and characterization of chitin and chitosan from Callinectes amnicola and Penaeus notialis shell wastes. Journal of Chemical Engineering and Material Science 12(1):1-30.
Padder MS, Majumder CB (2016). Studies on removal of As(III)and As(V) through their adsorption onto granular activated carbon/$MnFe_20_4$ composite: isotherm studies and error analysis. Composite Interface 23(4):327-372.
Padmesh TVN, Vijayaraghavan K, Sekaran G, Velan M (2006). Application of two-and three-parameter isotherm models: b iosorption

of acid red 88 onto Azolla microphylla. Bioremediation Journal 10(1-2):37-44.

Pandey S, Mishra SB (2011). Organic–inorganic hybrid of chitosan/organoclay bionanocomposites for hexavalent chromium uptake. Journal of Colloid and Interface Science 361(2):509-520.

Periolatto M, Ferrero F (2013). Cotton Filter Fabrics Functionalization by Chitosan UV grafting for Removal of Dyes. Chemical Engineering Transactions 32:85-90.

Poots VJP, McKay G, Healy JJ (1976). The removal of acid dye from effluent using natural adsorbents—I peat. Water Research 10(12):1061-1066.

Popoola LT (2019). Characterization and adsorptive behavior of snail shell-rice husk (SS-RH) calcined particles (CPs) towards cationic dye. Heliyon 5(1):1-38.

Pourali P, Behzad M, Arfaeinia H, Ahmadfazeli A, Afshin S, Poureshgh Y, Rashtbari Y (2020). Removal of acid blue 113 from aqueous solutions using low cost adsorbent adsorption isotherms, thermodynamics, kinetics and regeneration studies. Separation Science and Technology. Available at: https://doi.org/10.1080/01496395.2020.1867583

Rahman MM, Pal A, Uddin K, Thu K, Saha BB (2018). Statistical analysis of optimized isotherm model for maxsorb III/ethanol and silical gel/water pairs. Evergreen Joint Journal of Novel Carbon Resources Sciences and Green Asia Strategy 5(4):1-12.

Rahmi HF, Susilawati, Ismaturrahmi, Nilawati (2018). Preparation of sulfonated magnetic chitosan for methylene blue adsorption. International Proceeding ASEAN YOUTH Conference, PPI-Malaysia 1:379-384.

Ramadoss R, Subramaniam D (2018). Adsorption of chromium using blue green algae-modeling and application of various isotherms. International Journal of Chemical Technology 10(1):1-22.

Razavi Z, Mirghaffari N, Rezaei B (2013). Adsorption of crude and engine oils from water using raw rice husk. Water Science and Technology 69(5):947-952.

Redlich O, Peterson DL (1959). A useful adsorption isotherm. Journal of physical chemistry 63(6):1024-1024. Available at: http://dx.doi.org/10.1021/j150576a611

Reichenberg D (1953). Properties of ion-exchange resins in relation to their structure. III. Kinetics of exchange. Journal of the American Chemical Society 75(3):589-597.

Sabar S, Aziz HA, Yusof NH, Subramaniam S, Foo KY, Wilson LD, Lee HK (2020). Preparation of sulfonated chitosan for enhanced adsorption of methylene blue from aqueous solution. Reactive and Functional Polymers 151:104584. Available at: http://dx.doi.org/10.1016/j.reactfunctpolym.2020.104584

Saha P, Chowdhury S (2011). Insight into adsorption thermodynamics. Thermodynamics 16:349-364. Available at: https://doi.org/10.5772/13474

Saleh TA, Gupta VK (2014). Processing methods, characteristics and adsorption behavior of tire derived carbons: A review. Advances in Colloid and Interface Science 211:93-101.

Salimi A, Roosta A (2019). Experimental solubility and thermodynamic aspects of methylene blue in different solvents. Thermochimica Acta 675:134-139.

Saravanam E, Khan MM, Gracia F, Qin J, Gupta VK, Stephen A (2016). Ce^{3+}-ion-induced visible-light photocatalytic degradation and electrochemical activity of ZnO/CeO_2 nanocomposite, Scientific Reports 6(1):1-11. Available at: https://doi.org/10.1038/srep31641

Saravanan R, Gupta VK, Thanigainathan P, Narayanan V, Arumainathan S (2013a). Synthesis, characterization and photocatalytic activity of novel Hg doped ZnO nanorods prepared by thermal decomposition method. Journal of Molecular Liquids 178:88-93.

Saravanan R, Joicy S, Gupta VK, Narayanan V, Stephen A (2013c). Visible light induced degradation of methylene blue using CeO_2/V_2O_5 and CeO_2/CuO catalysts. Materials Science and Engineering: C 33(8):4725-4731.

Saravanan R, Karthikeyan S, Gupta VK, Sekaran G, Narayanan V, Stephen A (2013b) Enhanced photocatalytic activity of ZnO/CuO nanocomposite for the degradation of textile dye on visible light illumination. Materials Science and Engineering: C 33(1):91-98.

Saravanan R, Karthikeyan N, Gupta VK, Thirumal E, Thangadurai P, Narayanan V, Stephen A (2013d). ZnO/Ag nanocomposite: An efficient catalyst for degradation studies of textile effluents under visible light. Materials Science & Engineering: C 33(4):2235-2244.

Saravanan R, Khan MM, Gupta VK, Mosquera E, Gracia F, Narayanan V, Stephen A (2015). ZnO/Ag/CdO nanocomposite for visible light-induced photocatalytic degradation of industrial textile effluents. Journal of Colloid and Interface Science 452:126-133.

Sarode S, Upadhyay P, Khosa MA, Mak T, Shakir A, Song S, Ullaha A (2019). Overview of wastewater treatment methods with special focus on biopolymer chitin-chitosan. International Journal of Biological Macromolecules 121:1086-1100.

Senthilkumaar S, Varadarajan PR, Porkodi K, Subbhuraam CV (2005). Adsorption fiber carbon: kinetics and equilibrium of methylene blue onto jute fiber carbon: kinetics and equilibrium studies. Journal of Colloid and Interface Science 284(1):78-82.

Shajahan A, Shankar S, Sathiyaseelan A, Narayan KS, Narayanan V, Kaviyarasan V, Ignacimuthu S (2017). Comparative studies of chitosan and its nanoparticles for the adsorption efficiency of various dyes. International Journal of Biological Macromolecules 104:1449-1458.

Sharififard H, Shahraki ZH, Rezvanpanah E, Rad SH (2018). A novel natural chitosan/activated carbon/iron bio-nanocomposite: sonochemical synthesis, characterization, and application for cadmium removal in batch and continuous adsorption process. Bioresource Technology 270:562-569.

Sharma P, Das MR (2012). Removal of a cationic dye from aqueous solution using graphene oxide nanosheets: investigation of adsorption parameters. Journal of Chemical & Engineering Data 58(1):151-158.

Sheshmani S, Ashori A, Hasanzadeh S (2014). Removal of acid orange 7 from aqueous solution using magnetic graphene/chitosan: A promising nano-adsorbent. International Journal of Biological Macromolecules 68:218-224.

Sivarajasekar N, Baskar R (2014). Adsorption of basic red onto activated carbon derived from immature cotton seeds: isotherm studies and error analysis. Desalination and Water Treatment 52(40-42):7743-7765.

Slimani R, Anouzla A, Abrouki Y, Ramli Y, Antri SE, Mamouni R, Lazar S, Haddad ME (2011). Removal of a cationic dye-methylene blue from aqueous media by the use of animal bone meal as a new low cost adsorbent. Journal of Materials and Environmental Science 2(1):77-87.

Sugiura N (1978). Further analysis of data by Akaike's information criterion and the finite corrections. Communications in Statistics – Theory and Methods A7(1):12-26.

Sun L, Tian C, Wang L, Zou JL, Mu G, Fu HG (2011). Magnetically separable porous graphitic carbon with large surface area as excellent adsorbents for metal ions and dye. Journal of Materials Chemistry 21(20):7232-7239.

Sutherland C, Venkobachar C (2010). A diffusion-chemisorption kinetic model for simulating biosorption using forest macro-fungus, fomes fasciatus. International Research Journal of Plant Science 1(4):107-117.

Tahir SS, Rauf N (2006). Removal of a cationic dye from aqueous solutions by adsorption onto bentonite clay. Chemosphere 63(11):1842-1848.

Temkin M, Pyzhev V (1940). Kinetics of ammonia synthesis on promoted iron catalyst. Acta Physiochimica 12:327-356.

Tóth J (1971). State equation of the solid gas interface layer. Acta Chimica (Academiae Scientiarum) Hungaricae 69:311-317.

Tran VS, Ngo HH, Guo W, Zhang J, Liang S, Ton-That C, Zhang X (2015). Typical low cost biosorbents for adsorptive removal of specific organic pollutants from water. Bioresource Technology 182:353-363.

Turner BD, Henley BJ, Sleap SB, Sloan SW (2015). Kinetic model selection and the Hill model in geochemistry. International Journal of Environmental Science and Technology 12:2545-2558.

Vakili M, Rafatullah M, Salamatinia B, Abdullah AZ, Ibrahim MH, Tan KB, Gholami Z, Amouzgar P (2014). Application of chitosan and its derivatives as adsorbents for dye removal from water and wastewater: A review. Carbohydrate Polymers 113:115-130.

Vandevivere PC, Bianchi R, Verstraete W (1998). Treatment and reuse

of wastewater from the textile wet-processing industry: Review of emerging technologies. Journal of Chemical Technology and Biotechnology 72(4):289-302.
Vijayaraghavan K, Padmesh TVN, Palanivelu K, Manickam V (2006). Biosorption of Nickel(II) Ions onto Sargassum wightii: Application of two-parameter and three-parameter isotherm models. Journal of Hazardous Materials 133(1-3):304-308.
Wagenmakers E, Farrell S (2004). AIC model selection using Akaike weights**.** Psychonomic Bulletin Review 11(1):192-196.
Walker GM, Weatherley LR (1997). Adsorption of acid dyes on to granular activated carbon in fixed beds. Water Research 31(8):2093-2101.
Wan Ngaha WS, Teonga LC, Hanafiaha MAKM (2011). Adsorption of dyes and heavy metal ions by chitosan composites: A review. Carbohydrate Polymers 83(4):1446-1456.
Wang QL, Apul OG, Xuan P, Luo F, Karanfil T (2013). Development of a 3DQSPR model for adsorption of aromatic compounds by carbon nanotubes: comparison of multiple linear regression, artificial neural network and support vector machine. RSC Advances 3(46):1-32.
Wang S, Li L, Wu H, Zhu ZH (2005). Unburned carbon as a low-cost adsorbent for treatment of methylene blue-containing wastewater. Journal of Colloid and Interface Science 292(2):336-343.
Wang XS, Qin Y, Li ZF (2006). Biosorption of zinc from aqueous solutions by rice bran: kinetics and equilibrium studies, Separation Science and Technology 41(4):747-756.
Weber TW, Chakravorti RK (1974). Pore and solid diffusion models for fixed-bed adsorbers. AIChE Journal 20(2):228-238.
Yanev ZL, Koumanova BK, Georgieva NV (2013). Linear and nonlinear regression methods for equilibrium modelling of p-nitrophenol biosorption by Rhizopus Oryza: comparison of error analysis criteria. Journal of Chemistry 2013:1-10.
Yao YJ, Xu FF, Chen M, Xu ZX, Zhu ZW (2010). Adsorption behavior of methylene blue on carbon nanotubes. Bioresource Technology 101(9):3040-3046.
Yoro KO, Singo M, Mulopo JL, Daramola MO (2017). Modelling and experimental study of the CO_2 capture. Energy Procedia 114:1643-1664.
Zarrouk AH, Zarrok B, Al-Salem, Sultan H, Messali M (2011). Temperature effect, activation energies and thermodynamic adsorption studies of l-cysteine methyl ester hydrochloride as copper corrosion inhibitor in nitric acid 2M. International Journal of Electrochemical Science 6(12):6261-6274.
Zbair M, Anfar Z, Khallok H, Ahsaine HA, Ezahri M, Elalem N (2018). Adsorption kinetics and surface modeling of aqueous methylene blue onto activated carbonaceous wood sawdust. Fullerenes, Nanotubes and Carbon Nanostructures 26(7):433-442.
Zhai Y, Wei X, Zeng G, Zhang D, Chu K (2004). Study of adsorbent derived from sewage sludge for the removal of Cd^{2+}, Ni^{2+} in aqueous solutions. Separation and Purification Technology 38(2):191-196.